Integration of design and control for large-scale applications: a back-off approach

by

Seyedehmina Rafieishishavan

A thesis

presented to the University of Waterloo

in fulfillment of the

thesis requirement for the degree of

Doctor of Philosophy

in

Chemical Engineering

Waterloo, Ontario, Canada, 2020

Examining Committee Membership

The following served on the Examining Committee for this thesis. The decision of the Examining Committee is by majority vote.

External Examiner	Lorenz T Biegler Professor Chemical Engineering, Carnegie Mellon University
Supervisor(s)	Luis A. Ricardez-Sandoval Associate Professor Chemical Engineering, University of Waterloo
Internal Member	Hector Budman Professor Chemical Engineering, University of Waterloo
	Nasser Mohieddin Abukhdeir Associate Professor Chemical Engineering, University of Waterloo
Internal-external Member	Fatih Safa Erenay Associate Professor Management Sciences, University of Waterloo

I hereby declare that I am the sole author of this thesis. This is a true copy of the thesis, including any required final revisions, as accepted by my examiners.

I understand that my thesis may be made electronically available to the public.

Abstract

Design and control are two distinct aspects of a process that are inherently related though these aspects are often treated independently. Performing a sequential design and control strategy may lead to poor control performance or overly conservative and thus expensive designs. Unsatisfactory designs stem from neglecting the connection of choices made at the process design stage that affects the process dynamics. Integration of design and control introduces the opportunity to establish a transparent link between steady-state economics and dynamic performance at the early stages of the process design that enables the identification of reliable and optimal designs while ensuring feasible operation of the process under internal and external disruptions. The dynamic nature of the current global market drives industries to push their manufacturing strategies to the limits to achieve a sustainable and optimal operation. Hence, the integration of design and control plays a crucial role in constructing a sustainable process since it increases the short and long-term profits of industrial processes.

Simultaneous process design and control often results in challenging computationally intensive and complex problems, which can be formulated conceptually as dynamic optimization problems. The size and complexity of the conceptual integrated problem impose a limitation on the potential solution strategies that could be implemented on large-scale industrial systems. Thus far, the implementation of integration of design and methodologies on large-scale applications is still challenging and remains as an open question. The back-off approach is one of the proposed methodologies that relies on steady-state economics to initiate the search for optimal and dynamically feasible process design. The idea of the surrogate model is combined with the back-off approach in the current research as the key technique to propose a practical and systematic method for the integration of design and control for large-scale applications.

The back-off approach featured with power series expansions (PSEs) is developed and extended to achieve multiple goals. The proposed back-off method focuses on searching for the optimal design and control parameters by solving a set of optimization problems using PSE functions. The idea is to search for the optimal direction in the optimization variables by solving a series of bounded PSE-based optimization problems. The approach is a sequential approximate optimization method in which the system is evaluated around the worst-case variability expected in process outputs. Hence, using PSE functions instead of the actual nonlinear dynamic process model at each iteration step reduces the computational effort. The method mostly traces the closest feasible and near-optimal solution to the initial steady-state condition considering the worst-case scenario. The term near-optimal refers to the potential deviations from the original locally optimum due to the approximation techniques considered in this work.

A trust-region method has been developed in this research to tackle simultaneous design and control of large-scale processes under uncertainty. In the initial version of the back-off approach proposed in this research, the search space region in the PSE-based optimization problem was specified *a priori*. Selecting a constant search space for the PSE functions may undermine the convergence of the methodology since the predictions of the PSEs highly depend on the nominal conditions used to develop the corresponding PSE functions. Thus, an adaptive search space for individual PSE-optimization problems at every iteration step is proposed. The concept has been designed in a way that certifies the competence of the PSE functions at each iteration and adapts the search space of the optimization as the iteration proceeds in the algorithm. Metrics for estimating the residuals such as the mean of squared errors (MSE) are employed to quantify the accuracy of the PSE approximations. Search space regions identified by this method specify the boundaries

of the decision variables for the PSE-based optimization problems. Finding a proper search region is a challenging task since the nonlinearity of the system at different nominal conditions may vary significantly. The procedure moves towards a descent direction and at the convergence point, it can be shown that it satisfies first-order KKT conditions.

The proposed methodology has been tested on different case studies involving different features. Initially, an existent wastewater treatment plant is considered as a primary medium-scale case study in the early stages of the development of the methodology. The wastewater treatment plant is also used to investigate the potential benefits and capabilities of a stochastic version of the back-off methodology. Furthermore, the results of the proposed methodology are compared to the formal integration approach in a dynamic programming framework for the medium-scale case study. The Tennessee Eastman (TE) process is selected as a large-scale case study to explore the potentials of the proposed method. The results of the proposed trust-region methodology have been compared to previously reported results in the literature for this plant. The results indicate that the proposed methodology leads to more economically attractive and reliable designs while maintaining the dynamic operability of the system in the presence of disturbances and uncertainty. Therefore, the proposed methodology shows a significant accomplishment in locating dynamically feasible and near-optimal design and operating conditions thus making it attractive for the simultaneous design and control of large-scale and highly nonlinear plants under uncertainty.

Acknowledgments

First, I would like to express my sincere gratitude to my supervisor Prof. Luis A. Ricardez-Sandoval. This work could not happen without his continuous encouragement, support and valuable input. Luis! Thanks for your valuable time and endless support even on Sundays which are supposed to be only for family!

I would like to thank my examining committee: Prof. Lorenz T. Biegler, Prof. Hector Budman, Prof. Nasser Mohieddin Abukhdeir, and Prof. Fatih Safa Erenay for their time and valuable comments.

I wish to acknowledge the financial assistance provided by Natural Sciences and Engineering Research Council and University of Waterloo.

My special thanks go to my loving family and dear in-laws for their infinite love and support, especially during difficult times. You are one of the reasons why I smile.

I want to thank all of my dear friends, especially Lena, Navid, Amir, Mahshad, Kimia, Mariana, and Nina for all their encouragement, support, and invaluable friendship. Many thanks go to my dear friends in the research group, especially Grigoriy, Kavitha, Yue, Donovan, Oscar, Yael and all other colleagues who encouraged me, supported me and made my PhD journey a pleasant adventure.

In the end, I would like to extend my heartfelt appreciation to my loving husband, Sepehr, for all his endurance, support, and encouragement. Honey! I cannot thank you enough for all you have done for me. You are my sky, a sky full of stars!

Dedication

In memory of my beloved father, Taher Rafieishishavan, the kindest man in the world whom I still miss every day every moment.

Baba! I can deal with anything in the world except your absence. I wish I had you by my side.

Table of contents

List of figures

List of tables

List of abbreviations

AI	Artificial intelligence
ANN	Artificial neural network
CFD	Computational fluid dynamic
DFO	Derivative-free optimization
GBD	Generalized benders decomposition
GWP	Global warming potential
HTPE	Human toxicity potential by exposure
HTPI	Human toxicity potential by ingestion
MC	Monte Carlo
MIDO	Mixed-integer dynamic optimization
MINLP	Mixed-integer nonlinear programming
MLMC	Multilevel Monte Carlo
MPC	Model predictive control
MSE	Mean squared error
NLP	Nonlinear programming
NMPC	Nonlinear model predictive control
OA	Outer approximation
ODE	Ordinary differential equation
PSE	Power series expansion
SSV	Structured singular value
RGA	Relative gain array

List of symbols

c_s	Oxygen specific saturation
c_w	Dissolved oxygen concentration(mg/L)
$c_{w_{sp}}$	Dissolved oxygen set-point in the reactor (mg/L)
$\boldsymbol{d}$	Time-varying disturbances
$\boldsymbol{d}_{nom}$	Disturbances at nominal condition
f_d	Fraction of death biomass
f_k	Turbine speed
g	Process inequality constraints
g_{ss}	Process equality constraints at steady-state
g_{PSE}	PSE of process inequality constraints
h	Process equality constraints
h_{PSE}	PSE of process equality constraints
h_{ss}	Process equality constraints at steady-state
i	Index in the iterative back-off algorithm
j	Index of uncertain parameters ($\boldsymbol{\zeta}$)
k	Index in the procedure of finding required MC samples/stepwise search for trust interval
k_s	Saturation constant
k_d	Biomass death rate
k_c	Specific Cellular activity
k_{la}	Oxygen transfer into the water constant
k_{01}	Oxygen demand constant
l	Order of gradient in the PSE
lr_d, lr_b , lr_r	Depth of the first, second and bottom layers in the decanter (m)
n	Potential model structure error
n_x	Number of system states
n_y	Number of system algebraic equations
p	Index of decision variables
q	Index of equality constraints
q_o	Outlet flow from reactor (m^3/hr)
q_i	Feed flowrate (m^3/hr)
$q_{i_{nom}}$	Nominal condition of the inlet flowrate (m^3/hr)
q_p	Purge flowrate (m^3/hr)
q_r	Recycle flowrate (m^3/hr)
q_1	Outlet flow from decanter (m^3/hr)
q_2	Recycle flow that leaves the decanter (m^3/hr)
s	Index of inequality constraints
s_i	Inlet organic substrate concentration(mg/L)
s_{ir}	organic substrate concentrations entering the bioreactor (mg/L)
s_w	Organic substrate concentrations in the bioreactor (mg/L)
$s_{w_{sp}}$	Substrate set-point in the reactor (mg/L)
s_w^{up}	upper bund (saturation limit) on the substrate concentration
r	Return on investment, TE plant

t	Time
t_f	Final process time
t_{wc}	Time at the worst-case scenario
$\boldsymbol{u}$	Time-varying control variables
$\boldsymbol{u}_U^*$	Lagrangian multipliers for the upper bound multipliers
$\boldsymbol{u}^*$	Lagrangian multipliers for the inequality constraints
$\boldsymbol{u}_L^*$	Lagrangian multipliers for the lower bound multipliers
vsd, vsb, vsr	Rate of settling for the activated sludge at first, second and bottom layers in the decanter
$\boldsymbol{x}$	System states
$\dot{\boldsymbol{x}}$	Differential of system states
x_d, x_b, x_r	Biomass concentrations at first, second and bottom layers in the decanter (mg/L)
x_i	Inlet biomass concentration (mg/L)
x_{ir}	Biomass concentrations entering the bioreactor (mg/L)
x_w	Biomass concentrations in the bioreactor (mg/L)
$\boldsymbol{x_0}$	States at initial condition
$\boldsymbol{y}$	System algebraic variables
A	Amplitude of the sinusoidal changes in the inlet flowrate (m^3/hr)
A_d	Cross-sectional area of the decanter (m^2)
CC_w	Capital cost of the wastewater treatment plant ($/a)
$\mathbb{CI}^{\rho}$	Confidence interval at coverage probability of ρ
D	Diameter of the process units, TE plant
F	Process DAE model
F_{ss}	Process model at steady-state
F_0	Process DAE model at initial condition
F_1	System of DAEs of first-order sensitivity analytical sensitivity calculation
F_2	System of DAEs of second-order sensitivity analytical sensitivity calculation
K_{c1}	Proportional gain of the PI controller of the purge flowrate
K_{c2}	Proportional gain of the PI controller of the turbine speed
M_1	Big-M method penalty term for inequality constraints
M_2	Big-M method penalty term for equality constraints
N	Number of samples in each batch of MC samples
N_c	Convergence examination period, back-off methodology
N_{iter}	Maximum number of iterations allowed in the back-off algorithm
N_T	Maximum number of steps in the stepwise search for trust interval
OC_w	Operating cost of the wastewater treatment plant ($/a)
P	Number of decision variables in the optimization problem
P	Pressure, TE plant
Q	Number of equality constraints in the optimization problem
R	Data set (simulation results) collected from *N* MC samples
S	Number of inequality constraints in the optimization problem
R_1^{lo}	Lower bound on feasible ratio between the purge to the recycle flowrate
R_1^{up}	Upper bound on feasible ratio between the purge to the recycle flowrate
R_2^{lo}	Lower bound on feasible purge age in the decanter
R_2^{up}	Upper bound on feasible purge age in the decanter
V_r	The volume of the aeration tank (m^3)

VC_w	Variability cost of the wastewater treatment plant ($/a)
Greek symbols	
$\boldsymbol{\alpha_d}$	Statistical properties of probability distribution function of disturbance
$\boldsymbol{\alpha_\zeta}$	Statistical properties of probability distribution function of uncertainty
$\boldsymbol{\gamma}$	Weights assigned to the standard deviation of the constraints
δ	Search space of optimization variables in PSE-based optimization
ϵ	Tolerance criterion for convergence, back-off methodology
ϵ_{MC}	Tolerance criterion for convergence, PSE functions
ϵ_{TR}	Tolerance criterion of the validity of PSE functions
$\boldsymbol{\zeta}$	Uncertainty (parameter uncertainty, model structure error)
$\boldsymbol{\zeta}_{nom}$	Uncertainty at nominal condition
$\boldsymbol{\eta}$	Optimization variables
$\boldsymbol{\eta}_{nom}$	Optimization variables at nominal condition
$\boldsymbol{\eta}^{up}$	Upper bounds on the optimization variables
$\boldsymbol{\eta}^{lb}$	Lower bounds on the optimization variables
$\boldsymbol{\eta}^{+}$	Optimization variables at forward point for gradient calculation
$\boldsymbol{\eta}^{-}$	Optimization variables at backward point for gradient calculation
$\boldsymbol{\eta}_0$	Optimization variables estimated at steady-state
$\boldsymbol{\lambda}$	Feasibility variables to ensure feasibility of inequality constraints
$\boldsymbol{\mu}$	Feasibility variables to ensure feasibility of equality constraints
μ_w	Specific growth rate
ρ	Confidence level
$\boldsymbol{\varsigma}$	Integer decision variables
τ_{i1}	Time integral constant of the PI controller of the purge flowrate
τ_{i2}	Time integral constant of the PI controller of the turbine speed
Θ	Cost function
$\boldsymbol{\chi}$	System variables
ω	Index for number of states
$\boldsymbol{\delta}^U$	Maximum allowable trust interval
$\Delta\eta$	step size for the finite-difference calculations
$\boldsymbol{\nu}^*$	Lagrangian multipliers for the equality constraints

1 Introduction

The dynamic nature of the current global market is driving industries to push manufacturing strategies to their limits to achieve a sustainable and optimal operation. For a long period of time, profitability was one of the main concerns of manufacturers; however, lately, that attitude has shifted towards the development and optimal operation of profitable and sustainable processes. The alarming conditions of climate change, conflict and resource scarcity, and waste production are the main motivations to include sustainability in the chemical process industries. Nowadays, sustainability embraces almost all aspects of company policies related to economics, social, safety, and environmental attitudes. Traditionally, several aspects of the processes are handled independently. This outlook has great potential to be upgraded for most real-world case studies. Clearly, the desired improvement is possible by incorporating multiple aspects of the process that encompass long-term process sustainability.

One of the core fragments of that combined problem is the simultaneous optimization of process design and control. In the past, these two aspects of the process, i.e., steady-state process design economics and dynamic behaviour, were treated independently and solved in a sequential fashion. However, this approach may lead to poor control performance or overly conservative and thus expensive designs (Luyben, 2004). The naive designs stem from neglecting the inherent connection of choices made at the process design stage that affects the process dynamics. Alternatively, integration of design and control introduces the opportunity to establish a transparent link between conflicting objectives of steady-state economics and dynamic performance at the early stages of the process design that enables the identification of reliable and optimal designs while ensuring feasible operation of the process under internal and external disruptions.

Over the past decade, there has been a dramatic increase in the development of multi-faceted approaches for the integration of multiple aspects; in particular, integration of design and control (Rafiei and Ricardez-Sandoval, 2020a). Hence, a large and growing body of the current literature in this field has attempted to propose novel methods that resolve some unanswered and challenging questions in the field. Simultaneous

process design and control as the core of the integrated approach can be formulated conceptually as dynamic optimization problems. The size and complexity of the conceptual integrated problem impose limitations on the potential solution strategies that could be implemented on large-scale industrial systems. Consequently, integration of design and control for a relatively large-scale application might become intractable even for high-performance computers. Indeed, the available methodologies applied multiple simplifying assumptions to make the problem tractable and have been implemented either on an isolated unit operation or simple industrial case studies (Alhammadi and Romagnoli, 2004; Diangelakis et al., 2016; Ricardez-Sandoval et al., 2011). This indicates a need for an efficient and applicable simultaneous design and control method for large-scale industrial applications. Then, to fill the gap in the applicable methods, the central goal pursued in this PhD study is to present a practical and systematic method for the integration of design and control for large-scale applications.

This work presents a new methodology for integration of design and control that is based on the back-off approach to initiate the search for optimal and dynamically feasible process design. For the purpose of steady-state optimal design and process, all process parameters are assumed at their nominal values; however, any type of model mismatch, simplification, linearization or parametric uncertainty may lead to imprecise model predictions. Therefore, the optimal solution obtained from the nominal condition can be infeasible or highly sub-optimal due to the uncertainties or disturbances, which can emerge from different sources. On the other hand, the conceptual formulation of a simultaneous design and control problem results in a dynamic nonlinear optimization problem that is often sensitive to initialization. Lack of educated initial conditions may result in failure to achieve convergence to an optimal solution. A back-off approach is an attractive option where the ideal steady-state optimal condition is used as the foundation to improve the regulation of optimality and dynamic feasibility (Perkins, 1989; Perkins et al., 1989). Back-off terms are originally defined as the required draw-backs of the steady-state condition from active constraints in order to maintain dynamic feasibility under uncertainty and disturbances (Bahri et al., 1995; Figueroa et al., 1996; Kookos and Perkins, 2016; Narraway and Perkins, 1994).

As mentioned above, the integration of design and control problem often leads to challenging and complex formulations. One of the central strategies in the engineering discipline to handle the size and complexity of the theoretical formulations of the integrated problem is to employ surrogate models and/or decomposition methods. Model-based approaches have been proposed where the nonlinear behaviour of the system is approximated using suitable model structures (Bettebghor et al., 2011; Bhosekar and Ierapetritou, 2018; Chawankul et al., 2007; Forrester and Keane, 2009; Gerhard et al., 2008, 2005; Ricardez-Sandoval et al., 2008; Sanchez-Sanchez and Ricardez-Sandoval, 2013a; Trainor et al., 2013; Viana et al., 2013). Likewise, dynamic high fidelity models of the process are represented using approximation and model reduction techniques for simultaneous design and control (Burnak et al., 2019a; Diangelakis et al., 2017; Malcolm et al., 2007; Moon et al., 2011; Pistikopoulos et al., 2015). Accordingly, in attempts to reduce the computational burden of the approach, power series expansions (PSEs) have been used as a basis to capture the behaviour of the system for optimal process improvement under uncertainty. The idea of the surrogate model is combined with the back-off approach in the current research as the key technique to propose a new and efficient methodology for simultaneous design and control.

1.1 Research objectives

Despite the extensive body of research on the integration of design and control, a systematic framework that addresses simultaneous design and control of large-scale systems under uncertainties is sparse. Thus, the main goal of the research is to propose and develop a methodology for the integration of design and control with the aim of achieving economical, environmentally friendly and computationally attractive process designs, particularly for large-scale applications. The specific objectives of the current study are as follows:

- Propose a practical method for integration of design and control that can address the simultaneous design and control of large-scale and highly nonlinear systems under uncertainty and disturbances. To accomplish this goal, the system is represented using low-order models with online

identification of the worst-case scenario while the validity of those replicas is certified in a trusted interval. The procedure sequentially moves toward a descent direction from an educated initial condition.

- Take into account probabilistic-based uncertainties for integration of design and control. To achieve this objective, variability in the process constraints and objective function are considered by means of statistical terms.
- Inspect the quality of the identified optimal solution for simultaneous design and control. Check if the surrogate models are sufficient for the replacement of the actual nonlinear behaviour of the process.

1.2 Research work contributions

The current PhD study is aimed to provide the following contributions:

- A new back-off methodology (trust-region) that performs simultaneous design and control of large-scale and highly nonlinear systems under uncertainty and disturbances. Significant reductions in the computational costs have been achieved by developing a decomposition algorithm that involves simple optimization problems that can lead to the optimal process designs. As a result, the proposed method empowers the simultaneous design and control of large-scale systems.
- A stochastic back-off approach that can address the simultaneous design and control of medium-scale processes under probabilistic-based uncertainty and disturbances. The method is designed in a way that provides the user with an additional degree of freedom to rank the significance of the constraints with a reasonable computational cost.
- A trust-region method that may guarantee convergence to a local optimum solution. The proposed methodology moves optimization variables towards a descent direction and the convergence satisfies the first-order KKT conditions.

- The proposed trust-region technique has the potential to deal with black-box models since piecewise surrogate models (PSEs) replace the actual behaviour of the process.

1.3 Outlines of the work

The remainder of this thesis is organized as follows:

Chapter 2 provides a general problem statement for the integration of design and control, followed by a discussion of the main challenges and proposed remedies in the literature. In addition to the literature review of the subject, the challenges that are currently being faced in the field of integration of design and control are identified so that academic and industrial practitioners can recognize the main obstacles and perceive the approaches that might be more relevant for their specific applications. Open problems and future research perspectives are identified. The literature review in this chapter has been published in (Rafiei and Ricardez-Sandoval, 2020a)

Chapter 3 presents a basic back-off approach that focuses on searching for the optimal design and control parameters by solving the set of optimization problems using mathematical expressions obtained from PSE. The PSE model coefficients, i.e. the sensitivity terms, can be calculated numerically and analytically. The benefits and limitations of numerical and analytical PSE coefficients are examined. The work presented in this chapter has been published in (Rafiei-Shishavan et al., 2017).

Chapter 4 presents a new stochastic back-off approach. The basic back-off presented in Chapter 3 was extended to accommodate probabilistic (stochastic)-based uncertainties and disturbances. The key idea in the present approach is to represent variability in the process constraints and objective function by means of statistical terms, e.g. confidence intervals. This approach provides the user with an additional degree of freedom to rank the significance of the constraints through the use of coverage probabilities. The present methodology has the potential to specify more economically attractive designs compared to the worst-case variability methodologies presented in Chapter 3. The results of this chapter have been published in (Rafiei-Shishavan and Ricardez-Sandoval, 2017; Rafiei and Ricardez-Sandoval, 2018).

Chapter 5 presents a trust-region approach to address the simultaneous design and control of large-scale systems under uncertainty. The approach is on the foundation of the basic back-off approach presented in Chapter 3. The concept is designed in a way that certifies the competence of the PSE functions at each iteration and systematically acquires the search space of the optimization as the iteration proceeds in the algorithm. The proposed approach was tested in a wastewater treatment plant and the Tennessee Eastman (TE) process. The results indicate that the proposed methodology leads to more economically attractive and reliable designs while maintaining the dynamic operability of the system in the presence of multiple disturbances. Part of the results presented in this chapter has been publication in (Rafiei and Ricardez-Sandoval, 2020b).

In Chapter 6 incentives directed towards the evolution of an integrated approach are identified. Emerging trends are discussed as the possible pathways the industry and academy might take to achieve the ideal framework of integrating all the decision levels, considering the complexities, obligations, and dimensions of a real-world enterprise. Promising strategies that are often implemented individually and that can expand the operating window of an integrated approach are outlined under the emerging trends. Potential applications of an integrated scheme are presented. The discussions presented in this chapter have published in (Rafiei and Ricardez-Sandoval, 2020a).

Finally, Chapter 7 presents the conclusions obtained from the present research work and outlines potential future work that can be considered for this research.

2 Literature review

Reasonably, a sustainable enterprise aims to protect nature and human and ecological health without sacrificing economic efficiency, innovations and business improvements. Thus, the key features for the specification of a sustainable process involve profitability, controllability, flexibility, reliability, and product quality satisfaction, safety, and environmental inducements (Kuhlman and Farrington, 2010). In general, a cost-effective and profitable process is defined based on the capability of the system to generate profit. Controllability is known as the ability of a system to retain desired outputs variables in specific bounds by changing available manipulate variables in spite of external/internal disruptions. In view of that, using a flexible process that can maintain and fulfill all significant constraints such as safety and environmental incentives under varying operating conditions plays a vital role in the success of the process. Another key factor is reliability which refers to the dependability of the system and probability of the failure of a system or component to function under stated conditions for the process lifecycle.

Over the past decade, there has been a dramatic increase in the development of multi-faceted approaches for the integration of multiple aspects, in particular, integration of design and control. Additionally, recent technological and computational advances have empowered the development of efficient solution strategies. Hence, a large and growing body of the current literature in this field has attempted to propose novel methods that resolve some unanswered and challenging questions in the field. There have been a few reviews that have classified the contributions in this area, see e.g. (Burnak et al., 2019b; Ricardez-Sandoval et al., 2009a; Sakizlis et al., 2004; Sharifzadeh, 2013; Vega et al., 2014a; Yuan et al., 2012). There are advantages but also significant challenges in promoting the integration of design and control strategies. Every solution strategy holds a number of features that have been proposed to tackle specific challenges of the subject in a certain way. This chapter presents the main challenges in simultaneous design and control along with some of the solution techniques which have been published in the literature. While this chapter provides a brief review of the subject, the main goal is to identify the challenges that are currently being

faced in this area. The discussion and literature review of this chapter has been published in (Rafiei and Ricardez-Sandoval, 2020a).

The chapter initially presents a general problem statement for the integration of design and control, followed by a discussion of the main challenges and proposed remedies in the literature (Section 2.2). Current applications of an integrated scheme are presented in Section 2.3.

2.1 Problem statement

The integration of design and control problem can be conceptually formulated as a mixed-integer nonlinear dynamic optimization (MIDO) formulation in which the design and control parameters are the key decision variables, i.e.

$$\min_{\boldsymbol{\eta}(t),\boldsymbol{\gamma}(t),\boldsymbol{u}(t)} \Theta = \Theta^{dyn}\left(\dot{\boldsymbol{x}}(t),\boldsymbol{x}(t),\boldsymbol{y}(t),\boldsymbol{\eta}(t),\boldsymbol{\varsigma}(t),\boldsymbol{u}(t),\boldsymbol{d}(t),\boldsymbol{\zeta},t\right) \tag{2-1}$$

Subject to:

$$F(\dot{\boldsymbol{x}}(t),\boldsymbol{x}(t),\boldsymbol{y}(t),\boldsymbol{\eta}(t),\boldsymbol{\varsigma}(t),\boldsymbol{u}(t),\boldsymbol{d}(t),\boldsymbol{\zeta},t) = 0$$
$$F_0(\dot{\boldsymbol{x}}(t_0),\boldsymbol{x}(t_0),\boldsymbol{y}(t_0),\boldsymbol{\eta}(t_0),\boldsymbol{\varsigma}(t_0),\boldsymbol{u}(t_0),\boldsymbol{d}(t_0),\boldsymbol{\zeta},t_0) = 0$$
$$h(\dot{\boldsymbol{x}}(t),\boldsymbol{x}(t),\boldsymbol{y}(t),\boldsymbol{\eta}(t),\boldsymbol{\varsigma}(t),\boldsymbol{u}(t),\boldsymbol{d}(t),\boldsymbol{\zeta},t) = 0$$
$$g(\dot{\boldsymbol{x}}(t),\boldsymbol{x}(t),\boldsymbol{y}(t),\boldsymbol{\eta}(t),\boldsymbol{\varsigma}(t),\boldsymbol{u}(t),\boldsymbol{d}(t),\boldsymbol{\zeta},t) \leq 0$$
$$\boldsymbol{\eta} \in [\boldsymbol{\eta}^L,\boldsymbol{\eta}^U]$$
$$\boldsymbol{u} \in [\boldsymbol{u}^L,\boldsymbol{u}^U]$$
$$\boldsymbol{\varsigma} \in \{\varsigma_1,\dots,\varsigma_N\}$$
$$t \in (0,t_f]$$

where F represent the system of differential-algebraic equations (DAEs) with their initial conditions F_0; h and g are equality and inequality constraints. The DAE model represents the essential aspects of the process including material and energy balances, transport phenomena, thermodynamics, chemical kinetics, equilibrium relations, logical constraints, and other physical property relationships. In addition to the fundamental mathematical model, other key features and relations particular to the system such as the product qualifications and demands, geometry considerations and operational limitations can be considered as equality and inequality constraints (h and g). $\boldsymbol{x},\dot{\boldsymbol{x}} \in \mathbb{R}^{n_x}$ are system's states and their differentials that

are functions of time (t); $\boldsymbol{y} \in \mathbb{R}^{n_y}$ are algebraic variables. Through this study, $\boldsymbol{\eta}$ is a vector of continuous design variables such as equipment sizes and continuous operating conditions that can take different values at different time intervals, e.g. product quality set-points. On the other hand, $\boldsymbol{u}$ are time-varying control variables, e.g. manipulated variables that can be used for control. $\boldsymbol{\varsigma}$ represents integer decision variables including the choice and sequencing of process units or the control structure selection. These continuous and discrete decision variables can be time-invariant or time-varying, e.g. they can take on different values for different time periods. $\boldsymbol{d}$ represents time-dependent disturbances and $\boldsymbol{\zeta}$ is a vector containing uncertain parameters. Deviations from the steady-state conditions are most likely due to the time-invariant or rather slowly time-varying uncertainties, process time-varying disturbances, and transition between different operating modes. The deviations can be originated from different sources, including imperfect knowledge of the behaviour of the system, raw material impurities, equipment failure, measurement error, and production target fluctuations. Not only is the aim of simultaneous design and control to identify an optimal process design but also to maintain an acceptable level of operation in the presence of parameter uncertainty and disturbances. Representation of uncertainties and corresponding recognition enables decision-makers to account for possible undesirable scenarios that may occur during operation and reduce process variability. Consideration of uncertainty and disturbances is one of the challenges of the field. Further thoughts on this challenge are provided in Section 2.2.1.

2.2 Challenges

Typically, simultaneous design and control is an optimization-based approach that carries all the challenges associated with mixed-integer nonlinear programming (MINLP) and mixed-integer dynamic optimization (MIDO). There is no generally accepted methodology that covers all the aspects of a given problem and that can explicitly solve Problem (2-1). However, academic practitioners have attempted to resolve a few obstacles while performing integration of design and control. The challenges in this field may be classified as follows: a) uncertainty and disturbances, b) multiple objectives, c) problem size inflation, d) structural

(integer) decision variables, f) local vs. global optimality, and e) incorporation of advanced control strategies.

The available techniques were originally classified into three main categories: controllability index-based approaches, dynamic optimization, and robust-based approaches (Ricardez-Sandoval et al., 2009a). Later on, Yuan et al. (2012) added two other categories to the previous classifications: embedded control optimizations and black-box optimization approaches. An objective of the current study is to identify the most common challenges in the integration of design and control and provide a summary of methodologies and their contributions to address the challenges in this subject.

2.2.1 Uncertainty and disturbances

Uncertainty can be classified into four categories (Pistikopoulos, 1995):

I. Model inherent uncertainty; e.g. physical properties.
II. Process inherent uncertainty; e.g. flowrate fluctuations.
III. External uncertainty; e.g. product demand, price, and environmental incentives.
IV. Discrete uncertainty; e.g. equipment availability.

In chemical engineering applications, all types of uncertainties may occur. Any kind of model mismatch, simplification, linearization, or parametric uncertainty may lead to imprecise model predictions. Process disturbances are the changes in the input variables that affect the output of the process and are often referred to as external perturbations that are typically time-dependent. Therefore, the optimal solution obtained from the nominal condition can become infeasible or sub-optimal due to these deviations. A sensible description of the uncertainties and disturbances enables the integrated methodologies to remain feasible in the presence of perturbations. Handling uncertainty becomes more crucial when constraint violations raise safety or environmental concerns. In order to incorporate the uncertainty into the process models, multiple techniques have been introduced in the literature.

Uncertainty quantification techniques aim to assess process variability. In general, uncertainty quantification is graded in terms of deterministic (definite a finite number of scenarios) and stochastic (uncertainty is treated as random variables). In the deterministic approaches, the occurrence of the uncertainty and process disturbances are limited to pre-defined finite situations (i.e. scenarios) in which the realization of each perturbation/uncertainty are assumed to be known *a priori*. The multi-scenario approach is one of the most widely used methods for handling uncertainty and disturbances. Multi-scenario optimization is a tool for semi-infinite problems that need to operate under a variety of different conditions (Laird and Biegler, 2006). Most of the contributions in the simultaneous design and control mainly focus on this type of uncertainty description. The majority of the robust approaches are developed for the deterministic approaches which could be too limiting in practice since the specific occurrence of the uncertainty and disturbances are assumed to be perfectly known *a priori*. Therefore, there is a need for a more realistic and efficient representation of uncertainties and process disturbances.

One of the open-ended challenges in the field is the specification of process designs that can tolerate stochastic descriptions with probability distribution functions of uncertain parameters and disturbances. In stochastic modeling, probability distributions of the process outputs are estimated in the presence of uncertainties. Uncertainty is often introduced assuming random realizations of the uncertain parameters, which are typically estimated from observations based on historical data or process heuristics. Stochastic optimization is a tool to deal with the inherent system noise and probabilistic-based uncertainties and disturbances. In general, excessive function evaluations are required by the stochastic methods, which make them highly expensive. Also, the volume of the search region grows rapidly as the dimension of the uncertainty/disturbance set grows, which also limits the application of these methods. Challenges associated with stochastic programming makes the approach intractable for large-scale systems. A few researchers have implemented a stochastic optimization approach with embedded control that adaptively optimizes control choices for a given design (Malcolm et al., 2007; Moon et al., 2011). A number of studies have performed a worst-case variability distribution analysis for simultaneous design and control under random

realizations in the disturbances. In the latter studies, uncertainty propagation is performed using Monte Carlo sampling technique (Bahakim and Ricardez-Sandoval, 2014; Koller et al., 2018; Rafiei-Shishavan et al., 2017; Rafiei and Ricardez-Sandoval, 2018; Ricardez-Sandoval, 2012; Valdez-Navarro and Ricardez-Sandoval, 2019a). Meeuse and Tousain (2002) defined a measure to assess the relationship between design and a closed-loop performance in the presence of stochastic disturbances. In another study, a Gaussian process model has been trained in an iterative manner to represent the uncertainty as the input to the simultaneous design and control framework (Chan and Chen, 2017). Washington and Swartz (2014) proposed a parallel computing approach for dynamic optimization using a multiple shooting of process under stochastic uncertainty through a set of possible parameter scenarios based on a discrete probability distribution. Vega et al. (2014b, 2014a) used controllability indices to translate integrated design and control into MINLP problems for different uncertainty sources, and solved the mathematical problem using genetic algorithms. It is worthy of note that some stochastic programming approaches such as random search, stochastic approximation, and genetic algorithms have the potential to achieve the global optimal solution, which is highly desired but the required computational effort is still excessive even for offline design optimizations (Gentle et al., 2012). Global optimization is still an open challenge that requires further developments. This subject is further discussed in Section 2.2.5.

Robust approaches have been employed to deal with uncertainty and other sources of unknown parameters in the system. The maximum process variability aims to search for the worst-case scenario where the largest violation of the constraints occurs; then, the system is optimized in a way to deal with that critical (worst-case) condition. In previous studies, robust control approaches on a basis of a representative nominal linear model have been implemented to assess the effects of model uncertainty and nonlinearity with respect to the nominal model (Chawankul et al., 2007, 2005). Robust control tools borrowed from Lyapunov theory and structured singular value analysis have also been used to develop metrics to identify the worst-case process variability, process feasibility, and stability (Ricardez-Sandoval et al., 2009b, 2009c, 2008). In addition, critical realizations in the disturbances can be estimated from structured singular value and then

combined with a simulation-based calculation of the responses to that worst disturbance to identify the worst-case condition; this method has been referred to as the hybrid worst-case approach (Ricardez-Sandoval et al., 2011, 2010). In an iterative approach, the amount of back-off required to achieve dynamic feasibility is calculated under the worst-case (maximum) deviation in the cost function and process constraints (Mehta and Ricardez-Sandoval, 2016; Rafiei-Shishavan et al., 2017). Despite these efforts, it has been realized that such robust approaches tend to be highly conservative since the worst-case scenario might be unlikely to occur during operation. This problem becomes strictly critical in the presence of uncertainties with large domains. Accordingly, methods have been recently proposed to achieve robustness to a user-defined level of process variability due to stochastic realizations. Statistical quantification of the uncertainty provides the flexibility to assign different levels of satisfaction to each constraint depending on their relevance or significance. Therefore, a degree of freedom is authorized by the decision-maker to reduce the conservatism in the integrated solutions (Koller et al., 2018; Rafiei-Shishavan and Ricardez-Sandoval, 2017; Rafiei and Ricardez-Sandoval, 2018). In summary, in the simultaneous design and control framework, companies aim to have a prescription against potential extreme situations that may put in risk the operation and or create an undesirable event, e.g. safety hazard. However, those extreme conditions might not happen very often and the corresponding arrangements oblige additional financial burden on the overall cost. While some constraints must be ensured at a high probability level, e.g. safety constraints, others may not be critical, e.g. levels in storage tanks. Full compliance of the process constraints under the worst-case scenario in the disturbances and uncertain parameters may result in overly conservative and expensive designs. Therefore, to reduce redundancy, it is essential to select a level of appropriate precautions while maintaining acceptable levels of satisfaction for the process goals and constraints.

2.2.2 Multiple objectives

Decisions made at the design stage according to the steady-state economics often conflict with those needed to maximize the dynamic controllability. For example, for a heat exchanger design, the smaller the heat-transfer area, the lower the steady-state economics but more aggressive control actions would be required

thus negatively affecting process performance, and eventually the operating costs. Accordingly, to take into account the trade-off between the conflicting goals of the process, a multi-objective framework can be applied which systematically optimizes a collection of objective functions. An index is required to assess the contribution of the controllability aspects into the overall profitability of the process. Therefore, controllability indexes are used to construct the link between process economics and process performance to investigate the interactions between process design and control goals. Taking these interactions into account enable designers to seek for conditions in which the system has the ability to reject process variability due to uncertainties and/or disturbances in an optimal fashion. Thus, one of the resolutions for the integration of design and control is to introduce the controllability of the system as one of the objectives in a multi-objective framework. Some controllability and flexibility metrics have been introduced as objectives or constraints within the simultaneous design and control optimization formulation. Relative gain array (Alhammadi and Romagnoli, 2004; Luyben and Floudas, 1994a), singular value decomposition (Palazoglu and Arkun, 1986), integral of squared error (Lenhoff and Morari, 1982), resilience index and condition number (Nguyen et al., 1988) have been used to quantify the dynamic performance. Although the calculation of the controllability indexes is straightforward, the main drawback is the lack of a clear and direct connection between the process economics and process controllability, i.e. the allocation of an economic cost to the process control strategy. In addition, most of the existing methods made use of linear models to assess process controllability, which restricts the accuracy of the methods for nonlinear constrained large-scale systems. Table 2-1 summarizes the approaches that carry out the multi-objective function approach for simultaneous design and control.

Table 2-1: Indicative list, multi-objective optimization approach

Authors	Contribution
(Lenhoff and Morari, 1982)	Bounding technique based on the Lagrangian theory
(Palazoglu and Arkun, 1986)	Robustness indices are used as the operability indicators appeared in the constraints that result in a semi-infinite programming problem
(Luyben and Floudas, 1994a, 1994b)	Open-loop controllability measures were used to translate a superstructure of design alternatives into a multi-objective (MINLP) problem
(Meeuse and Tousain, 2002)	Relative Gain Array (RGA) and singular value decomposition-based indices are employed in a multi-objective optimization method that provides clear insight for the trade-off between closed-loop variance and economics
(Blanco and Bandoni, 2003)	Dynamic convergence and stability were analyzed in an eigenvalue optimization framework
(Alhammadi and Romagnoli, 2004; Luyben, 1992)	RGA and condition number are used to indicate the pairing process between the variables and ease of control, respectively
(Asteasuain et al., 2006)	off-spec polymer and transition time are minimized along with capital cost during grade changeover between grades in the styrene polymerization process
(Sharifzadeh and Thornhill, 2013, 2012)	A multi-objective function is considered that is based on the assumption of perfect control and inversion of the process model
(Bernal et al., 2018)	Set-point tracking performance and economic costs are balances based on an offline utopia tracking procedure

Sustainability consists of numerous features, e.g. process economics, performance, flexibility, reliability, safety, and environmental impacts. Several metrics have been defined to represent those sustainability features. Some of the factors which can be used to quantify the environmental concerns are human toxicity potential by ingestion (HTPI), global warming potential (GWP), human toxicity potential by exposure (HTPE) (Kalakul et al., 2014). Figure 2-1 shows a schematic of the key objectives often pursued in optimal and sustainable process designs. As depicted in the figure, multiple aspects of the process are correlated, even if they do not seem correlated at first glance. Changes in one aspect can either directly or indirectly affect the remaining features of the process. For example, poor controllability of a chemical plant might lead to lower product qualities and thus higher utility and waste management costs as well as extreme environmental concerns. Accordingly, to design a sustainable process, further consideration of correlated factors is essential. The integration of multiple aspects of the process offers greater opportunities to improve

the process in terms of satisfying process economics, process operating goals and environmental criteria. The sustainability metrics and lifecycle assessment factors can be considered to allocate targets for the process in terms of the objective functions and constraints in a multi-objective framework. Several studies that have simultaneously determined economic operation and environmental criteria using sustainability metrics along with the operational aspects of the process have been reported (Li et al., 2009; Wang et al., 2013).

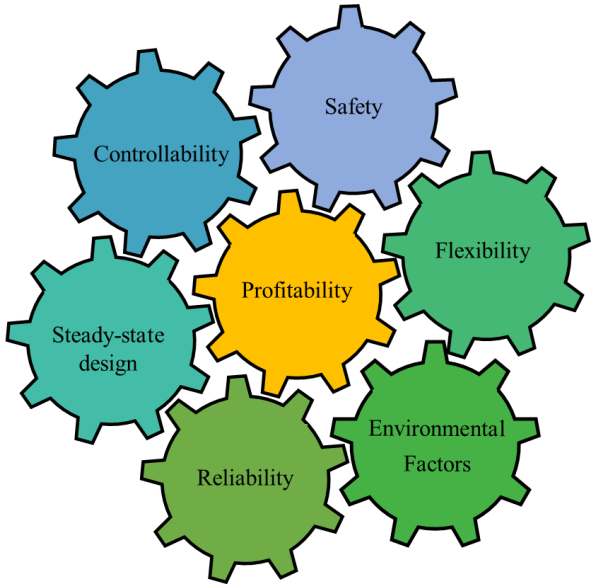

Figure 2-1: Interconnectivity of the multiple objectives

For a multi-objective optimization, there would be a set of solutions in which it is impossible to find a better outcome unless at least one individual or preference criterion worsens; this is known as the Pareto optimal solutions. The task is to systematically quantify the trade-offs in satisfying the different objectives and choose the appropriate Pareto solution. Ranking the objectives is a challenging task since the conflicting objectives of design and control performance must be balanced to ensure both steady-state economics and dynamic feasibility. Often, preference information is limited or simply is not available, particularly for highly interconnected systems. Moreover, the vague connection fails to detect systematically the importance of the objectives and complex preference information. Three major categories of multi-objective programming based on the decision-maker articulation are methods with *a priori* articulation of

preferences, *a posteriori* articulation of preferences, and with no articulation of preferences (Marler and Arora, 2004). In *a priori* articulation methods, the user specifies the preferences only in terms of objective functions; however, in the methods with *a posteriori* articulation, the potential solutions are available for the user to decide a preference. One of the most well-known classical methods for the multi-objective optimization framework is the weighted sum method in which all objective functions are combined to form a single function (Marler and Arora, 2004). However, the method is insufficient in the case of a highly correlated system due to the existence of constant weights or non-convex Pareto optimal solutions. Further discussions of the deficiencies of common multi-objective methods can be found elsewhere (Marler and Arora, 2004).

For the purpose of integrated approaches, adopting the weights becomes even more challenging when additional aspects need to be included in the problem such as sustainability, environmental and safety indexes. Alhammadi and Romagnoli (2004) proposed a methodology that incorporates economics, environmental, heat integration and operational considerations within a multi-objective optimization framework. Those authors implemented the proposed methodology on a Vinyl Chloride Monomer plant. The weights are usually selected from *a priori* trial-and-error simulations or from process heuristics. Therefore, there is a need to use systematic and practical multi-objective approaches that rely on intuitive weights. Accordingly, Luyben (1992) used a method with no articulation of preference to avoid assigning arbitrary weights. The authors utilized the trade-off information from the Pareto optimal solution using partial derivatives of a utility function that relates the various objectives in an interactive iterative approach. Bernal et al. (2018) employed the utopia point, which is an infeasible point that minimizes all the individual objectives of the multi-objective problem independently. Those authors aimed to find the closest optimal, feasible solution to the utopia point for the optimal design and control of a catalytic distillation column.

In general, most of the multi-objective solution strategies are sufficient for relatively small-scale problems; yet, the solutions might become intractable for a large-scale problem involving multiple objectives and a significantly large number of decision variables. This caveat with the complex system arises since the

integration of multiple aspects of the process mostly results in compound formulations for the integrated problems. In addition to the challenges regarding the efficiency of the multi-objective framework for integrated approaches, the inclusion of integer decision variables imposes another limitation to the multi-objective approaches. Although there are a few contributions that considered integer decision variables for integrated design and control in a multi-objective framework (Gebreslassie et al., 2012; Luyben and Floudas, 1994a, 1992), most of the current methods involving multi-objective optimization have been developed for formulations that only consider continuous variables. In the existence of the discrete variables, the feasible set is no longer convex. Therefore, the complexity of the multi-objective optimization problem increases and may become nearly intractable for large-scale applications. The mixed-integer multi-objective programming approaches in the presences of uncertainty is a challenging task and still remains as an open challenge in this area. A review of the methods devoted to multi-objective mixed-integer programming can be found elsewhere (Alves and Clímaco, 2007).

2.2.3 Problem size inflation

The integration of design and control is a complex problem by nature since it aims to account for conflicting aspects of the process. Generally, solution strategies require the need to specify a model that describes the dynamic behaviour of the process. As such, the size and complexity of the problem depend directly on the process model used in the analysis and the assumptions made while developing the model, e.g. model structure error, parameter uncertainty, external perturbations, etc. To reduce the complexity in the analysis, practitioners have therefore proposed multiple approaches to deal with the subject such as employing surrogate models and decomposition techniques.

2.2.3.1 Surrogate models

Process systems engineering consistently seeks efficient techniques in computational modeling and optimization to introduce novel solutions for highly complex problems. The performance of the systems can be presented using highly sophisticated mathematical models; however, in a broad view, sophisticated mechanistic models are not suitable, particularly when these high-fidelity models result in complex

formulations with high computational demands, e.g. computational fluid dynamic (CFD) models. Such high computational demands are commonly unaffordable using conventional computational resources. Furthermore, the parameters of high-fidelity models are often restricted to within a certain region. Instead of using high fidelity models that would require an intensive computational effort, surrogate models are introduced as a data-driven tool to develop a correlation between the input-output performance of the system and present approximate models to alleviate the burden of sophisticated replicas. By using low-order (surrogate) models, engineers attempt to estimate a fair approximation of the process behaviour with an acceptable level of accuracy. Several taxonomies for surrogate models have been developed (Bhosekar and Ierapetritou, 2018). They can be classified into non-interpolating and interpolating methods. Non-interpolating methods aim to minimize the sum of squared errors such as quadratic polynomials and other regression models whereas interpolating methods pass through all sample data such as radial basis functions and kriging models (Jones, 2001). Recently, artificial intelligence (AI) techniques such as the artificial neural network (ANN) has also been employed to approximate functions from sample data. Surrogate models are extremely convenient to reduce the complexity and computational demands of the problem when multiple evaluations of the cost and constraint functions are required. The models can be widely used in large-scale problems, stochastic and global optimization programming. Efficient, highly predictive surrogate models are key to predict systems' behaviour accurately with a fair amount of computational effort. The appropriate surrogate model must be decided based on the application and prescribed features. For example, plant behaviour can be captured using power series expansions (PSEs) as analytical representations that replace the nonlinear complex model of the system. PSE functions have been used as a basis to develop new approaches for the optimal design and control of dynamic systems under uncertainty. Previous works have used this modeling tool for optimal process improvement under uncertainty (Bahakim et al., 2014; Bahakim and Ricardez-Sandoval, 2015; Rasoulian and Ricardez-Sandoval, 2016, 2015, 2014). Model-based approaches have also been proposed where the nonlinear behaviour of the system is approximated using suitable model structures (Chawankul et al., 2007; Gerhard et al., 2008, 2005; Ricardez-Sandoval et al., 2008; Sanchez-Sanchez and Ricardez-Sandoval, 2013a; Trainor et al., 2013). Malcolm et

al. (2007) replaced the full nonlinear system equations with a simpler adaptive state-space to compute optimal control actions in an embedded control optimization procedure. Moon et al. (2011) extended the linearized embedded control optimization framework to a plantwide flowsheet and showed the effective complexity reduction of the method of integrating design and control. In a stepwise procedure, dynamic high fidelity models of the process are represented using approximation and model reduction techniques for simultaneous integration of design, scheduling, and control (Burnak et al., 2019a; Diangelakis et al., 2017; Pistikopoulos et al., 2015). Generally, it is essential to have a clear definition of the goals of the model to select a legitimate set of variables as inputs and outputs. The main challenge in the selection of surrogate models is the determination of the accuracy of the replicas in the corresponding region of the input space. A single surrogate model might fail to approximate a complicated function, especially when the original system features different responses depending on the input region. A common practice is to build several surrogate models on a similar learning basis to improve model prediction (Bettebghor et al., 2011). Likewise, discontinuous and derivative-discontinuous of the objective and constraint functions occurs quite often in complex dynamic models. If adequate information of the system is available, it may be possible to prevent discontinuities by dividing the input space into several continuous regions. The issue of discontinuity is the central downside of a surrogate model facing the optimization problem. Bhosekar and Ierapetritou (2018) classified the surrogate models with respect to the applications into three categories: prediction and modeling, derivative-free optimization (DFO), and feasibility analysis. The difference between available surrogate methods and advances in each section are discussed in that study. Surrogate models are widely used in engineering problems and global optimization techniques (Bhosekar and Ierapetritou, 2018; Forrester and Keane, 2009; Viana et al., 2013). Those models provide inexpensive evaluations of the functions and the gradients. Surrogate-based representation of the model is the key strategy to represent a highly nonlinear formulation in a certain way that it ensures the solution is attainable and the effort for obtaining the model is acceptable. Surrogate-based methods are extremely popular in the integrated optimization framework. The main point is to select the accuracy, the type, and the validity regions in an efficient way for every application. On the other hand, surrogate models may not provide

good estimations for the entire operating region and should be implemented cautiously. The faulty estimation of the functions and derivatives coming from such models may drive the integration of design and control problem to an infeasible condition. To overcome the latter, instead of defining a model for the entire process domain, the behaviour of the system is examined using piecewise surrogate models. For instance, the behaviour of the system is examined using piecewise PSE models in an iterative manner in which the nominal condition is updated as the iterative procedure converges to an optimal solution (Rafiei and Ricardez-Sandoval, 2018).

2.2.3.2 Decomposition approaches

The size of the original integration of design and control problem imposes a limitation on the potential solution strategies that can be implemented. The main idea in decomposition approaches is to partition the problem into a set of interconnected sub-problems that can be handled with inexpensive procedures. The susceptibility of such approaches stems from the complexity to maintain adequate information flow between the sub-problems of the optimization framework. In order to compensate for the limited information flow, decomposing techniques often succeed gradually, i.e. in an iterative manner. Abd Hamid et al. (2010) decomposed the simultaneous design and control problem into four sub-problems and solved the hierarchy of pre-analysis, design analysis, controller design analysis, and the final selection and verification to satisfy design, control and cost criteria. Some practitioners employed the decomposition-based solution approach to integrated design and control for binary and multiple element reactive distillation and a cyclic distillation processes in a systematic hierarchical manner (Andersen et al., 2018; Mansouri et al., 2016a, 2016b). Diangelakis et al., (2017) and Pistikopoulos et al., (2015) used multi-parametric programming to solve the integrated design and control as a function of one or multiple parameters. By decomposing the original system, those last studies built a foundation to explore the interactions between design and control. Most recently, the decomposition approach is used to develop offline maps of optimal receding horizon policies that allow a direct implementation in a MIDO formulation for process design optimization (Burnak et al., 2019a). To summarize, decomposition methods aim to

reduce large-scale problems to easier-to-solve optimization problems. The key is how to separate the problem and how to maintain information between those individuals without losing key information between the sub-problems.

As discussed in Section 2.2.3, several surrogate models and decomposition approaches have been proposed by academic practitioners to reduce computational costs associated with simultaneous design and control. As the integration is performed offline, the computational costs might not seem like a limiting barrier to most approaches. However, if the integrated approach is implemented on a relatively large-scale application, the computational demands might become intractable even for high-performance computers. For highly-nonlinear large-scale problems, global or even local optimal solutions might be unattainable. For that reason, attempts using surrogate models and decomposition approaches can be developed with the aim to reduce the computational burden of the framework and propose practical methods that can be successfully implemented in an industrial setting.

2.2.4 Structural (integer) decision variables

Equipment sizes, operating conditions, and controller tuning parameters are examples of continuous variables that must be specified while performing simultaneous design and control. In addition, integer variables associated with the topology of the process and the control scheme, e.g. control structure selection and the number of trays and feed location in a distillation column, are key integer (structural) decisions. Considering integer decision variables along with the continuous variables provide much greater flexibility for improving the economics and performance of a large variety of problems. However, discontinuity of the derivatives due to the presence of integer variables makes it an MINLP, thus increases the problem's complexity. Several algorithms have been proposed to solve MINLPs such as branch and bound algorithm (BB) (Dakin, 1965; Gupta and Ravindran, 1985), generalized benders decomposition (GBD) (Geoffrion, 1972), outer approximation (OA) (Duran and Grossmann, 1986; Viswanathan and Grossmann, 1990). A general classification of the methods can be found elsewhere (Biegler and Grossmann, 2004). As shown in Equation (2-1), taking into account the discrete decision variables for the integration of design and control

formulates a MIDO. Normally, MIDO problems can be approximated by MINLPs using advanced discretization techniques. The resulting MINLP problems can then be handled with an algorithm that suits the problem under consideration. Note that these MINLP methods have been mainly developed for deterministic approaches. The main limitation of the currently available methods is their shortage to deal with uncertainties and disturbances that follow a stochastic description. Adding stochastic considerations increases drastically the problem's complexity. Thus, the computational effort for process optimization under stochastic uncertainty descriptions may become prohibitive and may lead to intractable MIDO solutions for large-scale applications. Additionally, MIDO and NLP problems are often sensitive to initialization. Lack of an educated initial guess may also result in failure to achieve convergence. Table 2-2 provides a list of studies that have addressed the integration of design and control using MINLP techniques.

Table 2-2: Prominent works that have employed MINLP for integration of design and control

Authors	Contributions
(Papalexandri and Pistikopoulos, 1994a, 1994b)	A variable gain matrix is introduced to explore controllability and flexibility HENs for the purpose of synthesis and/or retrofit without decomposition
(Mohideen et al., 1997, 1996a, 1996b)	Robust stability criteria are considered to maintain desired dynamic characteristics in an MINLP formulation
(Bansal et al., 2003)	A decomposition approach to primal, dynamic optimization and master, mixed-integer linear programming sub-problems that doesn't require the solution of the adjoint intermediate master problem
(Asteasuain et al., 2006)	A multi-objective mixed-integer dynamic optimization approach was performed on grade transition in styrene polymerization
(Flores-Tlacuahuac and Biegler, 2007)	A robust solution for a MIDO using a simultaneous dynamic optimization approach
(Nie et al., 2015)	A discrete-time formulation optimization approach for the integration of production scheduling and dynamic process operation using Generalized Benders Decomposition (GBD) algorithm to solve the resulting large nonconvex mixed-integer nonlinear program
(Trainor et al., 2013)	Robust feasibility and stability analyses are formulated as convex mathematical problems and incorporated within the methodology to avoid the solution of MINLP for dynamic feasibility and stability evaluation
(Sanchez-Sanchez and Ricardez-Sandoval, 2013b)	Optimal process synthesis and control structure design are obtained using integrated dynamic flexibility and dynamic feasibility in a single optimization formulation
(Kookos and Perkins, 2016, 2001)	A bounding scheme to successively reduce the size of the search region to select an economic control structure using MINLP
(Meidanshahi and Adams, 2016)	A built-in optimization package of gPROMS is used to solve the MIDO via the deterministic outer approximation method for a semi-continuous distillation system
(Burnak et al., 2019a; Diangelakis et al., 2017; Diangelakis and Pistikopoulos, 2017)	A single prototype software system (PAROC framework) that uses multi-parametric programming for integrated design, control and scheduling

2.2.5 Local vs global optimality

Convexity is the curtail constraint for global optimality in most of the optimization approaches. In nonlinear programming (NLP), the global optimality of the local optimal point is satisfied under certain convexity assumptions (Tawarmalani and Sahinidis, 2004). Local solutions specify points that satisfy the objective function only within a neighborhood of the solution. Rigorous search methods are required to show that a particular local solution is also a global (Biegler, 2010). However, there has been significant progress in the field of global optimization solvers during the last decades. Global optimization methods are categorized

as deterministic and stochastic methods according to their convergence abilities. Kronqvist et al. (2019) presented a review of deterministic software for solving convex MINLPs.

There is a relatively small body of literature that is concerned with searching for global optimality in problems involving process integration. Nonconvex generalized Benders decomposition (NGBD) has been developed to solve simultaneous design and operation problems (Li et al., 2012, 2011b, 2011a). The performance of the proposed method has been compared to BARON (Tawarmalani and Sahinidis, 2004) and showed a more efficient convergence routine. Simultaneous scheduling and control of continuous processes (Chu and You, 2012) and batch processes (Chu and You, 2013) have been studied in a decomposed framework. The main disadvantage of the proposed method is that the resulting problem may lead to a large-scale problem, which might be computationally intractable. Several relaxation techniques have been proposed to reduce the complexity of the problem and being able to achieve global solutions within reasonable computational times. Further details regarding the reformulations and relaxation techniques of the global optimization approaches can be found elsewhere (Ruiz and Grossmann, 2017). Although global MINLP methods might seem promising in converging to the global optimal solution, the computation load remains unaffordable for complex integrated problems (Nie et al., 2015). Thus far, any firm conclusion cannot be drawn on the performance of solvers for nonconvex problems and for that kind of problems we still rely on local MINLP solvers; particularly for problems like that shown in Equation (2-1), which rely on functions that may depend on uncertainties and disturbances.

The stochastic global optimality solvers are usually incapable of handling equality and inequality constraints except when they represent the boundaries on the decision variables (Matallana et al., 2011). The application of the methods is still restricted on highly constrained problems and convergence cannot be guaranteed. Stochastic optimization techniques such as particle swarm optimization (Lu et al., 2010), genetic algorithm (Revollar et al., 2010), and tabu search-based algorithm (Exler et al., 2008; Schluter et al., 2009) have been used in the literature to obtain a global optimal solution for simultaneous design and control. The existence of a global optimum is beneficial in terms of giving insights into the best possible

performance of the system as a tool for the decision-making process. The estimation of a global solution enables decision-makers to measure how far the system operates from the optimum and design operating policies that can reduce that gap. Furthermore, such information helps to decrease the incidence of convergence to the suboptimal conditions.

NLP problems are usually sensitive to the initial guesses. In the absence of a feasible initial point, many of the currently available algorithms may fail to converge (Bajaj et al., 2018). A back-off approach is an appealing option where the steady-state optimal point is used to establish the economic incentive to improve the regulation of key process variables and maintain feasibility in the transient domain. There is a large number of published studies that consider ad hoc initial guesses, i.e. optimal steady-state designs, and proposed several methodologies to estimate how far the design must be placed from active dynamic path constraints. (Bahri et al., 1996, 1995; Figueroa et al., 1996; Kookos and Perkins, 2016, 2001; Narraway and Perkins, 1994, 1993; Perkins et al., 1989). To this regard, several methodologies have calculated back-off terms in a series of simple optimization problems that moved away in a systematic fashion from the optimal steady-state design to a new feasible operating condition (Rafiei-Shishavan et al., 2017; Rafiei-Shishavan and Ricardez-Sandoval, 2017; Rafiei and Ricardez-Sandoval, 2018). One limitation of this approach is that they rely on an optimal steady-state solution to initiate the search for the dynamically feasible condition. However, in the case of intrinsically dynamic processes (periodic systems), which do not have a steady-state condition, back-off approaches lose that key feature. Intrinsically dynamic processes such as periodic dynamic systems never reach a steady-state. The issue of intrinsically dynamic operations is discussed in (Swartz and Kawajiri, 2019). Transitions between different operating conditions need to be taken into account while optimizing such dynamics systems.

In summary, most of the available solvers have acceptable performance for smooth (convex) problems. Integrated framework results in complex formulations in particular for real-life applications. In order to guarantee convergence to a global optimum, the actual problems must often be simplified and reduced in size using multiple assumptions, e.g. surrogate models. Further algorithmic research and solver software

developments for non-convex systems are required to bring the promise of efficient global optimization closer to reality.

2.2.6 Incorporation of advanced control strategies

Advanced process control strategies have evolved over the past few decades. These strategies offer both economic improvement and process performance upgrades. Model predictive control (MPC) is an advanced multivariable optimization-based control algorithm that has been in use in chemical process industries over the last two decades. Consideration of the MPC into the simultaneous design and control was first articulated by Brengel and Seider (1992). Those authors evaluated the economic objectives, as well as controllability, within MPC algorithms in response to multiple disturbances. The use of MPC is expected to improve the performance of the designed system since the optimal control actions implemented in the plant are obtained from the solution of a constrained optimization problem. Furthermore, the ability of the MPC to handle the interactions and process constraints among the process variables may result in better optimal process designs than those obtained from decentralized control strategies. On the downside, advanced control schemes require solving an optimization problem online that increases the complexity of the integrated design framework (Sakizlis et al., 2003). In general, the key issues in the field are *a priori* stability and feasibility considerations for MPC. Thus, integration of design and control strategies should take these aspects into account to specify a stable and feasible process design that can efficiently operate in closed-loop. Sakizlis et al. (2003) incorporated MPC into a simultaneous process design and control problem. Those authors decomposed the problem into a control design primal problem with a linearized version of the process model and a control design master problem with the rigorous dynamic model. Chawankul et al. (2007) integrated the cost of variability and capital and operating costs into one objective function to the simultaneous calculation of the process design variables and the MPC tuning parameter. Francisco et al. (2011) used MPC to decide plant dimensions, control system parameters, and a steady-state condition. In another study, an iterative decomposition framework for the simultaneous process flowsheet and MPC design that includes dynamic flexibility and robust feasibility tests has been introduced (Sanchez-

Sanchez and Ricardez-Sandoval, 2013a). Moreover, Gutierrez et al. (2014) selected controller structure based on a communication cost term that penalizes pairings between the manipulated and the controlled variables. Both centralized and decentralized control strategies are considered through an MPC-based control superstructure. Multi-parametric MPC approach has been used for simultaneous consideration of design and control problems (Burnak et al., 2019a; Diangelakis and Pistikopoulos, 2017). In a different approach, Li et al. (2016) integrated an advanced control strategy with sustainability assessment tools to identify and assess the optimal process operation in terms of sustainability performance.

Based on the above, most of the applications presented in the literature have considered an internal linear model in the MPC framework. However, linear MPC formulation is limited since it is based on the linear approximations of nonlinear dynamics and path constraints, as opposed to Nonlinear MPC (NMPC) which relies on the nonlinear constraints and dynamics of the problem. Evidently, linear MPC results in a convex underlying optimization problem which guarantees the global solution at every time horizon. In contrast, the non-convexity of the optimization problem of NMPC formulation prevents such guarantees to be provided. To the authors' knowledge, the performance of NMPC for simulations design and control has yet to be attempted. It is still an open challenge since the non-convexity of the nonlinear problem will be added to the size of the integrated problem, which would obviously increase the problem's complexity and computational effort. A deeper investigation is needed to evaluate the pros and cons of the NMPC embedded in simultaneous design and control and fair comparison of the associated features and limitations such as computational costs.

2.3 Current applications

The complexity of the resulting problem is the main burden that prevents the implementation of the integrated approach on industrial-scale applications. Recent technological advances in computer science have facilitated the implementation of more advanced methodologies for industrial case studies. For most of the industrial applications, the process flowsheet is assumed to be known *a priori* when performing

simultaneous design and control; however, there is no guarantee that the process flowsheet is the best choice since the flowsheet synthesis and its effects on the optimality of the process are often not considered. Yuan et al. (2012) indicated that, if the process flowsheet synthesis is expected to be considered, heuristics can then be used to narrow down the selection of promising configurations. Obtaining a superstructure that involves the optimum flowsheet candidates is often considered as a non-trivial task. Besides, constructing a comprehensive superstructure for a large-scale industrial problem may become intractable as it adds a significant number of integer variables to the original optimization. In order to provide a systematic basis for the evaluation and optimization of synthesis alternatives, Papalexandri and Pistikopoulos (1996) proposed a generalized modeling framework based on fundamental mass/heat-transfer principles. Recently, there is a growing interest in process intensification (PI), which can be achieved through the integration of operations, functions, and phenomena with the aim to establish sustainable production levels in the industry (Lutze et al., 2010). Systematic phenomena based identification of flowsheet alternatives has also been presented using a decomposition-based solution approach (Babi et al., 2014; Lutze et al., 2013). More recently, phenomenological descriptions, mass and energy conservation, logical and thermodynamic relations, and operational restrictions were used to define an objective function and constraints within a single MINLP framework (Demirel et al., 2017). PI techniques are introduced to increase process efficiency and lower the process economics by reducing the required equipment and specifying an optimal flowsheet. This definition strictly complies with the targets aimed for integration of design and control. Tian et al., (2018) provided a comprehensive review of the development of various PI technologies with the focus on the separation, reaction, hybrid reaction/separation, and alternative energy sources. The operability of the proposed intensified processes is still an open question (Baldea, 2015; Dias and Ierapetritou, 2019; Tian et al., 2018; Tian and Pistikopoulos, 2019). As reported in the latter works, accounting simultaneously for operability, controllability, and safety aspects at the design stage are the main challenges in these conceptual designs. The solution for this issue is an opening to establish an integrated approach for promising flowsheet specified using PI techniques.

To the best of authors' knowledge, the application of simultaneous design and control methodologies on large-scale industrial processes is sparse. Indeed, the available methodologies applied multiple simplifying assumptions to make the problem tractable. The existing methods have been implemented either on an isolated unit operation, simple industrial case studies or as a retrofit option for a large-scale process instead of full design/flowsheet considerations. Combined heat and power (CHP) network (Diangelakis et al., 2016), production of vinyl chloride monomer (VCM) (Alhammadi and Romagnoli, 2004), and the widely known Tennessee Eastman process (Ricardez-Sandoval et al., 2011) are examples of industrial large-scale case studies for which simultaneous design and control have been considered. Despite significant achievements and numerous publications in the field, there is still a large gap between proposed theoretical methods and practical industrial applications. One of the reasons for this gap might be the lack of an industrial benchmark that could be used to examine the convenience of proposed methodologies for real-life applications. There is no generally accepted benchmark that includes the multi-facet characteristics needed for a comprehensive case study such as conflicting objectives, multiple sources of uncertainties with a known distribution, and operating mode transitions. The existence of a benchmark case study would enable academic and industrial practitioners to make a fair comparison of the proposed methods and gain insight into the limitations and features of each approach.

In summary, enterprise-wide sustainability involves aspects from molecular-scale design to macroscale facilities. Typically, these aspects are treated as independent sub-problems. Maintaining consistent information flow among the sub-problems in an integrated fashion provides additional opportunities in pursuing the ultimate goals of sustainable environmentally-friendly processes. Integration of design and control represents the core and foremost component of such an integrated approach. Simultaneous process design and control mostly results in the specification of a relatively complex and computationally intensive formulation, which can be conceptually formulated as a mixed-integer dynamic optimization problem. The size and complexity of the original integrated problem impose limitations on the potential solution strategies that can be implemented on large-scale industrial cases. In this chapter, the main challenges of the

integration of design and control were classified. There are still a few open questions and challenges in the field that require further investigation.

3 Basic back-off approach

As mentioned in Chapter 2, simultaneous design and control mostly results in NLP, MINLP or MIDO formulations. Those nonlinear programming problems are often sensitive to initialization. Lack of educated initial conditions may result in failure to achieve convergence to an optimal solution. A back-off approach is an attractive alternative that relies on steady-state economics to initiate the search for the optimal and dynamically feasible process design. Furthermore, in attempts to reduce the computational burden of the nonlinear programming PSE are used as the surrogate model for the proposed methodology.

A new back-off approach to those previously reported in the literature is presented for simultaneous design and control. The key idea is to combine PSE with the concept of the back-off approach to simultaneously specify the optimal design and control scheme that remains dynamically feasible under a given set of process disturbances and uncertainty in the parameters. The basic back-off methodology and results presented in this chapter have been published in Rafiei-Shishavan et al. (2017).

This chapter initially presents the idea of back-off followed by a discussion of the PSE models. The proposed basic methodology has been discussed in Section 3.3. The results of the implementation on a medium-scale case study are shown in Section 3.4.

3.1 Back-off approach

The idea of back-off was originally proposed by Perkins et al. (1989) and also discussed by Perkins (1989), i.e. steady-state optimization might be used to establish the economic incentive to improve regulation of key process variables in the transient domain. Narraway et al. (1991) formulated a combined steady-state/dynamic economic analysis in order to assess the economic performance under disturbances. Narraway and Perkins (1993) proposed an optimization framework that makes use of linear process models to calculate the required amount of back-off; that framework was later extended to consider nonlinear process models, which were used to estimate how far the design must be moved away from active

constraints (Narraway and Perkins, 1994). Dimitriadis and Pistikopoulos (1995) presented a unified approach for the quantification of dynamic feasibility and flexibility for optimal process design, which led to further development in this field. Bahri et al. (1996, 1995) developed a method for determining the essential open-loop back-off from a steady-state optimal point to ensure dynamic feasibility. A joint optimization-flexibility problem that can be solved in an iterative fashion at the steady-state was formulated. The proposed formulation involved a decomposition method that included two levels of optimization problems. The first optimization formulation aimed to search for the optimality of the system at the steady-state with flexibility for a fixed set of process disturbances. The second optimization formulation assesses the feasibility of the design identified in the previous stage using different disturbance profiles. Figueroa et al. (1996) extended the method proposed by Bahri et al. (1996, 1995) and provided a criterion to ensure the dynamic feasibility of the system, i.e. that study presented a joint dynamic optimization-flexibility analysis where the optimization of the design parameters and controllers tuning parameters were also considered in the analysis. Kookos and Perkins (2016, 2001) used the back-off approach for simultaneous process and control design. In their work, a sequence of combined configurations of design and control were solved using a bounding scheme to successively reduce the size of the search region. The main idea in those works was to progressively generate tighter upper and lower bounds on the optimal dynamically feasible design and control scheme. In addition to simultaneous design and control, the back-off concept has also been used for integration of control and scheduling (Valdez-Navarro and Ricardez-Sandoval, 2019a, 2019b) and integration of design, control, and scheduling (Koller et al., 2018).

Back-off terms ensure dynamic feasibility in spite of uncertainty especially in the case of safety and environmental constraints; however, they can be difficult to formulate and implement particularly for large-scale applications. The main challenge in the back-off methods is to calculate in a systematic fashion the amount of back-off required to accommodate the transient operation of the process. The back-off term can be imposed on constraints or optimization variables to compensate for transient behaviour. Different techniques have been employed to calculate the amount of back-off in the literature. Visser et al. (2000)

linearized both constraints and state-space models of the original optimization problem to calculate the back-off magnitude in constraints to compensate uncertainty. Diehl et al. (2006) employed a linearization technique of the uncertainty set based on constraint derivatives which lead to the amount of penalty term (back-off) for robust nonlinear optimization. Srinivasan et al. (2003) updated the initial back-off term in an iterative routine using state probability density function computed at the optimal solution. Alternately, a robust optimization formulation applied through the incorporation of back-off terms in the constraints was presented by Shi et al. (2016). In that work, the back-off terms were calculated from MC simulations.

Implementation of a new back-off method has been developed in the current research. In this work, the back-off amount was identified from a series of simple optimization problems. The optimum design obtained by recursive steps moving away from the optimal steady-state design to a new feasible operating condition that can accommodate pre-defined realizations in the uncertain parameters and time-dependent disturbances. The proposed back-off approach is taking into account the dynamic behaviour of the system caused by any kind of disruptions and estimates the amount of compensation with respect to the initial steady-state condition. Back-off terms are used to determine the required modifications to move the operating point away from the active constraints into the feasible region. Figure 3-1 illustrates the basic idea behind the proposed back-off approach. Figure 3-1(a) shows the optimal design point which is feasible at the steady-state condition. However, this point might violate constraints when transient changes are accounted in the analysis as schematically illustrated by a red dotted region in Figure 3-1(a). In order to maintain dynamic feasibility, the optimal steady-state design has to be moved away (back-off) to a new dynamically feasible operating region. Figure 3-1(b) shows the direction and the magnitude of back-off that is required to specify a new dynamic feasible operating point under process disturbances and parameter uncertainty. The key challenge in this method is to determine the magnitude of back-off required to accommodate the transient operation of the process in the presence of process disturbances and parameter uncertainty.

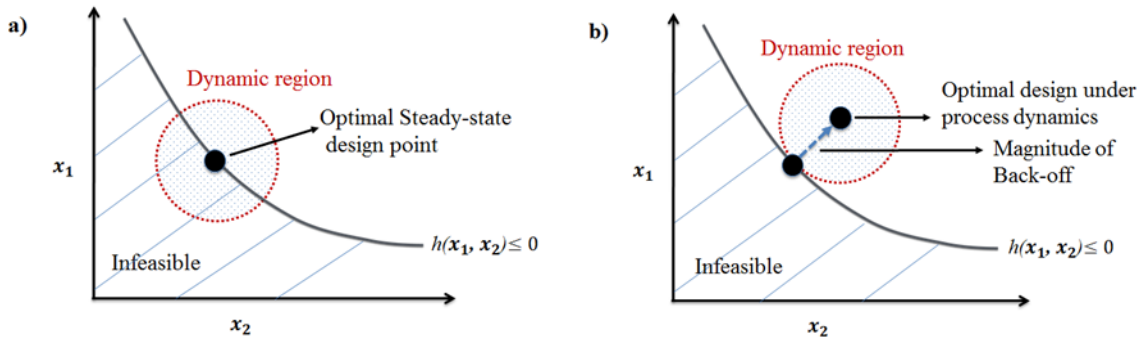

Figure 3-1: Idea of Back-off: a) dynamically infeasible steady-state design, b) Optimal feasible design under process dynamics

3.2 Power series expansion (PSE)

The simultaneous consideration of design and control results in an optimization problem as mentioned in Equation (2-1). In an attempt to reduce the computational burden of the nonlinear programming of the conceptual formulation (Equation 2-1), surrogate models are used in this study to represent the cost and constraint functions in the optimization problem. PSE is an analytical representation of a function as an infinite sum of expressions that are calculated based on the sensitivities, i.e. derivatives of the function in terms of its variables around a nominal condition. A complex function ($f(\chi)$) can be represented around χ_0 using PSE approximation as follows:

$$f(\chi) = f(\chi_0) + \sum_{l=1}^{\infty} \frac{1}{l!} \nabla^l f(\chi)^T|_{\chi_0} (\chi - \chi_0)^l \tag{3-1}$$

$\nabla^l f(\chi)$ is the l^{th} order gradient of the $f(\chi)$. Thus, model behaviour is quantified using a series expansion that replaces the nonlinear complex model of the system. The process constraints and the cost function are represented as PSE functions, which are explicitly defined in terms of the optimization variables at the vicinity of the worst-case scenario. The worst-case variability for each constraint and the cost function is evaluated from time-dependent realizations in the disturbances and time-invariant uncertain parameters. That is, the process model is simulated using the nominal condition defined by $\boldsymbol{\eta}_{nom}$ for all discrete realizations considered in the uncertain parameters $\boldsymbol{\zeta}$ using the pre-defined set of time-dependent

realizations in the disturbances $\boldsymbol{d}(t)$. Once the largest (worst-case) variability in the constraints has been identified, the time and the realization where the condition occurred are located, i.e. t_{wc} and ζ_j (see Figure 3-2). PSE representations for each constraint are only valid around a worst-case scenario in the optimization variables $\boldsymbol{\eta}$ and for each realization j considered for the uncertain parameters, i.e. ζ_j. Thus, s^{th} actual process constraint can be represented as a PSE constraint function as follows:

$$g_s(\boldsymbol{x},\boldsymbol{y},\boldsymbol{\eta},\boldsymbol{d},\boldsymbol{\zeta},t) \leq 0 \iff g_{s_{PSE}}(\boldsymbol{\eta})|_{t_{wc},\zeta_j} \leq 0 \tag{3-2}$$

$\boldsymbol{x} \in \mathbb{R}^{n_x}$ are system's states; $\boldsymbol{y} \in \mathbb{R}^{n_y}$ are algebraic variables. $\boldsymbol{\eta}$ is a vector of continuous design variables such as equipment sizes and continuous operating conditions, e.g. product quality set-points and control variables. $\boldsymbol{d}$ represents time-dependent disturbances and $\boldsymbol{\zeta}$ is a vector containing uncertain parameters. t_{wc} is used to denote the time that the largest (worst-case) variability in the process constraint g_s happens due to the time-varying disturbances.

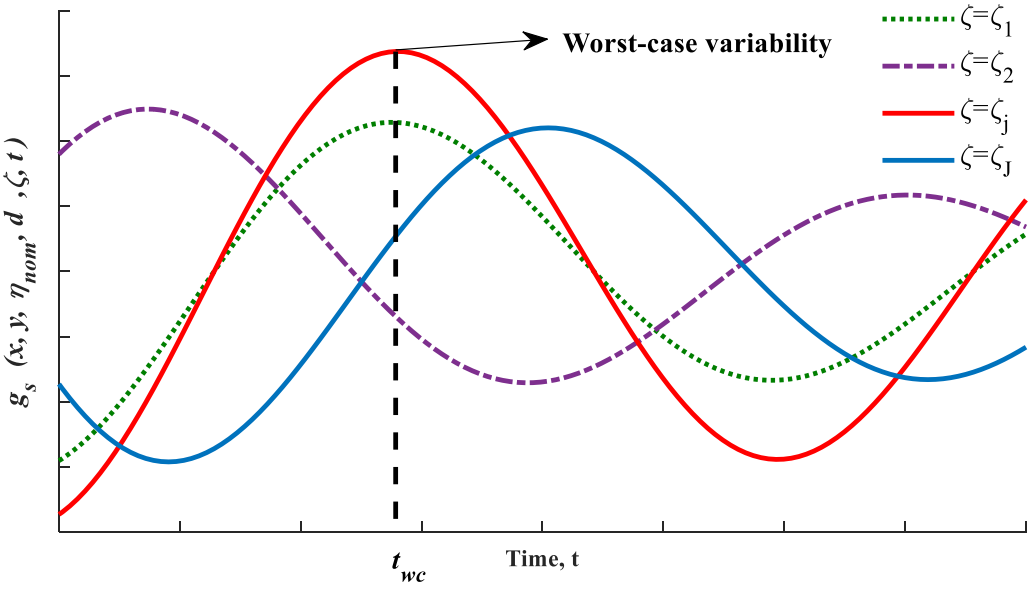

Figure 3-2: Worst-case variability point around which PSE functions are developed

Once the worst-case variability point is identified the expansions can be built around it. In order to compute the PSE, the gradients of the system are required. Accordingly, the PSE function of s^{th} inequality constraint is as follows:

$$g_{s_{PSE}}(\boldsymbol{\eta}) = g_s(\boldsymbol{\eta}_{nom})|_{t_{wc},\zeta_j} + \sum_{p=1}^{P} \left.\frac{\partial g_s}{\partial \eta_p}\right|_{t_{wc},\zeta_j} \left(\eta_p - \eta_{p_{nom}}\right) + \sum_{p=1}^{P} \frac{1}{2} \left.\frac{\partial^2 g_s}{\partial \eta_p^2}\right|_{t_{wc},\zeta_j} \left(\eta_p - \eta_{p_{nom}}\right)^2 + R_2(\boldsymbol{\eta}) \qquad (3\text{-}3)$$

Likewise, the PSE of the cost function can also be constructed. Note that Equation (3-3) can be expanded to higher-order approximations, which will improve the quality of the PSE approximation ($g_{s_{PSE}}$) at the expense of higher computational costs spent on calculating higher-order sensitivity terms. The error incurred in approximating a function by its n^{th}-order expansion, residual, is denoted by the function $R_n(\boldsymbol{\eta})$. The order of approximation is generally chosen depending on the degree of nonlinearity in the system, the number of optimization variables ($\boldsymbol{\eta}$), the desired accuracy of the results, and the budget available for estimation of the high-order sensitivity terms.

Sensitivities are required to construct the PSE functions in Equation (3-3). The sensitivities can be calculated either numerically or analytically. Each method has its own pros and cons which are discussed next.

3.2.1 Numerical sensitivity calculation

The numerical sensitivities for the PSE functions have been calculated using finite-differences. The procedure is as follows:

The closed-loop system of equations (F) is simulated around a nominal condition defined by $\boldsymbol{\eta}_{nom}$ (and for a particular realization j in the uncertain parameters $\boldsymbol{\zeta}_j$) using a pre-defined set of time-dependent realizations in the disturbances $\boldsymbol{d}(t)$ and worst-case variability is identified, i.e. j^{th} uncertain parameter at t_{wc}. This procedure is then repeated for forward and backward points assigned to each optimization variable η_p while keeping the rest of the optimization variables constant and equal to their nominal values, i.e. $\boldsymbol{\eta}_{nom}$

(see Figure 3-3). Function evaluations for the forward ($\boldsymbol{\eta}^{+}$) and backward ($\boldsymbol{\eta}^{-}$) points around the nominal condition ($\boldsymbol{\eta}_{nom}$) are used to calculate gradients as follows:

$$\left.\frac{\partial g_s}{\partial \eta_p}\right|_{t_{wc},\zeta_j} = \left(g_s(\eta_p^{+})|_{t_{wc},\zeta_j} - g_s(\eta_p^{-})|_{t_{wc},\zeta_j}\right)/2\Delta\eta_p \tag{3-4}$$

$$\left.\frac{\partial^2 g_s}{\partial \eta_p \partial \eta_p}\right|_{t_{wc},\zeta_j} = \left(g_s(\eta_p^{+})|_{t_{wc},\zeta_j} - 2g_s(\eta_{p_{nom}})|_{t_{wc},\zeta_j} + g_s(\eta_p^{-})|_{t_{wc},\zeta_j}\right)/\Delta\eta_p{}^2 \tag{3-5}$$

where $\Delta\eta_p$ is the finite-difference step used to calculate forward and backward points of p^{th} decision variable, i.e. $\Delta\eta_p = \eta_{p_{nom}}(\Delta\eta)$. The existence of an explicit closed-loop model in the PSE approach is not necessary since the analytical expression can be approximated using numerical approaches, i.e. the sensitivities required in expansion can be calculated numerically. Following this reasoning, the method can be implemented for black-box models.

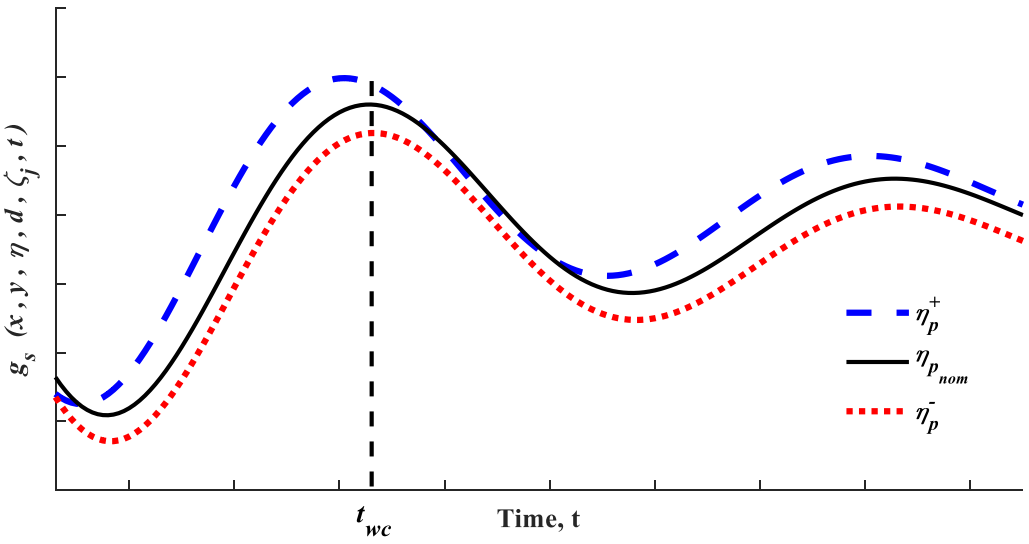

Figure 3-3: Simulations for the nominal condition, forward and backward points at the worst-case scenario

3.2.2 Analytical sensitivity calculation

The closed-loop dynamic model (F) can be represented as follows:

$$F(\dot{\boldsymbol{x}}, \boldsymbol{x}, \boldsymbol{y}, \boldsymbol{\eta}, \boldsymbol{d}, \boldsymbol{\zeta}, t) = 0 \tag{3-6}$$

where $\boldsymbol{x}$ and $\boldsymbol{y}$ are the states of the system and algebraic variables, respectively; $\boldsymbol{u}$ represents manipulated variables, $\boldsymbol{d}$ is the disturbances affecting the process, and $\boldsymbol{\zeta}$ denotes the uncertain parameter set; $\boldsymbol{\eta}$ represents the optimization variables and includes the process design variables, e.g. the size of the unit, and the controller tuning parameters, e.g. the controller's gain; t represents time. In the analytical approach, the sensitivity of the ωth closed-loop state variable with respect to the p^{th} optimization variable, $\Phi_{\omega,p}$, is calculated by taking the derivative of the closed-loop dynamic model (F) with respect to each optimization variable, (Maly and Petzold, 1996), i.e.

$$F_1: \quad \frac{\partial F}{\partial x_\omega}\Phi_{\omega,p}\Big|_{\zeta_j} + \frac{\partial F}{\partial x'_\omega}\Phi'_{\omega,p}\Big|_{\zeta_j} + \frac{\partial F}{\partial \eta_p} = 0\,; \quad \forall \omega = 1, \dots, \Omega \quad ; \quad \forall p = 1, \dots, P \tag{3-7}$$

where:

$$\Phi_{\omega,p}\Big|_{\zeta_j} = \left.\frac{dx_\omega}{d\eta_p}\right|_{\zeta_j} \tag{3-8}$$

Note that $\Phi_{\omega,p}$ needs to be calculated for every j^{th} realization of the uncertain parameter. As shown in (3-7), the computation of the first-order sensitivity requires an additional (ΩxP) system of equations (denoted as function F_1), which need to be integrated simultaneously with the closed-loop dynamic model equations (F). Thus, the first-order gradients for s^{th} constraint function (g_s) can be calculated in terms of first-order sensitivity of states $\Phi_{\omega,p}\Big|_{\zeta_j}$:

$$\left.\frac{\partial g_s}{\partial \eta_p}\right|_{\zeta_j}(t) = \Gamma\left(\boldsymbol{x}, \boldsymbol{y}, \boldsymbol{u}, \Phi_{\omega,p}\Big|_{\zeta_j}, \boldsymbol{\eta}, \boldsymbol{d}, \boldsymbol{\zeta}_j, t\right) \tag{3-9}$$

Note that $\left.\frac{\partial g_s}{\partial \eta_p}\right|_{\zeta_j}$ is slightly different from the sensitivity descriptions presented in (3-4) since it represents a function that determines the sensitivity of g_s with respect to η_p at every time t, i.e. numerical sensitivities in Equation (3-4) denote local sensitivities. As shown in Figure (3-4), the sensitivity at the worst-case

variability in g_s ($\left.\frac{\partial g_s}{\partial \eta_p}\right|_{t_{wc},\zeta_j}$)can be extracted from $\left.\frac{\partial g_s}{\partial \eta_p}\right|_{\zeta_j}(t)$ by searching for the point in time (t_{wc}) at which the worst-case variability in the s^{th} constraint function (g_s) is observed due to changes in the disturbances and at a particular realization in the uncertain parameters.

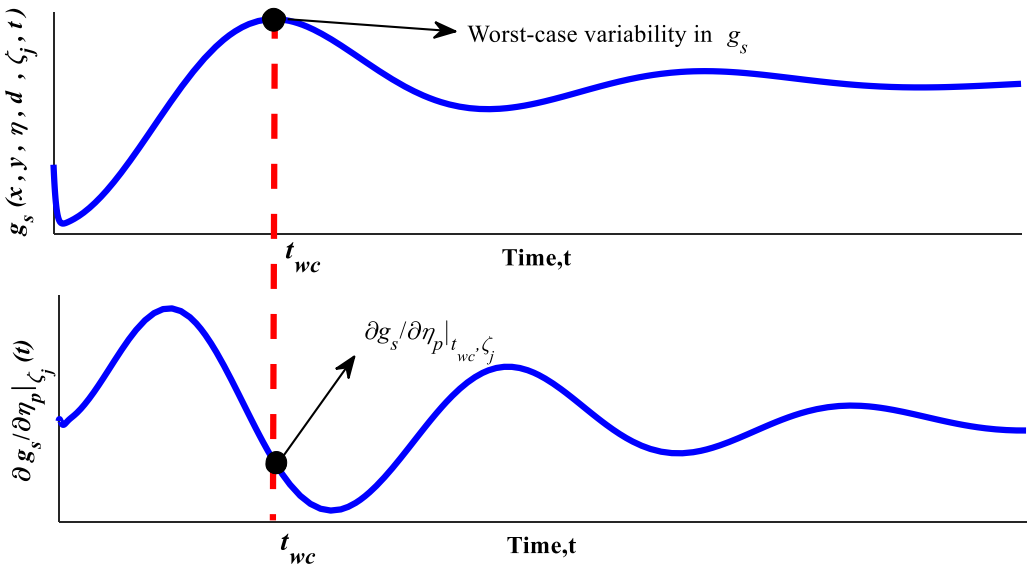

Figure 3-4: Gradient calculation using the analytical approach

This same approach can be used to estimate the sensitivities for the rest of the constraints and of the cost function (Θ). Second-order sensitivity can be calculated by taking the derivative of the first-order sensitivity functions (F_1) shown in (3-7) with respect to each optimization variable, i.e.

$$F_2 : \frac{\partial F_1}{\partial \Phi_{\omega,p}} \Psi_{\omega,p,\varsigma}\Big|_{\zeta_j} + \frac{\partial F_1}{\partial \Phi'_{\omega,p}} \Psi'_{\omega,p,\varsigma}\Big|_{\zeta_j} + \frac{\partial F_1}{\partial \eta_\varsigma} = 0\,; \quad \forall \omega = 1,\dots,\Omega \;;\; \forall p = 1,\dots,P \;;\; \forall \varsigma = 1,\dots,P \qquad (3\text{-}10)$$

$$\Psi_{\omega,p,\varsigma}\Big|_{\zeta_j} = \left.\frac{d\Phi_{\omega,p}}{d\eta_\varsigma}\right|_{\zeta_j} \qquad (3\text{-}11)$$

where the second-order sensitivity function F_2 has dimensions ΩxPxP. Thus, second-order sensitivity can be obtained by the simultaneous integration of functions F_2, F_1 and F. Hence, second-order sensitivities can be obtained as follows:

$$\left.\frac{\partial^2 g}{\partial \eta_p \partial \eta_\varsigma}\right|_{\zeta_j}(t) = \Upsilon\left(\boldsymbol{x}, \boldsymbol{y}, \boldsymbol{u}, \Phi_{\omega,p}\big|_{\zeta_j}, \Psi_{\omega,p,\varsigma}\big|_{\zeta_j}, \boldsymbol{\eta}, \boldsymbol{d}, \boldsymbol{\zeta}_j, t\right) \tag{3-12}$$

The local second-order sensitivity at the worst-case variability, i.e. Equation (3-5), can be extracted from $\left.\frac{\partial^2 g}{\partial \eta_p \partial \eta_\varsigma}\right|_{\zeta_j}(t)$ using the same procedure described above for the first-order sensitivity function (see Figure 3-4). In general, the l^{th} order sensitivity term can be obtained by defining a function F_l with dimensions $\Omega \text{x} P_1 \text{x} P_2 \text{x} \ldots \text{x} P_l$, which will need to be integrated simultaneously with the previous sensitivity functions, $F_{l-1}, F_{l-2,} \ldots, F_1$, and the closed-loop function F. Note that a new index ς of the same dimensions as index p was introduced in equations (3-10)-(3-12) to indicate the calculation of mixed-partial second-order derivatives, i.e. derivatives involving two or more independent variables.

3.3 Methodology

This section summarizes the procedure of the basic back-off methodology employed to address the integration of design and control under process disturbances and parameter uncertainty. The key calculation that needs to be performed multiple times in this methodology is the identification of a PSE function, which is used to represent the process constraints and cost function considered in the optimal design and control formulation. The current methodology focuses on the computation of continues optimization variables. This approach can be potentially extended to deal with structural decisions by adding integer optimization variables in the analysis.

The procedure proposed for the present back-off methodology is presented in Figure 3-5. The step-by-step back-off procedure is described next to address simultaneous design and control.

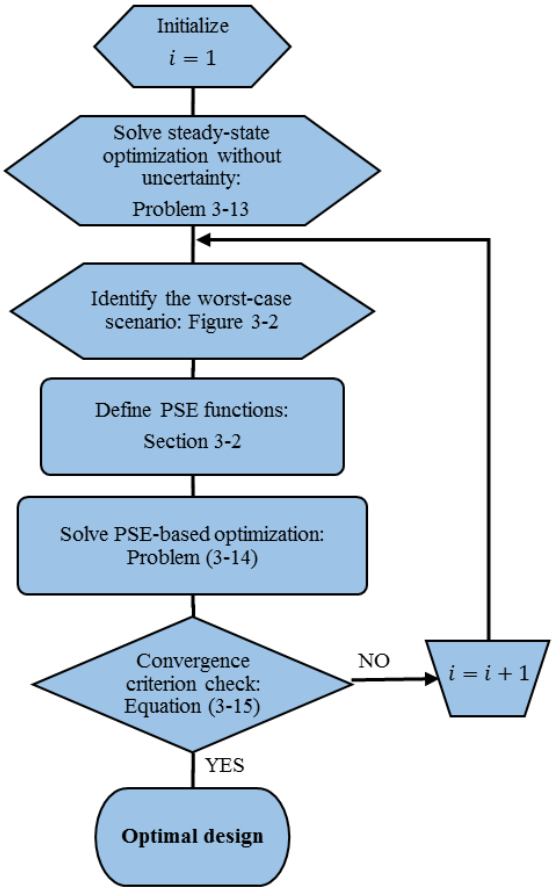

Figure 3-5: Basic back-off algorithm for integration of design and control

Step 1 (initialization)

Define upper ($\boldsymbol{\eta}^U$) and lower bounds ($\boldsymbol{\eta}^L$) for optimization variables ($\boldsymbol{\eta}$). Specify the maximum number of iterations (N_{iter}). Define step size for the finite-difference calculations ($\Delta\eta$). Also, define a tolerance criterion (ϵ) and a convergence examination period (N_c) that will be used later on to terminate the algorithm. Set the iteration index to $i = 1$.

Step 2 (Optimal steady-state design without uncertainty and disturbances):

In this step, the initial point of the procedure is specified which is used to back-off from. The optimal steady-state design can be obtained as follows:

$$
\begin{aligned}
&\min_{\boldsymbol{\eta}_0} \quad \Theta_{ss}(\boldsymbol{x},\boldsymbol{y},\boldsymbol{\eta}_0,\boldsymbol{d}_{nom},\boldsymbol{\zeta}_{nom}) \\
&\text{Subject to:} \\
&\quad F_{ss}(\boldsymbol{x},\boldsymbol{y},\boldsymbol{\eta}_0,\boldsymbol{d}_{nom},\boldsymbol{\zeta}_{nom}) = 0 \\
&\quad h_{ss_q}(\boldsymbol{x},\boldsymbol{y},\boldsymbol{\eta}_0,\boldsymbol{d}_{nom},\boldsymbol{\zeta}_{nom}) = 0\ ,\forall q = 1,\dots Q \\
&\quad g_{ss_s}(\boldsymbol{x},\boldsymbol{y},\boldsymbol{\eta}_0,\boldsymbol{d}_{nom},\boldsymbol{\zeta}_{nom}) \le 0\ ,\forall s = 1,\dots S \\
&\quad \boldsymbol{\eta}^L \le \boldsymbol{\eta}_0 \le \boldsymbol{\eta}^U
\end{aligned}
\tag{3-13}
$$

where Θ_{ss} is the cost function at steady-state; $h_{ss}: \mathbb{R}^P \rightarrow \mathbb{R}^Q$ and $g_{ss} \in \mathbb{R}^P \rightarrow \mathbb{R}^S$ are equality and inequality constraints; $x \in \mathbb{R}^{n_x}$ represents the system's states. F_{ss} includes process model equations, i.e. F in Problem (2-1) at the steady-state. Upper ($\boldsymbol{\eta}^U$) and lower ($\boldsymbol{\eta}^L$) bounds are imposed on decision variables and should be similar to those defined for Problem (2-1). Moreover, disturbances and uncertain parameters are set to their nominal values, i.e. $\boldsymbol{d}_{nom}$ and $\boldsymbol{\zeta}_{nom}$. The results of this optimization problem ($\boldsymbol{\eta}_0$) can be used as the starting (initial) point to search for the dynamically operable design that optimizes an objective function for this process. $\boldsymbol{\eta}_0$ defines the nominal condition ($\boldsymbol{\eta}_{nom}$) for the first iteration in the present procedure to develop the PSEs. The proposed trust-region method searches the closest dynamically feasible condition to the initial starting point.

Step 3 (Develop PSE-based functions):

The proposed back-off approach is a robust approach since the methodology aims to find the optimal solution which ensures that the system remains dynamically feasible in the presence of the largest (worst-case) variability observed in the constraints. The process model is simulated using the nominal condition defined by $\boldsymbol{\eta}_{nom}$ for all discrete realizations considered in the uncertain parameters $\boldsymbol{\zeta}$ using the pre-defined set of time-dependent realizations in the disturbances $\boldsymbol{d}(t)$ to evaluate the worst-case variability for each constraint and the cost function. Once the time and the uncertainty realization at the worst-case variability, i.e. t_{wc} and ζ_j, are identified, the PSE functions can be developed (see Section 3.2). The PSE sensitivities are calculated numerically or analytically as discussed in Section 3.2. Typically, second-order PSEs are used since they often provide sufficient accuracy for most engineering calculations. The order of the PSE depends on the process nonlinearity and also the required accuracy. Increasing the order of PSE is

computationally expensive. In order to calculate higher-order PSE additional forward and backward points are required.

Step 4 (Optimization of the PSE-based functions)

Once the PSE-based functions are constructed for each process constraint (g) and the optimization's cost function (Θ), a PSE-based optimization problem can be formulated as follows:

$$
\begin{aligned}
&\min_{\boldsymbol{\eta},\boldsymbol{\lambda}} \quad \sum_{j=1}^{J} w_j\, \Theta(\boldsymbol{\eta})|_{t_{wc},\zeta_j} + \sum_{j=1}^{J}\sum_{s=1}^{S} M_1 \lambda_{s,j} \\
&\text{Subject to:} \\
&\quad g_{s_{PSE}}(\boldsymbol{\eta})\big|_{t_{wc},\zeta_j} \le \lambda_{s,j} \quad ; \quad \forall s = 1,\dots,S \;;\; \forall\, j = 1,\dots,J \\
&\quad \boldsymbol{\eta}_{nom}(1-\delta) \le \boldsymbol{\eta} \le \boldsymbol{\eta}_{nom}(1+\delta) \\
&\quad \sum_{j=1}^{J} w_j = 1 \\
&\quad \lambda_{s,j} \ge 0
\end{aligned}
\tag{3-14}
$$

where δ is a user-defined tuning parameter that determines the lower and upper bounds imposed on the optimization variables ($\boldsymbol{\eta}$). This parameter determines the size of the search space region in the optimization variables that will be considered while solving Problem (3-14). The PSE functions will only be valid around a nominal region defined by $\boldsymbol{\eta}_{nom}$. Thus, δ specifies the space region for which the PSE-based optimization is allowed to explore for the optimal design and controller tuning parameters. $\lambda_{s,j}$ is an optimization variable used to avoid infeasibility, i.e. it represents the magnitude in the s^{th} constraint function g_s, and at the j^{th} realization in the uncertain parameter, that needs to be added to avoid infeasibility. The PSE-based optimization forces $\lambda_{s,j}$ to zero to specify a dynamically feasible system. M_1 represents a big number that needs to be degrees of magnitude higher than the actual cost function referred to as the big-M method. The weight M_1 in the penalty term needs to be large enough to force the feasibility variables ($\lambda_{s,j}$) to be driven to zero and therefore minimize the objective function. Conversely, an overly large value of M_1 can create convergence problems for the optimization since the calculation of the sensitivity of the cost function to the optimization variables may only be dominated by the penalty function term. Hence, M_1 is problem specific and needs to be selected in connection with the nature of the problem. w_j is a weight assigned to the

probability of occurrence of the j^{th} realization in the uncertain parameters; this parameter is user-defined and can be specified from process experience or historical data.

The solution obtained from Problem (3-14) aims to determine the search direction in which the optimization variables $\boldsymbol{\eta}$ need to be moved (backed-off) to specify an optimal process design and control scheme. As discussed earlier, PSE approximations provide inexpensive evaluations of the actual nonlinear behaviour of the system. However, the evaluations are valid for a certain vicinity (worst-case scenario) of the nominal condition and should be implemented cautiously. Accordingly, instead of defining a model for the entire process domain, the behaviour of the system is examined in an iterative manner in which the nominal condition is updated. Consequently, an iterative framework is needed in which optimal solutions obtained from (3-14) at the current iteration step are used to build a new PSE-based optimization in the subsequent iteration. The solution at each iteration represents an improvement in the search direction for the optimization variables. This procedure is carried out in an iterative manner until one of the convergence criteria described in *Step 5* in the algorithm is satisfied. It should be noted that the feasibility variables ($\boldsymbol{\lambda}$) should be zero at the convergence point for the design and control parameters to be dynamically feasible under the given process disturbances and parameter uncertainty. If any of the elements in $\boldsymbol{\lambda}$ fails to converge, then the tuning parameters such as δ and the order of the PSE functions need to be adjusted and the method restarts from *Step 1*.

Step 5 (Convergence Criterion)

A floating average convergence technique is considered here as a stopping criterion.

$$Tol_{float}^{\Theta} = \left(\sum_{v=i-2N_c+1}^{i-N_c} \Theta_v - \sum_{r=i-N_c+1}^{i} \Theta_r\right) \Big/ \sum_{r=i-N_c+1}^{i} \Theta_r \tag{3-15}$$

Θ_v and Θ_r represent the PSE cost (Θ_{PSE}) obtained from the solution of Problem (3-14) at the v^{th} and r^{th} iterations, respectively. Similarly, for the optimization variables:

$$Tol_{float}^{\boldsymbol{\eta}} = \left(\sum_{v=i-2N_c+1}^{i-N_c} \boldsymbol{\eta}_v - \sum_{r=i-N_c+1}^{i} \boldsymbol{\eta}_r\right) \Big/ \sum_{r=i-N_c+1}^{i} \boldsymbol{\eta}_r \tag{3-16}$$

where $\boldsymbol{\eta}_v$ and $\boldsymbol{\eta}_r$ represent optimization variables obtained from the solution of Problem (3-14) at the v^{th} and r^{th} iterations, correspondingly. As shown in (3-15), a sampling period N_c is specified first; then the mean of the PSE-based cost function (Θ_{PSE}) obtained from iterations $(i - 2N_c + 1)$ to $(i - N_c)$ is compared to the mean of the same function obtained from iterations $(i - N_c + 1)$ to (i). That is, the differences in means, i.e. the cost function values, are required to be less than a threshold value (ϵ). If $\left|Tol_{float}^{\Theta}\right|$ or $\left|Tol_{float}^{\boldsymbol{\eta}}\right|_p$ are below a threshold value (ϵ), then STOP, an optimal solution has been found, i.e. $\boldsymbol{\eta}^{i+1}$. Otherwise, set $i = i + 1$ and go back to *Step 3*. Alternatively, the algorithm is also terminated if the maximum number of iterations is reached, i.e. $i \geq N_{iter}$. Note that the stopping criteria are checked for $i \geq 2N_c$.

3.4 Case study: wastewater treatment plant

An existent wastewater treatment plant, located in Manresa, Spain plant was used as a case study to test the proposed methodology (Bahakim and Ricardez-Sandoval, 2014; Vega et al., 2014b). A general flowsheet of the plant is shown in Figure 3-6. The goal of the process is to regulate the level of the substrate concentration in the biodegradable waste stream due to the environmental incentives. The process consists of maintaining the substrate concentration (s_w) in the bioreactor and the dissolved oxygen concentration (c_w) in the settler at the desired levels in presence of process disturbances corresponding to the change in the feed properties (x_i, s_i, q_i). The control scheme considered for this case study includes two PI controllers that regulate the substrate concentration and the dissolved oxygen by adjusting the purge flowrate (q_p) and the turbine speed (f_k), respectively.

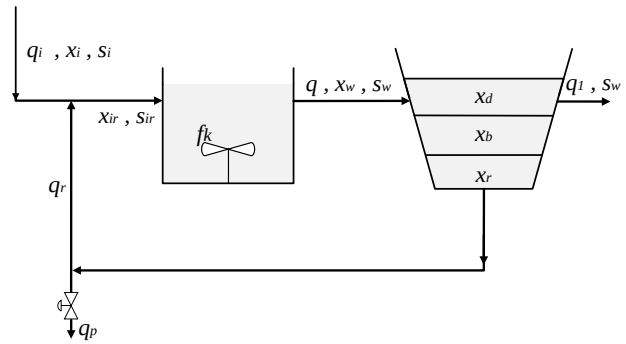

x_w	Biomass concentrations in the bioreactor
x_d , x_b , x_r	Biomass concentrations at the different layers in the clarifier unit
s_w	Organic substrate concentrations in the bioreactor
c_w	Dissolved oxygen concentration
q_p	Purge flowrate
f_k	Turbine speed
x_i , s_i	Inlet biomass and organic substrate concentration
q_i	Feed flowrate
q_r	Recycle flowrate

Figure 3-6: Flowsheet: wastewater treatment plant

Each of the layers in the decanter unit was assumed to have a uniform concentration across its spatial domain, i.e. spatial concentration gradients on each layer were neglected. Table 3-1 provides the model equations regarding the rate of the biomass and organic substrate concentrations (mg/L) inside the bioreactor as well as the difference in settling rate of biomass concentration among the different layers in the decanter.

Table 3-1: Model equations of the wastewater treatment plant

Description	Equations
Rate of change in biomass	$\frac{dx_w}{dt} = \mu_w\, y_w\, \frac{x_w\, s_w}{k_s + s_w} - k_d\, \frac{{x_w}^n}{s_w} - k_c\, x_w + \frac{q}{V_r}(x_{ir} - x_w)$
Rate of consumption of the organic substrate in the reactor	$\frac{ds_w}{dt} = -\mu_w\, \frac{x_w\, s_w}{k_s + s_w} + f_d k_d\, \frac{{x_w}^n}{s_w} + f_d\, k_c\, x_w + \frac{q}{V_r}(s_{ir} - s_w)$
The difference in settling rate of biomass concentration among different layers in the decanter	$\frac{dx_b}{dt} = \frac{1}{A_d\, lb}(q_i + q_2 - q_p)(x_w - x_b) + \frac{1}{lb}(vsd - vsb)$ $\frac{dx_d}{dt} = \frac{1}{A_d\, ld}(q_i - q_p)(x_b - x_d) - \frac{1}{ld} vsd$ $\frac{dx_r}{dt} = \frac{1}{A_d\, lr} q_2 (x_b - x_r) + \frac{1}{lr} vsb$
Rate of dissolved oxygen	$\frac{dc_w}{dt} = k_{la}\, f_k\, (c_s - c_w) - k_{01}\, \mu_w\, \frac{s_w\, x_w}{k_s + s_w} - \frac{q}{V_r} c_w$

Model parameters and their corresponding nominal values are described in Table 3-2.

Table 3-2: Process model parameters: wastewater treatment plant

Symbols	Description	Value
μ_w	Specific growth rate	0.1824 (hr^{-1})
y_w	The fraction of converted substrate to biomass	0.5948
k_s	Saturation constant	300 (hr^{-1})
k_d	Biomass death rate	$5x10^{-5}$ (hr^{-1})
k_c	Specific Cellular activity	$1.33x10^{-4}$ (hr^{-1})
k_{la}	Oxygen transfer into the water constant	0.7 (hr^{-1})
k_{01}	Oxygen demand constant	$1.00x10^{-4}$ (hr^{-1})
c_s	Oxygen specific saturation	8.0 (hr^{-1})
f_d	The fraction of death biomass	0.2
n	Potential model structure error	2

The following process constraints determine the feasible operational region for this process:

$$0.01 \leq \frac{q_p(t)}{q_2(t)} \leq 0.2$$
$$0.8 \leq \frac{V_r x_w(t) + A_d l r x_r(t)}{24\ q_p x_r(t)} \leq 15 \qquad (3\text{-}17)$$
$$s_w(t) \leq 100$$

The first two constraints shown above represent the feasible limits on the ratio between the purge to the recycle flowrates and the purge age in the decanter, respectively. Note that all three process constraints should be within their feasible limits during operation. For the present case study, the annualized total cost of the plant (Θ_w) is given by the summation of capital cost, operating cost and variability cost. A dynamic variability cost (VC_w) is considered and defined as a function of the largest variability observed in the substrate concentration throughout the process. One of the key constraints of this process is to maintain the substrate concentration below a certain threshold in the outlet stream (Equation 3-17). Since the substrate contains toxic components, the surge in the concentration from a specific level will lead to high penalty costs. Based on the above, the annual total cost (Θ_w) for this process is as follows:

$$\Theta_W = \underbrace{0.16(3500V_r + 2300A_d)}_{CC_w} + \underbrace{870(f_k + q_p)}_{OC_w} + \underbrace{10^5 s_{w\,max}(t)}_{VC_w} \qquad (3\text{-}18)$$

where $s_{w\,max}(t)$ is the largest variability in the substrate concentration at any time t. Note that a higher variable cost is assigned to the variability in the substrate concentration. For the present case study optimization variables are design variables and PI controller tuning parameters as follows:

$$\boldsymbol{\eta} = [A_d\ , V_r\ , s_{w_{sp}}\ , c_{w_{sp}},\ K_{c1}\ ,\ K_{c2}\ , \tau_{i1}\ , \tau_{i2}]. \tag{3-19}$$

where the volume of the reactor (V_r) and cross-sectional area for the decanter (A_d) are design variables. Substrate set-point ($s_{w_{sp}}$), controller gain (K_{c1}), and time constant (τ_{i1}) correspond to the controller that regulates the substrate (s_w) whereas $c_{w_{sp}}$, K_{c2}, and τ_{i2} correspond to the dissolved oxygen (c_w) control loop.

The optimal design and control problem presented above for the wastewater treatment plant was solved under different scenarios and conditions. In addition, the effect of key parameters for the present methodology is studied. Each of these analyses is described next.

3.4.1 Computation of the sensitivities

The aim of this scenario is to compare the performance of the methodology using an analytical and a numerical approach for the computation of the PSE sensitivity terms, i.e. the PSE model coefficients as shown in Section 3.2. A combination of step changes in the disturbances was considered shown in (3-20). The first realization in the disturbances corresponds to the disturbances' nominal values. Each combination of step changes in the disturbances was performed every 2,000 seconds. In the analysis, the maximum number of iterations N_{iter} was set to 200 whereas the floating average convergence criteria (ϵ) described in *Step 5* of the algorithm was set to 1x10^{-2} for the sampling period of $N_c = 20$. To simplify the analysis, the first-order approximation was used.

$$\begin{aligned}
&\boldsymbol{d_1}(t)\text{: } q_i\left(\frac{\text{m}^3}{\text{hr}}\right) = [500, 480\ ,520, 480, 500\ ,520\ ,520] \\
&\boldsymbol{d_2}(t)\text{: } x_i\left(\frac{\text{mg}}{\text{L}}\right) = [366\ ,371\ ,361, 366, 371\ ,366, 366] \\
&\boldsymbol{d_3}(t)\text{: } s_i\left(\frac{\text{mg}}{\text{L}}\right) = [80\ ,75, 85\ ,80\ ,75, 85\ ,80]
\end{aligned} \tag{3-20}$$

As shown in Figure 3-7 and Table 3-3, the optimal cost obtained when gradients were calculated numerically and analytically was found to be similar (difference of around 0.5%). This result suggests that the gradients calculated from the numerical approach are as efficient as those calculated analytically

provided that the step sizes ($\Delta\eta$) in the finite-difference sensitivity calculation are suitable. The system converged after 42 iterations for both the cases.

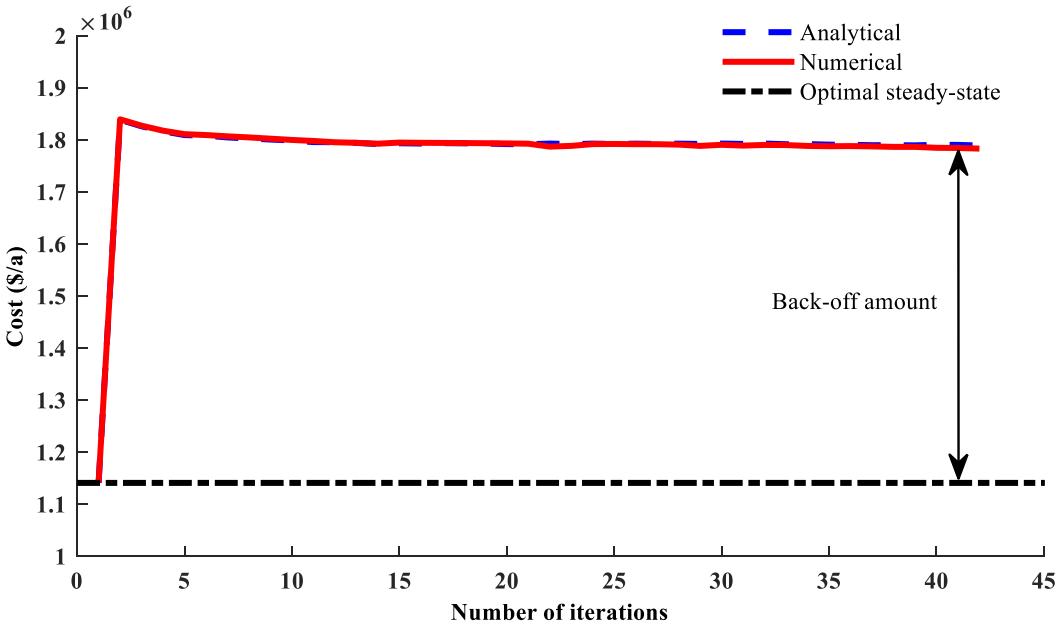

Figure 3-7: PSE-based cost function using analytical and numerical sensitivities, wastewater treatment plant

Table 3-3: PSE-based cost function using analytical and numerical sensitivities

	PSE-based approach		Formal Integration
	Analytical	Numerical	
Optimization variable			
Area (m^2)	1,366.7	1,329.7	1,441.2
Volume (m^3)	1,134.5	1,160.9	1,186.8
$s_{w_{sp}}$	93.6	93.6	93.14
$c_{w_{sp}}$	0.009	0.015	0.023
K_{c1}	0.09	0.16	0.32
K_{c2}	0.01	0.03	0.07
τ_{i1}	2.86	4.27	6.54
τ_{i2}	13.98	9.12	10.1
Total Cost ($/a)	1.7893 x10^6	1.7834 x10^6	1.9376 x10^6
Iterations	42	42	-
Total CPU Time (s)	332	134	543

As shown in Figure 3-7, a back-off of about 35% in terms of the total cost (θ_w) was obtained for this case study and represents the amount of back-off needed to accommodate the process dynamics due to disturbances. All feasibility variables (λ) for both cases converged to zero (not shown for brevity), which

indicates that the final optimal design and control scheme obtained by the present approach is dynamically feasible under the given set of process disturbances.

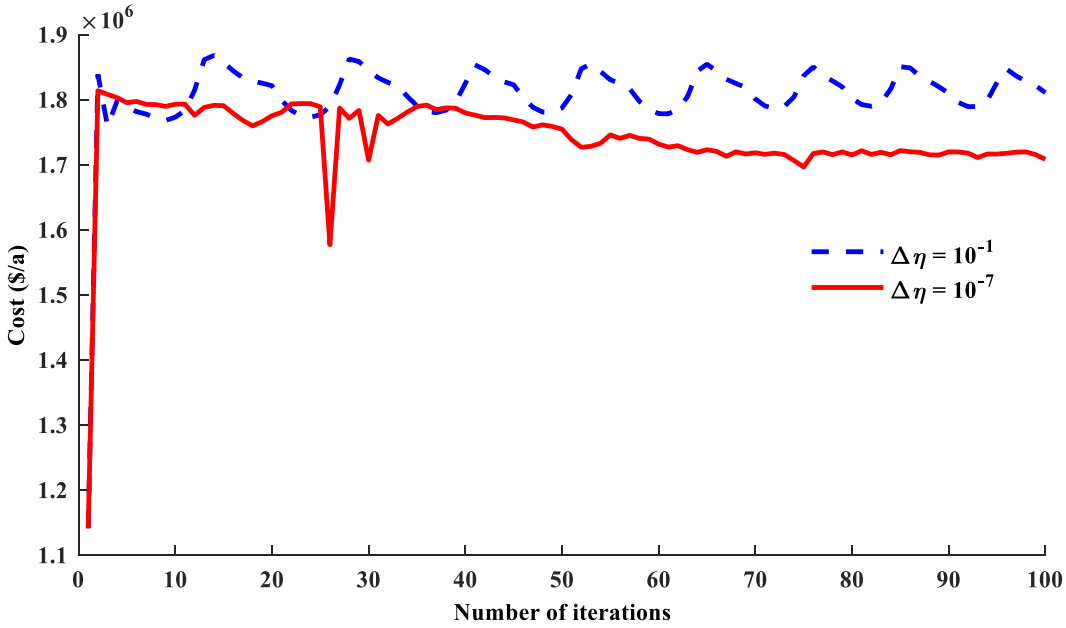

Figure 3-8: Cost function for different step sizes ($\Delta\eta$)

As shown in Table 3-3, the total CPU time required when the analytical approach was used was found to be more than twice the numerical approach. This is due to the fact that for the analytical approach a larger system of differential equations needs to be solved compared to the numerical approach. Note that the step size ($\Delta\eta$) used in the finite-difference method while calculating the numerical sensitivities is chosen offline. If the step size ($\Delta\eta$) is not tuned properly, an optimal or even a dynamically feasible solution may not be achieved. No step size is required using the analytical method, which is one of the advantages of calculating the gradients analytically at the expense of higher computational costs other than the accuracy. The step size ($\Delta\eta$) was set to 0.005 for the results shown in Table 3-3. As shown in Figure 3-8, the method failed to converge when a larger step size is used ($\Delta\eta$=1x10^{-1}); this is because the sensitivity gradients calculated may not be accurate around the worst-case variability point for the constraints and the cost function. On the other hand, when a very small step size is chosen ($\Delta\eta$1x10^{-7}) the gradient calculation may capture noise and also failed to converge to an optimal solution due to the miscalculation of the PSE sensitivity terms.

Therefore, tuning the step size to a proper value while using the numerical method to calculate the gradients is key to compute representative and accurate PSE functions of the system. In the analytical method, the number of ODE's increases significantly as the order of approximation is increased as discussed in Section 3.2.2. The design obtained from the basic back-off approach was validated using the formal integration approach. Formal integration of design and control is solved using a sequential dynamic optimization framework (Problem 2-1) in MATLAB. As shown in Table 3-3, the results obtained from the PSE-based method converge to a somewhat similar optimal design as that obtained from the formal integration process (less than 5% difference). However, the computational cost obtained from the proposed back-off approach is around 50% less as compared with the formal integration method. This result provides a guideline on how the total CPU time scales up with an increase in the problem size and the degree of nonlinearity.

3.4.2 Effect of tuning parameter δ

The effect of the tuning parameter (δ) on the optimal process design and control scheme configuration was studied. Four different δ values were chosen offline and compared, i.e. $\delta = \{0.05, 0.08, 0.1 \text{ and } 0.13\}$; second-order PSE approximations were employed to represent the cost function and process constraints in this study. The sensitivities were calculated using the numerical technique. As shown in Figure 3-9, the system converged after 82 and 62 iterations when δ was set to 0.05 and 0.08, respectively. Although the algorithm required a larger number of iterations to converge when δ=0.05, this specification also returned a lower cost (1.86×10^6 \$/a) when compared to that achieved with δ=0.08 (1.93×10^6 \$/a). The system did not converge after 200 iterations when δ was set to 0.1 and 0.13. In those cases, PSE functions may no longer be valid for wider search space regions. Since the lowest cost was obtained when $\delta = 0.05$, this is considered as an appropriate value for the present case study. Note that further decreasing the search space for the current case-study did not create significant changes in the obtained solution. Noteworthy, the order of the PSE functions can have an effect on δ value; however, their influence may not significantly improve convergence while using overly large δ values since the PSE approximations heavily rely on the fact that they are only valid around a nominal point. Thus, allowing the PSE optimization problem to move away

significantly far from the region where the PSE descriptions are valid by setting larger δ values may still result in inaccurate calculations of the back-off. For that reason, the order of PSE was studied to explore the impact on the convergence when using different δ values. As expected, increasing the order of PSE did not improve the convergence considerably while it was checked for first and second-order PSE, i.e. convergence criteria were met at roughly the same iterations (i.e. system converged after142 iterations for both first and second-order PSE) and total cost for a fixed δ value (i.e. 0.09) was found to be similar (i.e. within 0.2% error of tolerance) when using and first and second-order PSE approximations. As a consequence, the selection of this parameter is problem specific and also depends on the region that is being explored at each iteration step.

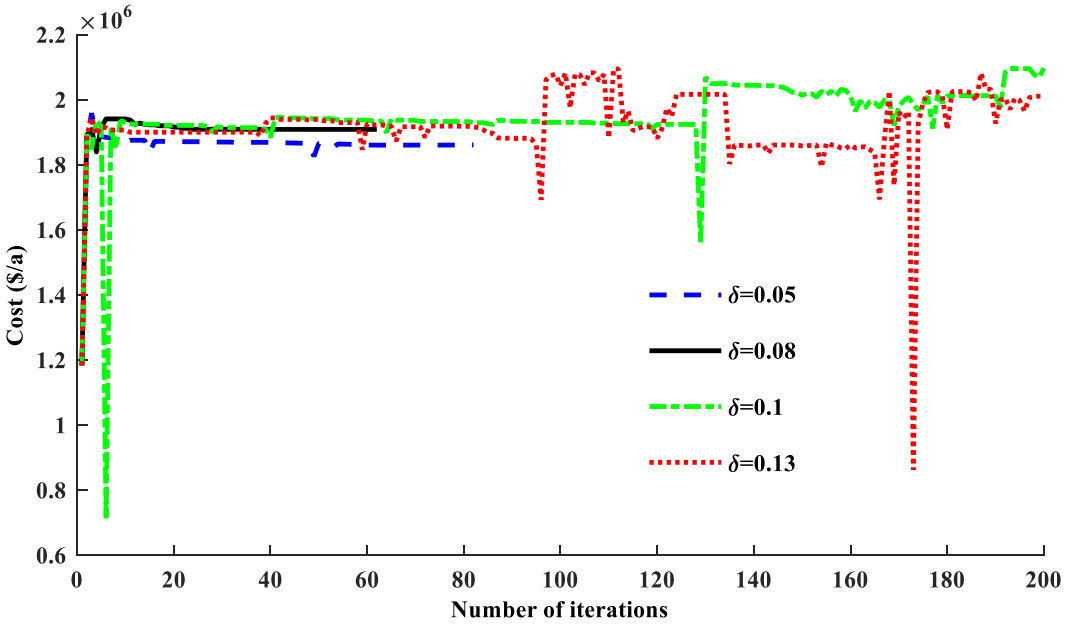

Figure 3-9: Cost function convergence chart for different tuning parameters δ

In summary, a new back-off approach for the integration of design and control of chemical processes has been presented using PSE functions. The PSE functions represent the actual process constraints and the cost function, which are explicitly defined in terms of the optimization variables, at the worst-case scenario and at a particular realization in the uncertain parameters. The present methodology is a model-based approach and assumes that a dynamic process model is available for simulations. However, the model might

associate with uncertainties and disturbances. The dynamic model is required for the sensitivity calculations. A wastewater treatment plant has been presented to evaluate the performance and benefits of the proposed method. A comparison between the computation of the PSE sensitivity terms using an analytical and a numerical approach was performed. The results show that both methods are equally efficient to calculate the PSE sensitivity terms; however, proper tuning of the finite-difference calculation is required offline. Higher computational costs were observed from the analytical calculation when compared with the numerical technique as more ODE's have to be solved in the first. Most of the CPU time required by the present approach is spent on the computation of the PSE sensitivity terms; thus, the total CPU time is expected to increase as more complex and highly nonlinear systems are considered. The proposed basic back-off approach considers deterministic uncertainty and disturbance profile and is the foundation of the proposed back-off algorithm which works efficiently for integration of design and control of small- to medium-scale processes.

4 Stochastic back-off approach

In modeling analysis, uncertainty can emerge due to multiple sources such as model structure error or the lack of knowledge in the actual model parameter values, i.e. parameter uncertainty (see Section 2.2.1). All types of uncertainties occur often in chemical engineering applications. Handling uncertainty becomes critical when the violation of constraints involves environmental or safety restrictions. A current challenge in simultaneous design and control is the specification of process designs that can accommodate stochastic descriptions of uncertain parameters and disturbances. In this regard, Tsay et al. (2017) formulated a dynamic optimization where the uncertain parameters are treated as dynamic disturbance variables with continuous pseudo-time trajectories. Wang and Baldea (2014a) used pseudo-random multilevel signals to impose uncertainty in an identification-based optimization for the optimal design of dynamic systems. Those same authors extended the approach using a control system with a switching control law at the design stage which allows obtaining designs at user-defined conservativeness (Wang and Baldea, 2014b). Koller et al. (2018) determined back-off terms to compensate for the effect of stochastic uncertainty and disturbances to provide an optimal solution for integration of design, control, and scheduling for multiproduct systems. Few studies have performed a worst-case variability distribution analysis for simultaneous design and control using random realizations in the disturbances (Bahakim and Ricardez-Sandoval, 2014; Ricardez-Sandoval, 2012). In those approaches, full compliance of process constraints may result in overly conservative designs since the worst-case scenario may not likely occur during operation. In most engineering applications, a high probability of satisfaction is often required for some constraints, e.g. safety restrictions, whereas others may not be critical, e.g. liquid level control in storage tanks. Therefore, performing an integrated stochastic-based design and control approach may result in more economically attractive designs compared with the worst-case scenario approach.

This chapter aims to present a new stochastic back-off technique for integration of design and control that can accommodate probabilistic (stochastic)-based uncertainties and disturbances. The stochastic back-off

approach is on the basis of the basic back-off approach presented in Chapter 3. The occurrence of the uncertainty for the basic back-off approach is limited to the finite realizations in the uncertainty and disturbances. The key idea in this chapter is to represent variability in the process constraints and objective function by means of statistical terms, e.g. confidence intervals. That is, PSE-based functions of the constraints specified at a user-defined coverage probability are explicitly identified in terms of the optimization variables in the presence of stochastic realizations in the uncertainty and disturbances. The results of this chapter have been published in (Rafiei-Shishavan and Ricardez-Sandoval, 2017; Rafiei and Ricardez-Sandoval, 2018).

In the current chapter, the methodology of the stochastic back-off is presented first. Later, the results of the implementation of the approach to the wastewater treatment plant are discussed.

4.1 Methodology

This section describes the stochastic back-off methodology introduced in this PhD research. Similar to basic back-off, the current stochastic approach aims to search for the optimal design and control parameters by solving a set of optimization problems using mathematical expressions obtained from PSE. PSE functions of statistical terms of the expected cost and process constraints are developed around the nominal conditions in the design variables and controller tuning parameters. Different types of statistical terms can be used to represent the expected cost and constraints, e.g. expected value, standard deviation, variance and confidence interval.

The present stochastic back-off methodology aims to find the optimal process design and control scheme under stochastic-based uncertainty and disturbances in an iterative manner. A schematic of the iterative stochastic back-off approach algorithm proposed in this chapter is shown in Figure 4-1. Each of the steps in the algorithm is described next.

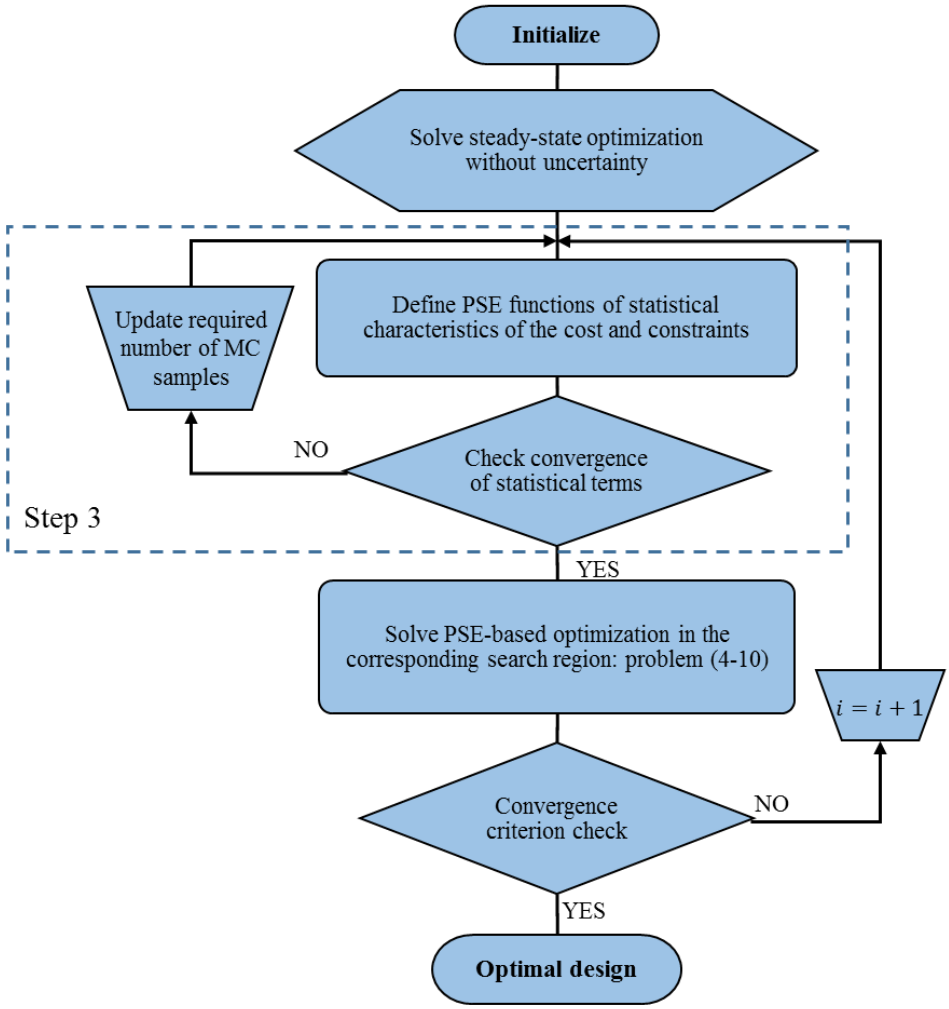

Figure 4-1: Algorithm for the stochastic back-off methodology

Step 1 (Algorithm Initialization):

Similar to *Step 1* in Chapter 3, specify the order of the PSE functions to be used in the analysis (i.e. the number of terms in the PSE function), upper and lower bounds for each optimization variable ($\boldsymbol{\eta}$), the maximum number of iterations (N_{iter}), the search space in the decision variables (δ), and a tolerance criterion (ϵ) that will be used to terminate the algorithm. In addition to those mutual parameters, define the acceptable tolerance for the convergence of the statistical terms (ϵ_{Mc}) and a minimum number of realizations (N). Set the iteration index to $i = 1$.

In the current work, the uncertain parameters and time-varying disturbances are considered as random variables correlated by probability distribution functions $PDF(\boldsymbol{\alpha}_{\boldsymbol{\zeta}})$ and $PDF(\boldsymbol{\alpha}_{d})$, respectively; where $\boldsymbol{\alpha}_{\boldsymbol{\zeta}}$ and $\boldsymbol{\alpha}_{d}$ represent the statistical parameters of the probability distribution (e.g. mean and variance for normal distribution or upper and lower bounds for uniform distribution). Historical data can be used to characterize the variability in the uncertain parameters. The mathematical description of the uncertain parameters and disturbances is as follows:

$$\begin{aligned} &\boldsymbol{\zeta} = \{\boldsymbol{\zeta} \,|\boldsymbol{\zeta} \sim PDF(\boldsymbol{\alpha}_{\boldsymbol{\zeta}})\} \\ &\boldsymbol{d}(t) = \{\boldsymbol{d}|\boldsymbol{d} \sim PDF(\boldsymbol{\alpha}_{\boldsymbol{d}})\}; 0 < t < t_f \end{aligned} \tag{4-1}$$

Step 2 (Optimal steady-state design without uncertainty and disturbances):

As discussed in Chapter 3, the result of this optimization problem ($\boldsymbol{\eta}_0$) is used as the starting (initial) point to search for the optimal dynamically operable design that can accommodate stochastic realizations in the uncertain parameters and disturbances.

Step 3 (Develop PSE-based functions: statistical terms):

As shown in (4-1), this algorithm assumes that the disturbances are stochastic time-varying random variables. Monte Carlo (MC) sampling was employed for the propagation of the uncertain parameters and disturbances into the system and the corresponding identification of the PSE functions for the constraints (h) and cost function (Θ). Two types of statistical terms have been considered to capture the behaviour of the cost and constraint functions, i.e. variance and confidence interval. If confidence interval has been chosen to develop the PSE-based functions, the procedure for *Step 3* is as follows:

The key idea is to develop PSE-based functions that describe the process variability in terms of the confidence interval for process constraints ($\mathbb{CI}^{\rho}(g_{PSE})$) and the expected value for the cost function ($\mathbb{E}(\Theta_{PSE})$). The confidence interval ($\mathbb{CI}$) is estimated from data obtained from simulations. The percentile bootstrap method has been used to compute the confidence interval from the simulated data (Davison and Hinkley, 1997). In order to ensure that the estimated confidence intervals are within a reasonable level of

accuracy, a systematic procedure has been considered to ensure that a sufficiently large number of MC samples are being used in the computation of these estimates, (see steps *a* through *e* below). Note that the confidence interval calculation is independent of the distribution of the process constraints since they are estimated from data collected from the simulations. Based on the above, MC realizations are generated for the disturbance ($\boldsymbol{d}$) and uncertain parameters ($\boldsymbol{\zeta}$) and are used as inputs for simulation of the dynamic model around a nominal condition in the optimization variables ($\boldsymbol{\eta}_{nom}$). The number of MC samples required to describe the probability distribution in the observables is determined based on the desired accuracy in the estimation and the available computational budget to perform the uncertainty propagation. In this regard, selecting an appropriate number of MC realizations is critical to identify the key statistical properties of the cost function and process constraints. An iterative approach is therefore employed in this work to determine the required number of MC samples. This procedure is as follows:

a) Specify a minimum number of realizations (N) and a tolerance criterion to check for convergence on the estimation of the statistical terms in the cost function and constraints due to uncertainty and disturbances (ϵ_{MC}). Also, initialize an index (k), which keeps track of the batches of the MC samples, i.e. set $k = 1$.

b) Using the descriptions provided in (4-1), generate a batch of MC samples that will contain N realizations of the uncertain parameters and disturbances.

c) For each realization included in the batch, simulate the system using fixed (nominal) values in the optimization variables ($\boldsymbol{\eta}_{nom}$). The N simulation results obtained from the current MC samples are collected in a set R. These results are appended to simulation results from past MC sample realizations, i.e.

$$R_k = \{R, R_{k-1}\} \tag{4-2}$$

d) where R_{k-1} represent the simulation results collected from $k = 1$ to $k - 1$.

e) Calculate the statistical terms of cost function and process constraints for the set R_k. That is, compute confidence intervals $\mathbb{C}I_{R_k}^{\rho_s}(g_s)$ at the desired coverage probability (ρ_s) for the process constraints (g_s).

f) Compare statistical terms of the current set (R_k) with the previous set (R_{k-1}) using the following formulation:

$$Tol_{MC} = \left(\mathbb{C}I_{\boldsymbol{R_k}}^{\rho_s}(g_s) - \mathbb{C}I_{\boldsymbol{R_{k-1}}}^{\rho_s}(g_s)\right) / \mathbb{C}I_{\boldsymbol{R_k}}^{\rho_s}(g_s) \tag{4-3}$$

If Tol_{MC} falls below a user-defined threshold (ϵ_{MC}), then STOP, convergence in the statistical terms have been obtained. Otherwise, update $k = k + 1$ and go back to *Step b*), i.e. generate another batch of *N* MC samples and add it to the previous set of samples. This procedure is repeated until the tolerance (ϵ_{MC}) is satisfied, which indicates that the statistical characteristics of the process constraints have converged. Note that k represents the index that keeps track of the number of *N* MC samples required by this method to comply with the tolerance criterion (see *Step e*) above).

The addition of multiple sources of uncertainty (each with their own probability distribution function) will directly impact the computational costs of the present approach. To achieve a satisfactory accuracy in the statistical terms, e.g. confidence interval in the cost function and process constraints, a larger set of combinations in the different realizations of the multiple uncertain parameters are needed. Hence, the number of required MC samples that need to be simulated will be increased significantly thus requiring additional computational resources. Note that the procedure described above is performed around a nominal condition in the optimization variables, i.e. $\boldsymbol{\eta}_{nom}$. Hence, the procedure needs to be repeated for forward and backward points assigned to each optimization variable while keeping the rest of the optimization variables constant and equal to their nominal values as shown in Figure 4-2. Calculation of forward and backward points is required in order to obtain sensitivity terms in the PSE for the constraints and cost function at the corresponding confidence interval for the specified coverage probability.

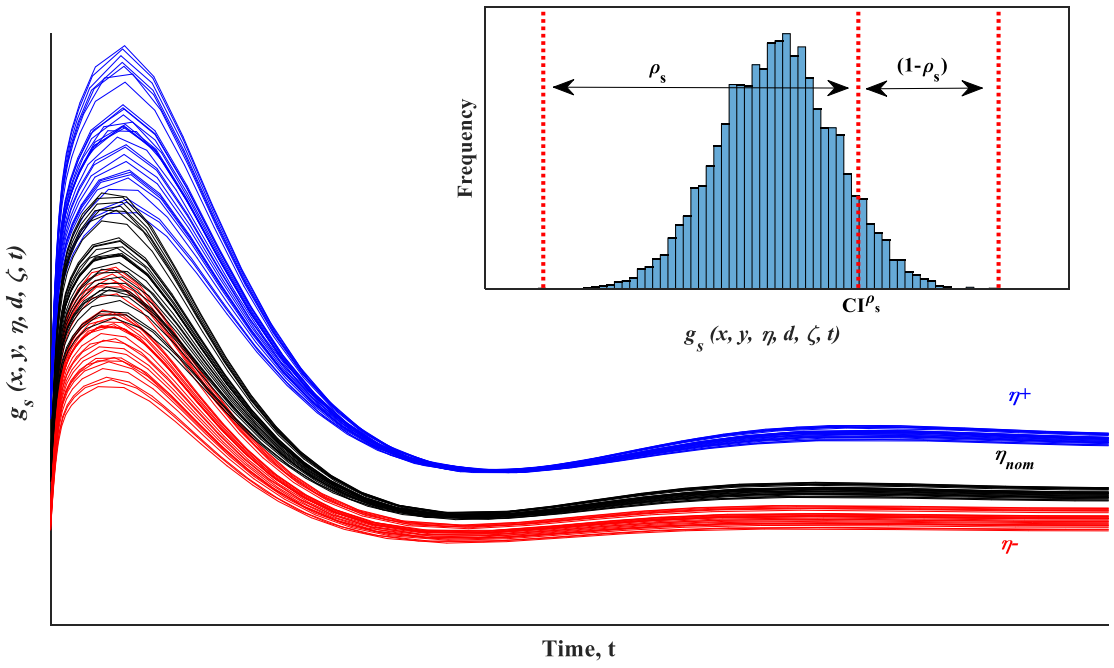

Figure 4-2: Simulations for the nominal condition, forward and backward points using uncertainties and disturbances realizations as input

Finite-differences have been used in this work to calculate the PSE sensitivities using data collected from simulations. For example, the first-order sensitivity term of the confidence interval of the s^{th} constraint at a coverage probability ρ_s in terms of the p^{th} decision variable can be calculated as follows:

$$\left.\frac{\partial \mathbb{CI}^{\rho_s}(g_s)}{\partial \eta_p}\right|_{d(t),\zeta} = \left(\mathbb{CI}^{\rho_s}(g_s(\eta_p^+))|_{d(t),\zeta} - \mathbb{CI}^{\rho_s}(g_s(\eta_p^-))|_{d(t),\zeta}\right)/2\Delta\eta_p \tag{4-4}$$

where $\mathbb{CI}^{\rho_s}(g_s)$ is the confidence interval of s^{th} constraints with the coverage probability of ρ_s; $\Delta\eta_p$ represents the difference between the forward points (η_p^+) and the backward points (η_p^-). Note that tuning the step size offline is required to compute representative PSE sensitivities. Similarly, the second-order sensitivity term can be calculated as follows:

$$\left.\frac{\partial^2 \mathbb{CI}^{\rho_s}(g_s)}{\partial \eta_p \partial \eta_p}\right|_{\boldsymbol{d}(t),\zeta} = \left(\mathbb{CI}^{\rho_s}(g_s(\eta_p^+))|_{\boldsymbol{d}(t),\zeta} - 2\mathbb{CI}^{\rho_s}(g_s(\eta_{nom}))|_{\boldsymbol{d}(t),\zeta} + \mathbb{CI}^{\rho_s}(g_s(\eta_p^-))|_{\boldsymbol{d}(t),\zeta}\right)/\Delta\eta_p{}^2 \tag{4-5}$$

Higher-order sensitivity terms can be identified in a similar fashion at the expense of higher computational costs since additional forward and backward points around the nominal point are required. Accordingly,

mathematical expressions for the expected value of the cost function (Θ) and confidence interval of the s^{th} constraint functions (g) using PSE approximations can be formulated as follows:

$$\mathbb{E}(\Theta_{PSE}(\boldsymbol{\eta}))|_{\boldsymbol{d}(t),\boldsymbol{\zeta}} = \mathbb{E}(\Theta(\boldsymbol{\eta}_{nom}))|_{\boldsymbol{d}(t),\boldsymbol{\zeta}} + \sum_{l=1} \frac{1}{l!} \nabla^l \mathbb{E}\big(\Theta(\boldsymbol{\eta})\big)\big|_{\boldsymbol{d}(t),\boldsymbol{\zeta},\boldsymbol{\eta}_{nom}} (\boldsymbol{\eta} - \boldsymbol{\eta}_{nom})^l \tag{4-6}$$

$$\mathbb{CI}^{\rho_s}(g_{s_{PSE}}(\boldsymbol{\eta}))\big|_{\boldsymbol{d}(t),\boldsymbol{\zeta}} = \mathbb{CI}^{\rho_s}(g_s(\boldsymbol{\eta}_{nom}))|_{\boldsymbol{d}(t),\boldsymbol{\zeta}} + \sum_{l=1} \frac{1}{l!} \nabla^l \mathbb{CI}^{\rho_s}\big(g_s(\boldsymbol{\eta})\big)\big|_{\boldsymbol{d}(t),\boldsymbol{\zeta},\boldsymbol{\eta}_{nom}} (\boldsymbol{\eta} - \boldsymbol{\eta}_{nom})^l \tag{4-7}$$

where $\mathbb{E}(\Theta_{PSE}(\boldsymbol{\eta}))$ is the PSE expansion of the expected value of the cost in terms of optimization variables ($\boldsymbol{\eta}$). Likewise, $\mathbb{CI}^{\rho_s}(g_{s_{PSE}}(\boldsymbol{\eta}))$ is the PSE expansion of the confidence interval the of the s^{th} constraint with the coverage probability of ρ_s; $\nabla^l \mathbb{E}\big(\Theta(\boldsymbol{\eta})\big)$ and $\nabla^l \mathbb{CI}^{\rho_s}\big(g_s(\boldsymbol{\eta})\big)$ represent the l^{th} sensitivity terms of the expected value of the cost function (Θ) and confidence interval of the s^{th} constraint (g) with the coverage probability of ρ_s, respectively. Note that the gradient terms are assessed at the nominal condition of optimization variables ($\boldsymbol{\eta}_{nom}$) due to random realizations in the disturbances ($\boldsymbol{d}(t)$) and uncertain parameters ($\boldsymbol{\zeta}$). Also, note that the expected value of the cost function is evaluated in the presence of stochastic realizations in the time-varying disturbances and time-invariant uncertainties. Admittedly, adding more decision variables results in higher computational expenses as it involves another set of sensitivity calculations, i.e. at nominal ($\boldsymbol{\eta}_{nom}$) forward (η_p^+) and backward (η_p^-) points, which would require MC simulations for each of these points.

Another alternative is to describe the process variability in terms of the expected value and variance /standard deviation. If variance has been chosen as the statistical term, calculation of *Step 3* Equation (4-7) is as follows:

The expected value and variance of the process constraints in the time domain are computed from the simulation of N MC samples and used to build the corresponding PSE functions. This procedure is then repeated for calculation of the variance of forward and backward points assigned to each optimization variable. Sensitivity terms for the expected value and variance are then calculated using the data collected

from simulations. Accordingly, mathematical expressions for the standard deviation s^{th} constraint functions (g_s) using PSE approximations can be formulated as follows:

$$\sigma(g_{s\,PSE}(\boldsymbol{\eta}))\big|_{\boldsymbol{d}(t),\boldsymbol{\zeta}} = \sigma(g_s(\boldsymbol{\eta}_{nom}))|_{\boldsymbol{d}(t),\boldsymbol{\zeta}} + \sum_{l=1} \frac{1}{l!} \nabla^l \sigma\big(g_s(\boldsymbol{\eta})\big)\big|_{\boldsymbol{d}(t),\boldsymbol{\zeta},\boldsymbol{\eta}_{nom}} (\boldsymbol{\eta} - \boldsymbol{\eta}_{nom})^l \tag{4-8}$$

where $\nabla^l \sigma\big(g_s(\boldsymbol{\eta})\big)$ are the l^{th} order gradients of the expected value and standard deviation of constraint (g_s). Note that a similar convergence approach (steps *a* through *e*) should be taken to ensure convergence of the standard deviation as discussed above.

S*tep 4 (Optimization of the PSE-based functions)*:

The PSE-based functions constructed in the previous step for the process constraints and the cost function are embedded within a PSE-based optimization problem, i.e.

$$\begin{aligned}
&\min_{\boldsymbol{\eta},\boldsymbol{\lambda}} \ \mathbb{E}(\Theta_{PSE}(\boldsymbol{\eta})|_{\boldsymbol{d}(t),\boldsymbol{\zeta}}) + \sum_{s}^{S} M_1 \, \lambda_s \\
&\text{Subject to:} \\
&\quad \mathbb{CI}^{\rho_s}(g_{s_{PSE}}(\boldsymbol{\eta}))\big|_{\boldsymbol{d}(t),\boldsymbol{\zeta}} \leq \lambda_s \,, \forall s = 1, \dots, S \\
&\quad \boldsymbol{\eta}_{nom}(1-\delta) \leq \boldsymbol{\eta} \leq \boldsymbol{\eta}_{nom}(1+\delta) \\
&\quad \lambda_s \geq 0 \,, \forall s = 1, \dots, S
\end{aligned} \tag{4-9}$$

where λ_s is an optimization variable used to avoid infeasibility in the s^{th} constraint function ($g_{s\,PSE}$). The weight M_1 is a sufficiently large penalty term use to drive the feasibility variables (λ_s) to zero and enable the specification of a dynamically feasible system that minimizes the expected value of the cost function. This method also referred to as the big-M method, is used here to ensure feasible solutions in Problem (4-9), particularly in the first iterations where the process constraints cannot accommodate dynamic feasibility. Setting values close the unity for the coverage probability (ρ_s) will seemingly reduce the possibility of violation of the constraints at the expense of specifying more conservative designs. As mentioned above, the PSE functions are only valid around the vicinity of nominal conditions in the decision variables ($\boldsymbol{\eta}_{nom}$); hence, the search space in the optimization variables is restricted by means of δ, which aims to specify a region where the PSE approximations remain valid. Accordingly, the present method requires an iterative

approach to identify an optimal design and control scheme that can comply with the process constraints at user-defined coverage probabilities. As shown in Figure 4-1, the solution of Problem (4-9) is used as the basis to search for a new direction in the optimization variables at each iteration step in the algorithm.

Alternatively, if the variance is chosen as the statistical term, PSE-based optimization problem will be as follows:

$$\begin{aligned}
&\min_{\boldsymbol{\eta},\boldsymbol{\lambda}} \quad \mathbb{E}(\Theta_{PSE}(\boldsymbol{\eta})|_{\boldsymbol{d}(t),\boldsymbol{\zeta}}) + \kappa\, \sigma(\Theta_{PSE}(\boldsymbol{\eta})|_{\boldsymbol{d}(t),\boldsymbol{\zeta}}) + \sum_{s}^{S} M_1\, \lambda_s \\
&\text{Subject to:} \\
&\quad \mathbb{E}\left(g_{s_{PSE}}(\boldsymbol{\eta})|_{\boldsymbol{d}(t),\boldsymbol{\zeta}}\right) + \gamma_s\, \sigma\left(g_{s_{PSE}}(\boldsymbol{\eta})|_{\boldsymbol{d}(t),\boldsymbol{\zeta}}\right) \leq \lambda_s\,, \forall s = 1, \ldots, S \\
&\quad \boldsymbol{\eta}_{nom}(1-\delta) \leq \boldsymbol{\eta} \leq \boldsymbol{\eta}_{nom}(1+\delta) \\
&\quad \lambda_s \geq 0\,, \forall s = 1, \ldots, S
\end{aligned} \tag{4-10}$$

where δ, M_1, and λ_s are similar to Problem (4-9). κ and γ_s are weights assigned to the cost function and s^{th} process constraint and are aimed to account for process variability as a function of the spread observed in the distribution of the cost function and process constraints. For example, setting γ_s=1 suggests that the s^{th} constraint should be satisfied at least in 83.9 % of the time (under the assumption of a normal distribution in g_s). Setting κ and γ_s to large values will surely reduce violation of the constraints at the expense of specifying more conservative designs. In general, the distributions for the constraints and cost function are expected to be non-Gaussian since process models are typically nonlinear. Thus, this approach is only an approximation to the actual distribution while using the above-mentioned weights.

Step 5 (Convergence Criterion):

A floating average convergence technique, i.e. the difference in means, is employed as a stopping criterion similar to the basic back-off approach in Chapter 3. If the criterion is satisfied, then STOP, an optimal solution has been found; otherwise, update the nominal condition and go to *Step 3*. Table 4-1 lists the tuning parameters that are required by the present methodology and their recommended values.

Table 4-1: Tuning parameters, Stochastic back-off methodology

Tuning parameter	Description	Recommended values[1]
N_c	Convergence examination period, the higher the value the longer to check for convergence of the back-off algorithm	10-30
N_{iter}	Maximum number of iterations allowed in the stochastic back-off algorithm	≥300
δ	Size of the search space region of the optimization variables at each iteration step. PSE functions are expected to be representative of the system's variability within this region	0.05-0.15
ϵ	Termination tolerance for the stochastic back-off algorithm	≤1x10^{-3}
ϵ_{MC}	Termination tolerance for the convergence of the statistical terms	≤1x10^{-3}
PSE order	Order of the PSE expansion. Problem-specific and directly correlated to the nonlinearity of the problem under consideration	1, 2
$\Delta\boldsymbol{\eta}$	Step size considered to estimate the sensitivity of the cost function and process constraints with respect to the optimization variables	$0.01\boldsymbol{\eta}_{nom}$-$0.02\boldsymbol{\eta}_{nom}$
M	Penalty term that forces the system to move within the dynamic feasibility region	$10^3\Theta$-$10^5\,\Theta$

4.2 Results

The wastewater treatment plant explained in Chapter 3 (Section 3.4) is used as a case study. Table 4-2 shows the cost function and the process constraints that determine the feasible operating region for this process. As shown in Table 4-2, a variability cost (VC_w) is considered to maintain the substrate concentration near a threshold (i.e. 100 mg/L) since any deviation in the substrate level leads to high penalty costs. While a positive deviation may impose a municipality penalty for the excessive deposition of this organic material to the environment, a drop in the substrate concentration below the threshold reduces plant performance and adversely affects the process economics. Note that all the three process constraints indicated in Table 4-2 must remain feasible during operation (up to a certain confidence level); hence, they are considered as dynamic path constraints.

[1] Recommended from previous experiences with different engineering applications.

Table 4-2: The objective and dynamic path constraints of the wastewater treatment plant

Description	Equations
Cost function: • CC_w : capital cost • OC_w : operating cost • VC_w : variability cost	$\Theta_W = \underbrace{0.16(3500\,V_r + 2300\,A_d)}_{CC_w} + \underbrace{870(f_k + q_p)}_{OC_w} + \underbrace{10^5(100 - \mathrm{s_w})^2}_{VC_w}$
Constraints:	
• Maximum allowable substrate concentration in the treated water that leaves the decanter	$s_w^{up}(t) \leq 100$
• Minimum and maximum allowed ratio between the purge to the recycle flowrates	$\mathrm{R}_1^{lo}: 0.01 \leq \frac{q_p(t)}{q_2(t)}$ $\mathrm{R}_1^{up}: \frac{q_p(t)}{q_2(t)} \leq 0.2$
• Allowed purge age in the decanter	$\mathrm{R}_2^{lo}: 0.8 \leq \frac{V_r x_w(t) + A_d l r x_r(t)}{24\ q_p x_r(t)}$ $\mathrm{R}_2^{up}: \frac{V_r x_w(t) + A_d l r x_r(t)}{24\ q_p x_r(t)} \leq 15$
Optimization variables	$[A_d, V_r, s_{w_{sp}}, c_{w_{sp}}, K_{c1}, K_{c2}, \tau_{i1}, \tau_{i2}]$

The stochastic back-off methodology presented in Section 4.1 has been implemented on the wastewater treatment plant. Second-order PSE expansions were used in the current analysis. In the present study, the accuracy of the PSE sensitivities was initially verified offline through simulations; similarly, they have been validated at the optimal condition for each scenario. This checking procedure can be embedded in the methodology to determine if, at each step in the iteration of the present back-off technique, the PSE expansions are constructed in a way that complies with the desired user-defined accuracy. This implementation requires higher computational efforts and is beyond the scope of this chapter. δ was set to 0.1 whereas the convergence criteria for the back-off technique were set to ϵ =1x10^{-3}. The computational experiments performed in this research were conducted using MATLAB2017a® on a computer running Microsoft Windows Server 2016 standard. The computer was equipped with 16 GB RAM and Intel® Xeon® CPU E5-2620 v4 @ 2.10GHz. To explore the potential benefits and limitations of the present method, the optimal design of the wastewater treatment plant was performed under different scenarios. Section 4.2.1 presents a comparison on the statistical terms that can be used in the present methodology to assess process variability under uncertainty, i.e. confidence intervals and expected value and variance. Section 4.2.2 explores the performance of the methodology using different sources of uncertainty, and with different

probability distribution functions. The effect of using different weights on the coverage probability of the constraints is discussed in Section 4.2.3 whereas Section 4.2.4 evaluates the computational cost of the present approach and discusses the scalability of the methodology.

4.2.1 Effect of statistical terms

As previously stated, different statistical terms can be used to represent the probability of the cost function and process constraints due to probabilistic-based descriptions for the disturbances and uncertain parameters in the PSE-based optimization problem. Two basic approaches are currently being adopted in the stochastic back-off methodology. Primarily, statistical terms of the cost function and process constraints in the PSE-based optimization problem were estimated using expected values and variances. However, the nonlinearity of the system that produces non-Gaussian distributions in the process constraints may result in poor estimations of expected value and variances. The issue of inaccurate estimation of probability characteristics due to the Gaussian distribution assumption can be avoided using the confidence intervals of process constraints at certain coverage probabilities. Both methods have been implemented on the wastewater treatment plant case study. As indicated in Table 4-3, the trajectory profile for the disturbances is assumed to be a series of step changes while magnitudes are described by a normal probability distribution function with a pre-specified mean and variance. In the case of using expected value and variance (*Sc1*), the constraints shown in Table 4-3 for this case study are required to be satisfied at the probability of $\mu + 3\sigma$, i.e. 0.99 whereas in the present approach, coverage probability of confidence intervals for the constraints was explicitly set to 0.99 (*Sc2*).

Table 4-3: Effect of using different statistical terms in the stochastic back-off methodology

	Sc1	*Sc2*
Confidence weights	All constraints @ $\boldsymbol{\mu + 3\sigma}$	All constraints @ $\mathbb{CI}^{0.99}$
Disturbances	Step changes $q_i \sim \mathcal{N}(600,20)$	Step changes $q_i \sim \mathcal{N}(600,20)$
Optimization variables		
Area (m^2)	3,034.21	1,945.31
Volume (m^3)	3,024.95	1,682.54
$s_{w_{sp}}$	70	94.74
$c_{w_{sp}}$	0.03003	0.01389
K_{c1}	0.032	3.26
K_{c2}	0.111	0.066
τ_{i1}	64.40	53.50
τ_{i2}	34.55	14.89
Cost ($/a)	9.2845×10^7	4.4539×10^6

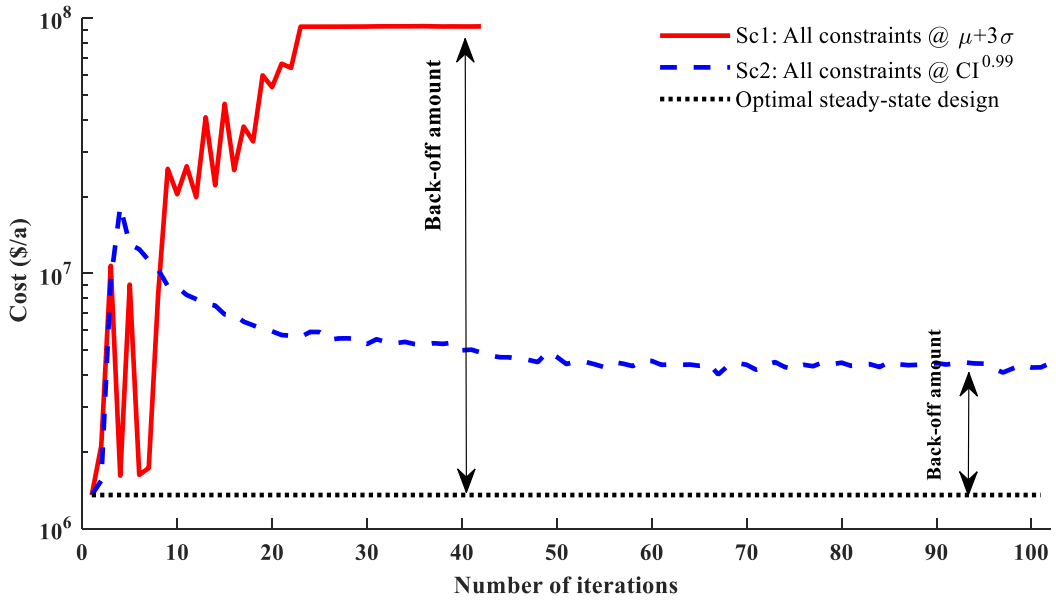

Figure 4-3: Cost function for *Sc1* and *Sc2*

As shown in Table 4-3 and Figure 4-3, the confidence interval approach (*Sc2*) produces a more economically attractive design since it captures accurately the variability in the constraints due to random step changes in the disturbance. *Sc1* specified design with a large volume of the aeration tank and a large cross-sectional area for the decanter (see Table 4-3). Similarly, *Sc1* specified overly conservative controllers that diminished plant performance. The results in Figure 4-3 indicate that the design obtained using larger weights on the constraints' variance is more conservative than that those specified by the confidence interval approach. As a result, the process design and control scheme for *Sc1* resulted in a plant cost that is

at least one order of magnitude higher than that obtained by *Sc2*. Figure 4-3 also reveals that there is a larger amount of back-off from the optimal steady-state design when using expected value and variance (*Sc1*) compared to the confidence interval-based approach (*Sc2*), i.e. back-off in *Sc1* is 97% larger than the back-off amount obtained for *Sc2*. Therefore, the variance-based approach produces a design and control scheme that is 95% more expensive than that obtained by the present method. Figure 4-4 shows the convergence of the substrate set-point for both scenarios. As expected, *Sc1* converged to the lowest allowable substrate set-point whereas *Sc2* specified a substrate set-point that is more economical since it is closer to the substrate constraint limit.

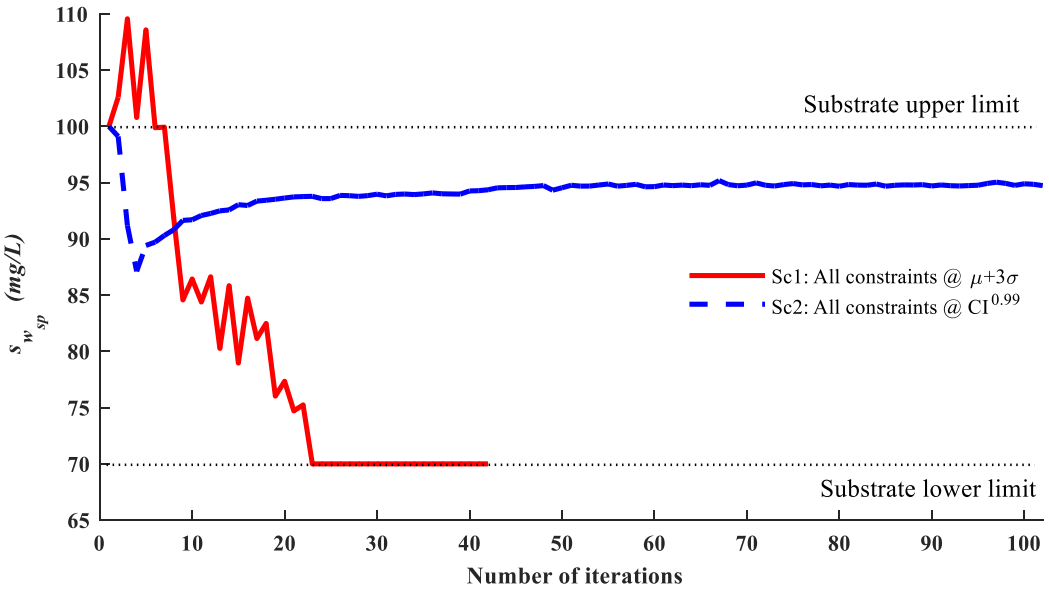

Figure 4-4: Substrate set-point for *Sc*1 and *Sc*2

Figure 4-5 shows the simulation results at the optimal solution obtained from *Sc1* and *Sc2*. These results were generated using a sufficiently large number of MC realizations in the disturbances so that convergence in the statistical terms was supposedly ensured. As shown in Figure 4-5, the process constraints do not follow a Gaussian distribution; thus, the Gaussian distribution assumption is not adequate for this system since the variance does not completely capture the behaviour of the constraints under the effect of disturbances. Different constraints are active for the two scenarios (red dashed lines in Figure 4-5). These

results confirm that the confidence interval approach proposed in this study is a more accurate representation of coverage of constraints whereas the variance-based approach fails to capture accurate approximations for the process nonlinear constraints; hence, the significant differences observed with respect to the confidence interval approach (*Sc2*).

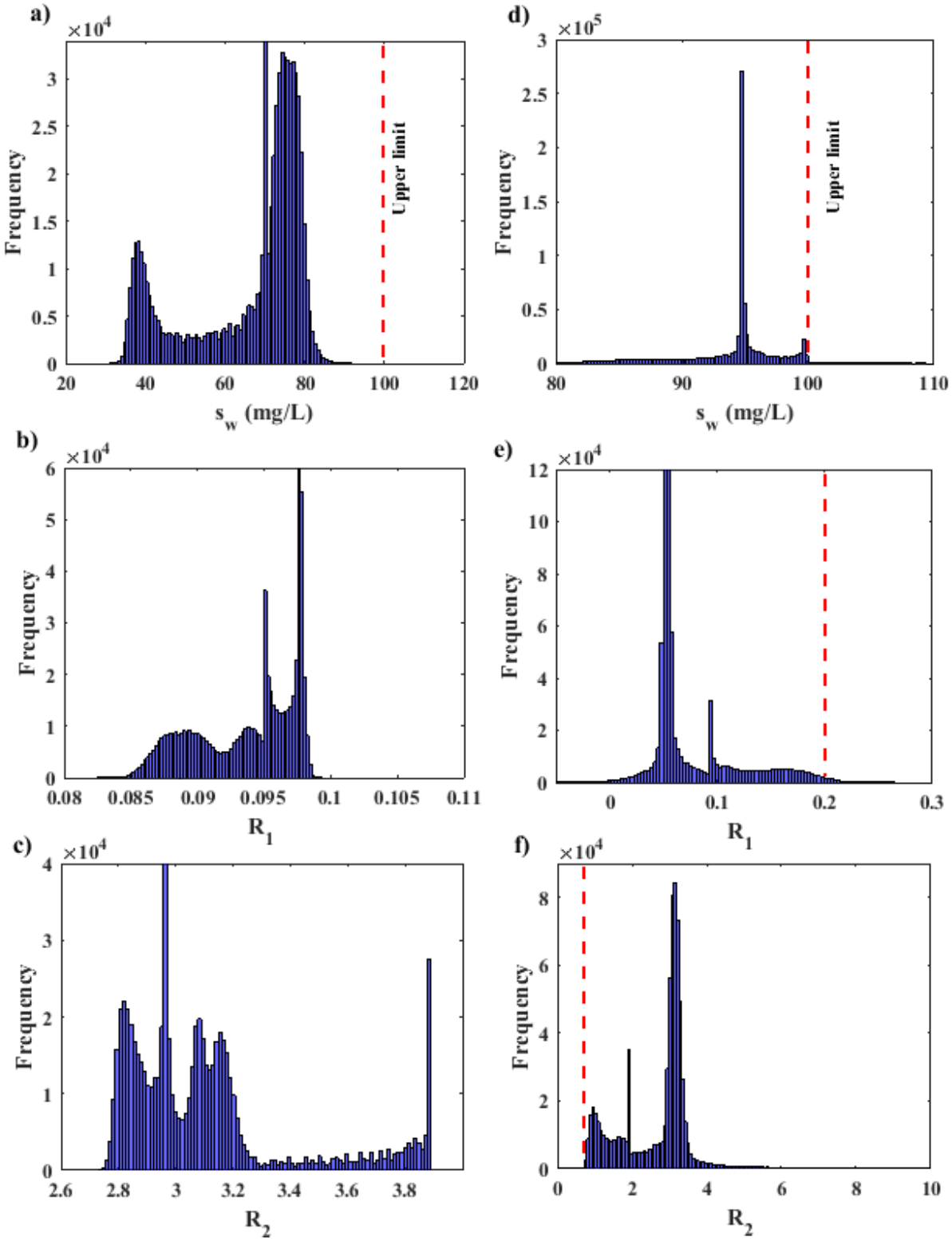

Figure 4-5: Simulation results. *Sc1*: using expected value and variance (a,b,c); *Sc2*: using confidence interval (d,e,f). Red dashed lines indicate input limits on the constraints.

Table 4-4: Effect of uncertainty

	Sc3	*Sc4*	*Sc5*
Confidence weights	All constraints @ $\mathbb{CI}^{0.99}$	All constraints @ $\mathbb{CI}^{0.99}$	All constraints @ $\mathbb{CI}^{0.99}$
	$q_i = Asin(wt) + q_{i_{nom}}$	$q_i = Asin(wt) + q_{i_{nom}}$	$q_i = Asin(wt) + q_{i_{nom}}$
Disturbances	$A = \mathcal{N}(10,10)$ $w = \mathcal{N}(0.001,0.001)$	$A = \mathcal{N}(10,10)$ $w = \mathcal{N}(0.001,0.001)$	$A = \mathcal{N}(10,10)$ $w = \mathcal{N}(0.001,0.001)$
Uncertainty	No time-invariant uncertain parameter	$\mu_w = \mathcal{U}(0.1,0.2)$	$\mu_w = \mathcal{U}(0.1,0.2)$ $k_c = \mathcal{U}(0.66\text{x}10^{-4}, 1.99\text{x}10^{-4})$ $k_d = \mathcal{U}(2.5\text{x}10^{-5}, 5.5\text{x}10^{-5})$ $s_i = \mathcal{N}(366,5)$ $x_i = \mathcal{N}(80,5)$
Optimization variables			
Area (m^2)	1,696.04	2,584.41	3,453.72
Volume (m^3)	1,402.68	2,469.10	2,240.45
$s_{w_{sp}}$	98.27	91.22	90.44
$c_{w_{sp}}$	0.006951	0.001214	0.003397
K_{c1}	12.50	1.24	1.25
K_{c2}	0.047113	0.042849	0.047749
τ_{i1}	10	42.27	52.26
τ_{i2}	35.44	64.04	69.21
Cost ($/a)	$1.7320\text{x}10^6$	$1.0073\text{x}10^7$	$1.1690\text{x}10^7$

4.2.2 Effect of uncertainty

The aim of this section is to evaluate the performance of the back-off methodology under the effect of disturbances, single and multiple uncertainties. As shown in Table 4-4, a time-varying sinusoidal disturbance in the inlet flowrate ($q_i = Asin(wt) + q_{i_{nom}}$) with a frequency and amplitude that follow normal distributions with specified means and variances are considered ($q_{i_{nom}} = 600$). In *Sc3-Sc5*, the coverage probability of confidence interval of all the process constraints shown in Table 4-2 was set to 0.99 (i.e. $\mathbb{CI}^{0.99}$). As shown in Figure 4-6 and Table 4-4, the present approach compensates for the various uncertainties and disturbances considered at the expense of economics; thus, the system moves further away from steady-state optimal design to compensate for the potential occurrence of single and multiple realizations. Consequently, the amount of back-off is generally seen as a factor strongly related to the significance, type and variation of the uncertainties, i.e. larger (or more drastic) changes in uncertainty may cause larger amounts of back-off. *Sc5* has the largest cost compared to *Sc3* and *Sc4* due to the multiple sources of uncertainties considered in that scenario. As shown in Table 4-4, *Sc5*, which considers the effect of disturbance and multiple uncertainties, specified a plant cost that is 91% higher than that specified by

Sc3, which only considers disturbance effects. Moreover, *Sc4* returned a plant that is 82% more expensive than that obtained for *Sc3*; this result provides an indication of the impact of single parameter uncertainty (μ_w) on the system. For the present case study, the area of the decanter (A_d), the volume of the reactor (V_r) and the substrate set-point ($s_{w_{sp}}$) dominate the process economics (see cost function in Table 4-2). Thus, changes in these variables will directly impact the process dynamics and therefore the selection of the optimal design and control scheme.

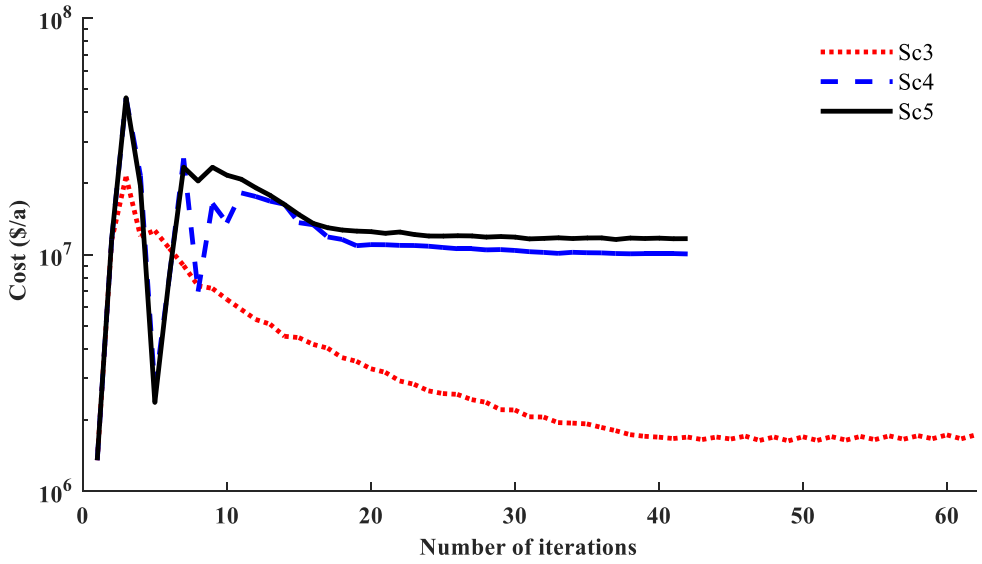

Figure 4-6: Cost function for different scenarios in uncertain parameters

As illustrated in Figure 4-7, the substrate set-point moves away from the threshold (100 mg/L) in exchange for the assurance of constraint satisfaction at the specified coverage probability limit in the presence of disturbances and uncertainties.

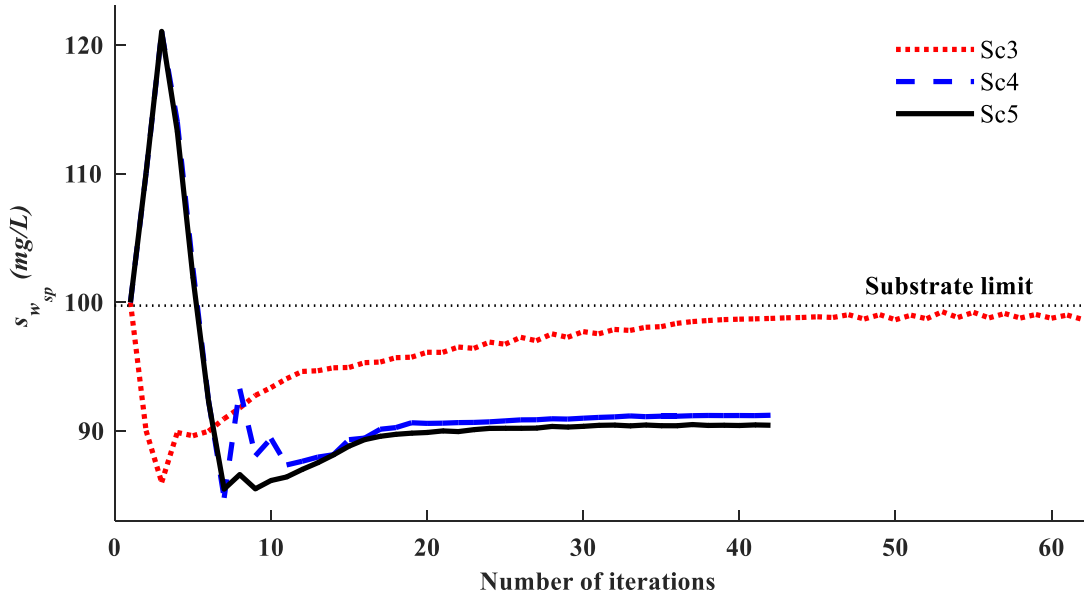

Figure 4-7: Substrate set-point different scenarios in uncertain parameters

4.2.3 Effect of coverage probability of process constraints

As mentioned above, this methodology provides an additional degree of freedom to the user to assign different probabilities of satisfaction to each constraint, i.e. coverage probability for the confidence interval of each constraint. While critical constraints need to be prioritized, violation of non-critical restrictions might be tolerated during operation. Table 4-5 shows the details and results of various scenarios considered in this section using different coverage probabilities for the confidence intervals of the constraints. The uncertainties and disturbance specifications outlined for *Sc5* in Table 4-4 were used to perform this analysis.

Table 4-5: Effect of coverage probability

Constraints	***Sc6***	***Sc7***	***Sc8***
s_w^{up}	@ $\mathbb{CI}^{0.5}$	@ $\mathbb{CI}^{0.99}$	@ $\mathbb{CI}^{0.9999}$
R_1^{lo}	@ $\mathbb{CI}^{0.9999}$	@ $\mathbb{CI}^{0.5}$	@ $\mathbb{CI}^{0.9999}$
R_1^{up}	@ $\mathbb{CI}^{0.9999}$	@ $\mathbb{CI}^{0.5}$	@ $\mathbb{CI}^{0.9999}$
R_2^{lo}	@ $\mathbb{CI}^{0.9999}$	@ $\mathbb{CI}^{0.5}$	@ $\mathbb{CI}^{0.9999}$
R_2^{up}	@ $\mathbb{CI}^{0.9999}$	@ $\mathbb{CI}^{0.5}$	@ $\mathbb{CI}^{0.9999}$
Optimization variables			
Area (m^2)	2,194.85	2,314.61	3,694.62
Volume (m^3)	1,820.07	2,248.86	2,495.53
$s_{w_{sp}}$	99.99	98.81	88.84
$c_{w_{sp}}$	0.008230	0.000595	0.070516
K_{c1}	0.226	20	1.032
K_{c2}	0.031928	0.029829	0.061932
τ_{i1}	57.81	70	47.18
τ_{i2}	70	61.91	13.66
Cost ($/a)	1.8530×10^6	2.3179×10^6	1.5230×10^7

As shown in Table 4-5, specifying a higher probability of satisfaction in the constraints, i.e. 0.9999 (*Sc8*) instead of 0.99 (*Sc5*), significantly impacts the process economics, i.e. *Sc8* produced a design and control scheme that is 23% more expensive than that obtained by *Sc5*. Figure 4-8 shows the convergence of the cost function for the different scenarios considered in this section. As shown in the figure, lowering the probability of satisfaction, particularly in the key process constraints, can potentially improve the process economics. For example, changing the coverage probability specification on constraint s_w^{up} from 0.9999 (*Sc8*) to 0.5 (*Sc6*) while keeping the rest at a constant coverage probability reduces the plant costs by almost 87%. Likewise, setting the coverage probability of constraint s_w^{up} to 0.99 while keeping the remaining constraints to 0.5 (*Sc7*) specified a plant design that is 80% less expensive than that obtained for *Sc5* (i.e. all the constraints were set to 0.99 probability of satisfaction).

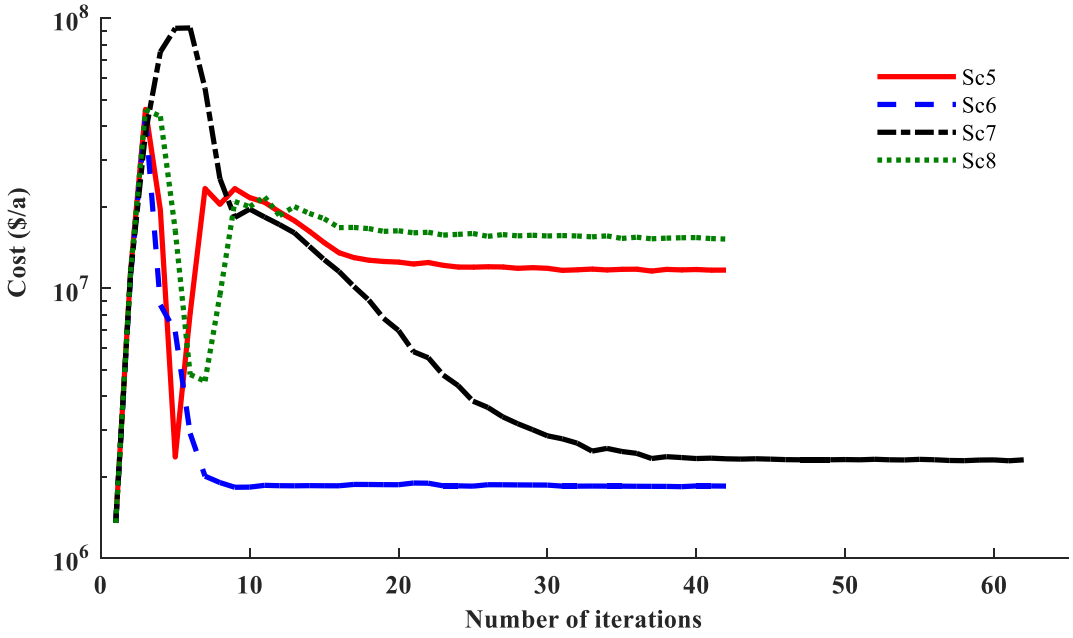

Figure 4-8: Cost, the effect of confidence weights

These results show that the substrate concentration in the decanter is a key constraint in this process since it directly impacts the process variability costs (Table 4-2). Figure 4-9 shows the simulation results using the optimal design and control scheme obtained from *Sc6*. This figure indicates that using a high coverage probability in the constraints interval forces the system to remain in the desired boundaries of constraints at the expense of higher cost. As a result, there is no violation of the constraints on the purge ratio (R_1) and purge age (R_2); however, the constraint on the maximum allowed substrate is tolerable to be violated at most 50%, which agrees with the coverage probability specified for this constraint (see Table 4-5).

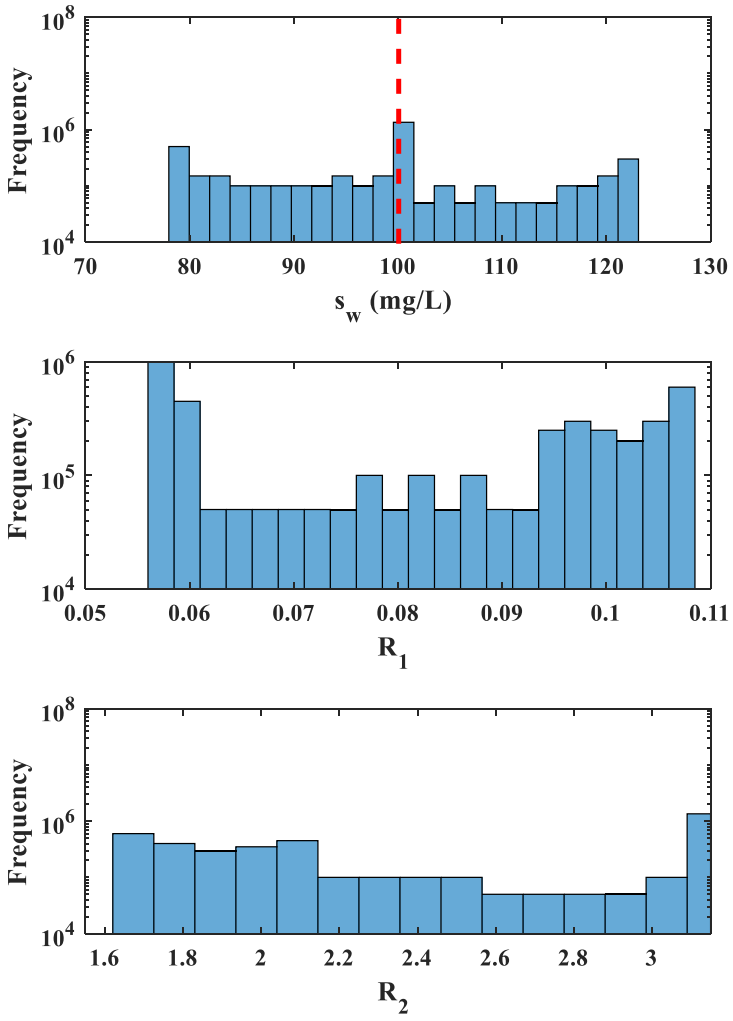

Figure 4-9: Simulation results (*Sc6*)

Table 4-6: Effect of multiple sources of uncertainty

	Sc9
Confidence weights	All constraints @ $\mathbb{CI}^{0.99}$
Disturbances	$q_i = Asin(wt) + q_{i_{nom}}$ $A = \mathcal{N}(10,10)$ $w = \mathcal{N}(0.001,0.001)$
Uncertainty	$\mu_w = \mathcal{U}(0.1,0.2)$ $k_c = \mathcal{U}(0.66\text{x}10^{-4}, 1.99\text{x}10^{-4})$ $k_d = \mathcal{U}(2.5\text{x}10^{-5}, 5.5\text{x}10^{-5})$ $s_i = \mathcal{N}(366,5)$ $x_i = \mathcal{N}(80,5)$ $n = \mathcal{U}(1.8,2.2)$
Area (m^2)	3,476.70
Volume (m^3)	2,273.37
$s_{w_{sp}}$	90.22
$c_{w_{sp}}$	0.006228
K_{c1}	1.24
K_{c2}	0.033603
τ_{i1}	49.42
τ_{i2}	63
Cost ($/a)	$1.2154\text{x}10^7$

4.2.4 Computational costs

This section aims to provide estimates on the computational demands associated with the present stochastic back-off methodology. Once the optimal problem has been defined, most of the CPU time required by the present approach is used to estimate the sensitivities needed to build the probabilistic-based PSE functions, i.e. see *Step 3* in the algorithm. The accuracy of the PSE functions is highly correlated with the number of MC samples required and the desired accuracy in the results, which is mostly controlled by the tolerance criterion (ϵ_{MC}). Table 4-6 shows the results of *Sc9* in which multiple sources of uncertainties and disturbances have been considered. Figure 4-10 shows the CPU time and the required number of MC samples per iteration that were needed to solve *Sc3* and *Sc9*. *Sc3* only considers a time-varying disturbance, i.e. it does not consider model parameter uncertainty. In addition to a stochastic disturbance, *Sc9* also considers multiple sources of uncertainties as well as a model structure error (see Table 4-6). Note that the uncertainty considered on power term n in the process (see Section 3.4) can be considered as a potential source of model structure error since it directly affects a time-dependent state variable for this system, i.e.

the biomass concentration. In the present analysis, the power term *n* in the differential state equation for the biomass concentration was assumed to follow a uniform distribution. As shown in Table 4-6, *Sc9* produced a design and control scheme that is 4% more expensive than that obtained by *Sc5*, which is the same scenario but without consideration of model structure error. As shown in Figure 4-10, there exists a correlation between CPU time and problem size. That is, *Sc9* required approximately 1.46 hours to converge (i.e. total CPU time), which is 46% higher than the total CPU time required by *Sc3*. On average, *Sc3* required 1.22×10^3 MC samples whereas *Sc9* involved 37% more samples i.e. 3.25×10^3. As shown in Figure 4-10, a few peaks in the required number of MC samples are observed for *Sc3*, e.g. around iteration 40. This behaviour suggests that sinusoidal changes in the disturbances (with random realizations in the frequency) together with the system nonlinearities around $\boldsymbol{\eta}_{nom}$ at those iterations directly affect the computation of the sensitivity terms in the PSE-based functions; hence, a larger number of simulations are needed to ensure convergence in the statistical terms.

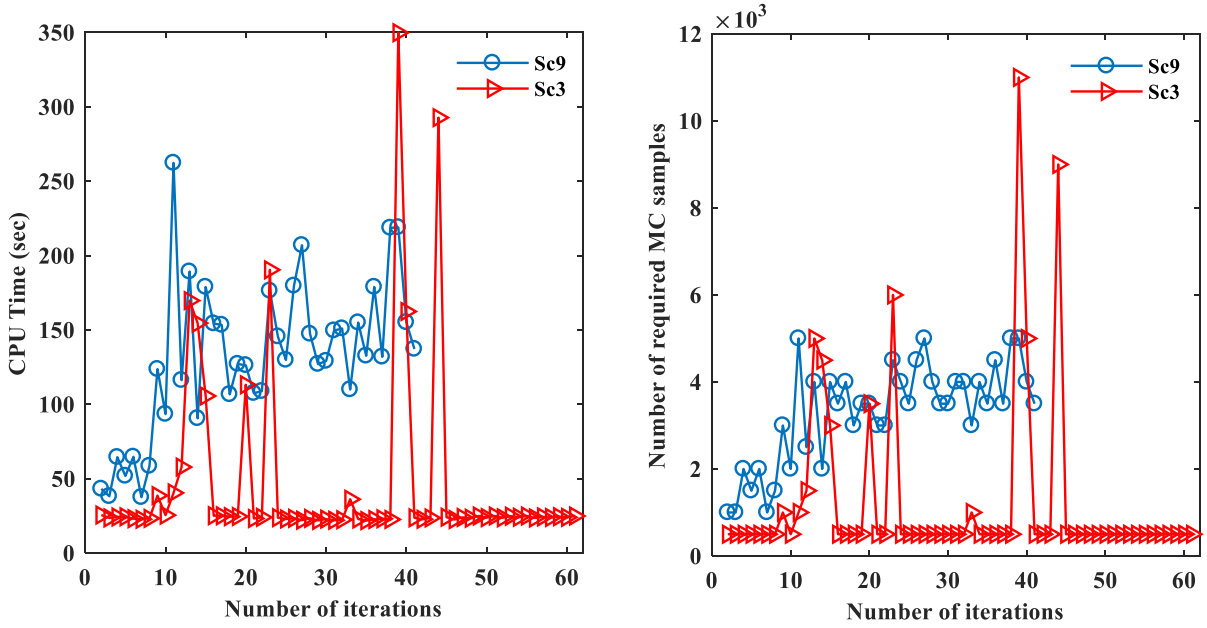

Figure 4-10: CPU time and number of required MC samples at different iterations for *Sc3* and *Sc9*

In terms of scalability, undoubtedly, adding more decision variables makes the problem more intense as it involves the computation of another set of sensitivity calculations. Also, the model complexity will increase

the computational costs, i.e. the more complex model the longer to simulate. Nevertheless, the main computational expenses in this method are directly correlated with the number and the nature of stochastic uncertain parameters considered in the analysis. Adding an additional uncertain parameter increases the domain of the uncertain space thus requiring the need to consider a larger set of realizations between the uncertain parameters, which requires the need to perform additional simulations and eventually increases the computational demands of the present approach.

In summary, a stochastic back-off methodology that addresses simultaneous design and control using stochastic uncertainty descriptions was presented. The key idea is to describe the confidence interval of process constraints at user-defined coverage probabilities using PSE-based functions. PSE functions are explicitly defined in terms of the optimization variables. The method provides an additional degree of freedom since it can allocate different levels of confidence for the process constraints using coverage probability of confidence intervals. The wastewater treatment plant introduced in Section 3.4 was used to illustrate the benefits and limitations of the present approach. The results presented in this study indicate that the proposed back-off approach leads to more economically attractive designs when compared to the variance-based approach. The main burden of the current stochastic-based technique is the need for numerous simulations of the system to obtain the PSE functions. For that reason, the next step in this research is to reduce the number of required samples in the analysis to achieve a certain level of accuracy in the calculations using advanced sampling and uncertainty quantification methods. In the current methodology, the search space region (δ) in the PSE-base optimization problem was specified *a priori*.

5 Trust-region approach

The aim of this chapter is to present a practical and systematic method for the integration of design and control for large-scale applications. In chapters 3 and 4, the search space region in the PSE-based optimization problem was specified *a priori*. Selecting a constant search space for the PSE functions may undermine the convergence of the methodology since the predictions of the PSEs highly depend on the nominal conditions used to develop the corresponding PSEs. In the current chapter, a trust-region framework is proposed that relies on an adaptive search space for individual decision variables in PSE-based optimization problems at every iteration. The concept is designed in a way that certifies the competence of the PSE functions at each iteration and systematically acquires the search space of the optimization as the iteration proceeds in the algorithm.

The key idea is to represent the system using PSEs as piecewise models in an iterative manner while the validity of those expansions is certified in a trusted interval. The mean of squared errors is used as a metric to quantify the accuracy of the PSE approximations. Identified search regions specify the boundaries of the decision variables for the PSE-based optimization problems. The proposed algorithm shows a significant accomplishment in locating dynamically feasible and near-optimal design and operating conditions. The proposed approach was tested for the integration of design and control of the wastewater treatment plant (introduced in Chapter 3) as an illustrative example and the Tennessee Eastman (TE) process. The results indicate that the proposed methodology has the potential to identify economical, computationally attractive and reliable designs for large-scale applications. Part of the results presented in this chapter has been published in (Rafiei and Ricardez-Sandoval, 2020b).

The chapter is organized as follows: Section 5.1 presents the methodology of the trust-region method followed by an illustrative example to discuss details of the implementation (Section 5.2). Later, the application of the proposed methodology on a large-scale application, i.e. the TE process, is presented (Section 5.3). The simultaneous design and control of the TE plant is studied in two stages. First, the design

and control of the reactor section are considered. Second, the trust-region method for simultaneous design and control of the complete TE plant is implemented.

5.1 Methodology

The basic back-off approach featured with PSEs was introduced earlier in Chapter 3. The basic back-off approach is extended to tackle simultaneous design and control of the large-scale process. The extended back-off approach is called trust-region approach since it systematically identifies trusted intervals for the validity of the surrogate models. Similar to the basic back-off, PSEs are employed to capture plant behaviour; in particular, they are used to represent the cost function and process constraints in Problem (2-1). Hence, PSE replicas in the optimization problem lessen the burden of nonlinear programming by approximating process nonlinear behaviour over a small region in the neighborhood of a nominal condition. Even though PSE models provide inexpensive evaluations of the functions, they are often limited to the vicinity of the nominal condition and cannot provide good estimations for the entire operating region. In that event, faulty estimations of the PSE function may lead to inaccurate or even unrealistic predictions. Thus, the accuracy of the expansions and their validity region must be carefully chosen. The predictability properties of the approximation are highly correlated to the nominal condition in which the PSEs are expanded upon. For that reason, the behaviour of the system is examined using piecewise PSE models in an iterative manner in which the nominal condition is updated as the procedure moves towards a solution.

The approach is a sequential approximate optimization method in which the system is evaluated around the worst-case variability expected in process outputs. The method mostly traces the closest feasible and near-optimal solution to the initial steady-state condition considering the worst-case scenario. A surrogate model (PSE) has been used to approximate the actual model behaviour of the process and alleviate the intense computational demands. The term near-optimal refers to the potential deviations from the original locally optimum due to the approximation techniques considered in this work, e.g. the use of a low-order process model to represent the system's behaviour around a nominal operating point. In the previous chapters, an

adequate (trust) region and thus a fixed search space for the PSE-based optimization problem at each iteration has been defined *a priori*. The key assumption made in those works is that a conservative region was specified that was identified offline. In addition, it is assumed that the search space region remains constant for all the decision variables during the implementation of the algorithm. The previous method works efficiently for small- and medium-scale applications. However, that approach might become cumbersome to handle large-scale and highly nonlinear systems. For highly nonlinear and large-scale processes, identification of a trust-region around a nominal value that remains valid for the entire back-off procedure is a challenging task and might become intractable. In the present approach, an adaptive search strategy is proposed to identify the trust-region for each decision variable systematically. Moreover, the trust-region is identified for every decision variable ($\boldsymbol{\eta}$) at each iteration. Accordingly, the adaptive approach may impose some restrictive boundaries on some decision variables regarding the effect of the decision variables in the deviation of the PSE function from the actual nonlinear process behaviour. Particularly for highly nonlinear systems, while the procedure chooses to retain those decision variables at their nominal values on some iterations, the rest of the decision variables may be allowed to be explored in a wider region. Furthermore, developing the trust-region offers the assurance of convergence to a locally optimum solution at the end of the sequential procedure, as it will be described in Section 5.1.2. The convergence of the approach to a locally optimal solution extremely depends on the qualifications of the PSE approximations during the entire sequence of the procedure. In addition, in the basic back-off approach the order of the PSE is decided *a priori* and remains constant for the entire procedure; however, in the current work, the approach can systematically update the order of PSE based on a user-defined level of accuracy.

The trust-region method presented in this chapter is an iterative framework; a schematic of the sequence of the proposed algorithm is presented in Figure 5-1. Each of the steps in the algorithm is described next.

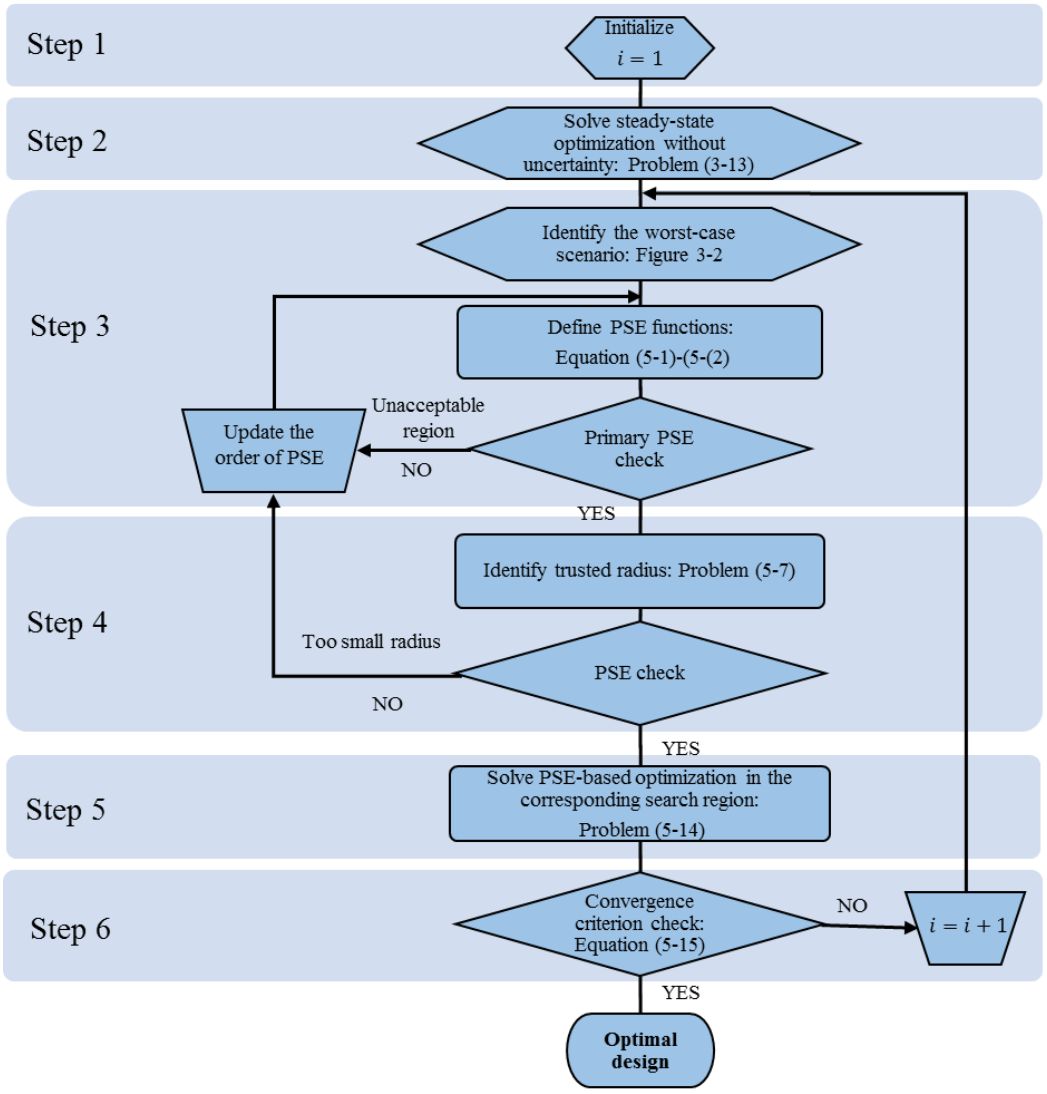

Figure 5-1: Algorithm for the trust-region approach

Step 1 (Algorithm Initialization):

This step is similar to *Step 1* of the basic back-off approach (Chapter 3). Upper ($\boldsymbol{\eta}^U$) and lower bounds ($\boldsymbol{\eta}^L$) for optimization variables ($\boldsymbol{\eta}$), the maximum number of iterations (N_{iter}). PSE validation tolerance (ϵ_{TR}), convergence tolerance (ϵ), convergence examination period (N_c) are defined similarly to the basic approach. Moreover, define the acceptable error range for the PSE validation that is used to define the trust-region (ϵ_{TR}) and step size for the finite-difference calculations ($\Delta\eta$) which is also used as the smallest acceptable trust-region.

Step 2 (Optimal steady-state design without uncertainty and disturbances):

In this step, the initial point for the procedure is specified. Original back-off approaches have been developed based on the idea of moving away from the ideal condition in which uncertain parameters and disturbances are set to their nominal values (Bahri et al., 1995; Kookos and Perkins, 2004; Narraway and Perkins, 1994; Perkins, 1989; Rafiei-Shishavan et al., 2017). Alternatively, the optimal steady-state design can be obtained by solving Problem (3-13) in Chapter 3. The results of the optimization problem ($\boldsymbol{\eta}_0$) can be used as the starting (initial) point to search for the dynamically operable design that optimizes an objective function for this process. The proposed trust-region method searches the closest dynamically feasible condition to the initial starting point. Typically, the idealistic steady-state condition is the most convenient condition to start the search for a new dynamically feasible condition in the presence of uncertainty and disturbances. However, the steady-state optimum might be unavailable or difficult to obtain, e.g. the optimal steady-state of a black-box model such as the Tennessee Eastman (TE) process. In those cases, the procedure can be initiated from a user-defined educated condition, e.g. current designs from similar plants.

Step 3 (Develop PSE-based functions):

The proposed trust-region framework aims to find the optimal solution which ensures that the system remains dynamically feasible in the presence of the largest (worst-case) variability observed in the constraints as discussed in Chapter 3. Function evaluations for the forward ($\boldsymbol{\eta}^+$) and backward ($\boldsymbol{\eta}^-$) points around the nominal condition are used to estimate the sensitivity of the cost and constraint functions to optimization variables (see Figure 5-2). The first- and second-order gradients of the s^{th} inequality constraints (g_s) are calculated as follows:

$$\left.\frac{\partial g_s}{\partial \eta_p}\right|_{t_{wc},\zeta_j} = \left(g_s(\eta_p^+)|_{t_{wc},\zeta_j} - g_s(\eta_p^-)|_{t_{wc},\zeta_j}\right)/2\Delta\eta_p \tag{5-1}$$

$$\left.\frac{\partial^2 g_s}{\partial \eta_p \partial \eta_p}\right|_{t_{wc},\zeta_j} = \left(g_s(\eta_p^+)|_{t_{wc},\zeta_j} - 2g_s(\eta_{p_{nom}})|_{t_{wc},\zeta_j} + g_s(\eta_p^-)|_{t_{wc},\zeta_j}\right)/\Delta\eta_p{}^2 \tag{5-2}$$

where $\Delta\eta_p$ is the finite-difference step used to calculate forward and backward points of p^{th} decision variable, i.e. $\Delta\eta_p = \eta_{p_{nom}}(\Delta\eta)$. Once the numerical sensitivities of cost function and constraints with regard to all decision variables have been identified, the quality of the constructed PSE is examined in a primary PSE check. The error between the actual functions and their PSE evaluations at the nominal condition ($\boldsymbol{\eta}_{nom}$) must remain negligible for all the cost and constraints (e.g. less than 1%). In the primary PSE check, if the error is not acceptable the default order of the PSE should be updated to ensure rigorous calculations at nominal condition since the entire procedure is constructed based on this calculation. Originally, second-order PSEs are used as the accuracy often is mostly acceptable for most engineering calculations. The order can later be updated if the default value is incapable of capturing the dynamic behaviour to a certain level of accuracy. The order of the PSE depends on the process nonlinearity and also the required accuracy. Increasing the order of PSE is computationally expensive. In order to calculate higher-order PSE additional forward and backward points are required.

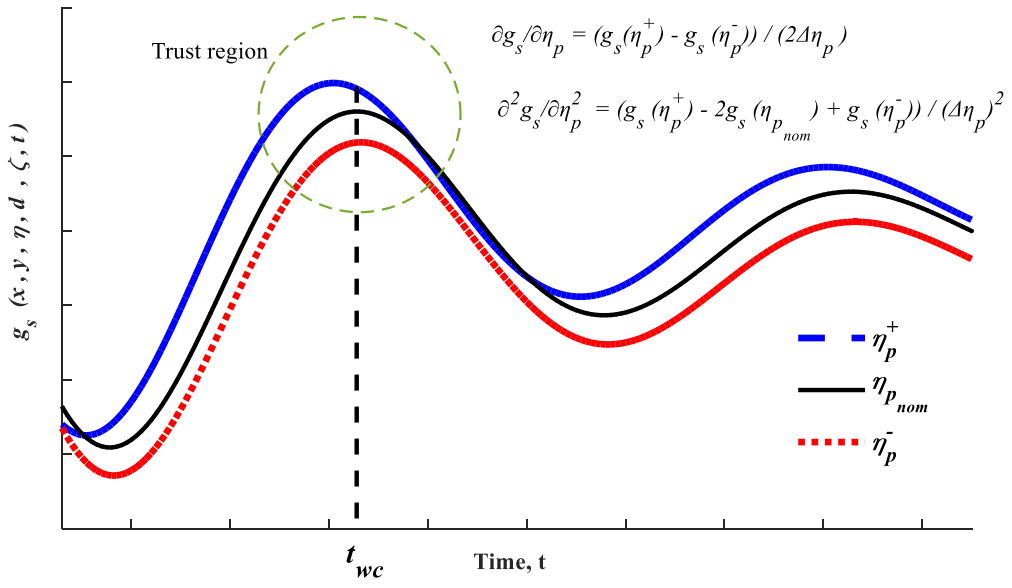

Figure 5-2: Simulations for the nominal condition, forward and backward points at the worst-case scenario

Step 4 (Identify the trust-region):

PSE functions are often valid for small vicinity around the nominal condition ($\boldsymbol{\eta}_{nom}$) at which they have been developed. The trust-region for each decision variable at each iteration of the procedure is identified to avoid inaccurate representations of the actual nonlinear system. To specify the trust-region at each iteration step i, the area is explored in which the error of the PSE evaluations compared to the actual functions remains within a certain threshold defined by the user (ϵ_{TR}). Once the gradients of the constraints and cost function are calculated and the PSE functions are built (*Step 3*), the constructed PSE functions can be used to evaluate the cost and constraint at different points ($\boldsymbol{\eta}^*$) away from the nominal condition. The mean squared error (MSE) is used as the performance metric to identify the region in which the PSEs are valid. The errors between the actual value of the cost function and process constraints and their corresponding PSE approximations are estimated as follows:

$$MSE_S = \frac{1}{2}\left\{\left(\frac{g_s(\boldsymbol{\eta}_{nom}+\boldsymbol{\delta}) - g_{s,PSE}(\boldsymbol{\eta}_{nom}+\boldsymbol{\delta})}{g_s(\boldsymbol{\eta}_{nom}+\boldsymbol{\delta})}\right)^2 + \left(\frac{g_s(\boldsymbol{\eta}_{nom}-\boldsymbol{\delta}) - g_{s,PSE}(\boldsymbol{\eta}_{nom}-\boldsymbol{\delta})}{g_s(\boldsymbol{\eta}_{nom}-\boldsymbol{\delta})}\right)^2\right\} \quad \forall s = 1, \dots S \tag{5-3}$$

$$MSE_\theta = \frac{1}{2}\left\{\left(\frac{\Theta(\boldsymbol{\eta}_{nom}+\boldsymbol{\delta}) - \Theta_{PSE}(\boldsymbol{\eta}_{nom}+\boldsymbol{\delta})}{\Theta(\boldsymbol{\eta}_{nom}+\boldsymbol{\delta})}\right)^2 + \left(\frac{\Theta(\boldsymbol{\eta}_{nom}-\boldsymbol{\delta}) - \Theta_{PSE}(\boldsymbol{\eta}_{nom}-\boldsymbol{\delta})}{\Theta(\boldsymbol{\eta}_{nom}-\boldsymbol{\delta})}\right)^2\right\} \tag{5-4}$$

where $\boldsymbol{\delta} \in \mathbb{R}^P$ represents the distance from the nominal value of the decision variables ($\boldsymbol{\eta}_{nom}$) and is defined for each decision variable ($\boldsymbol{\eta} \in \mathbb{R}^P$). The interval of the trust-region ($\boldsymbol{\delta}$) defines the region in which the PSE approximations are valid and can be used as equivalent representations of the actual nonlinear model. $g_{s,PSE}$ and Θ_{PSE} are the PSE function of s^{th} constraint and the cost function developed for the worst-case scenario as follows:

$$\Theta_{PSE}(\boldsymbol{\eta}^*) = \Theta(\boldsymbol{\eta}_{nom})|_{t_{wc},\zeta_j} + \sum_{p=1}^{P} \left.\frac{\partial \Theta}{\partial \eta_p}\right|_{t_{wc},\zeta_j} \left(\eta_p^* - \eta_{p_{nom}}\right) + \sum_{p=1}^{P} \frac{1}{2} \left.\frac{\partial^2 \Theta}{\partial \eta_p^2}\right|_{t_{wc},\zeta_j} \left(\eta_p^* - \eta_{p_{nom}}\right)^2 + R_2(\boldsymbol{\eta}^*) \tag{5-5}$$

$$g_{s,PSE}(\boldsymbol{\eta}^*) = g_s(\boldsymbol{\eta}_{nom})|_{t_{wc},\zeta_j} + \sum_{p=1}^{P} \left.\frac{\partial g_s}{\partial \eta_p}\right|_{t_{wc},\zeta_j} \left(\eta_p^* - \eta_{p_{nom}}\right) + \sum_{p=1}^{P} \frac{1}{2} \left.\frac{\partial^2 g_s}{\partial \eta_p^2}\right|_{t_{wc},\zeta_j} \left(\eta_p^* - \eta_{p_{nom}}\right)^2 + R_2(\boldsymbol{\eta}^*) \tag{5-6}$$

Likewise, g_s and Θ in (5-3) and (5-4) are the actual values of s^{th} constraint and the cost function, respectively. The trust-region interval is obtained from the following optimization problem:

$$\min_{\boldsymbol{\delta}} \frac{1}{MSE_{\Theta} + \sum_{s=1}^{S} MSE_s} \tag{5-7}$$

Subject to:

$$MSE_s \leq \epsilon_{TR} \,, \forall s = 1, \ldots S$$

$$MSE_{\Theta} \leq \epsilon_{TR}$$

$$\boldsymbol{\delta}^L < \boldsymbol{\delta} < \boldsymbol{\delta}^U$$

This optimization problem aims to search for the maximum acceptable region $\boldsymbol{\delta} \in \mathbb{R}^P$ for all decision variables around the nominal values ($\boldsymbol{\eta}_{nom}$) such that the MSE tolerance (ϵ_{TR}) is satisfied. The smallest acceptable interval ($\boldsymbol{\delta}^L$) is defined according to the finite-difference step size ($\Delta\eta$) that is used to estimate the PSE functions in *Step 3*. The upper bound of the interval ($\boldsymbol{\delta}^U$) is defined by the user. Problem (5-7) fails to converge if the original constructed PSEs are not accurate enough. In that case, higher-order PSE functions can be used to improve the quality of the expansions. Moreover, if small changes in the decision variables produce an unacceptable error, the system will be driven to update the order of the PSE with the aim to increase the prediction capabilities of these functions around ($\boldsymbol{\eta}_{nom}$) and therefore reduce the MSE. Figure 5-3 shows the schematic of the selection of trusted intervals.

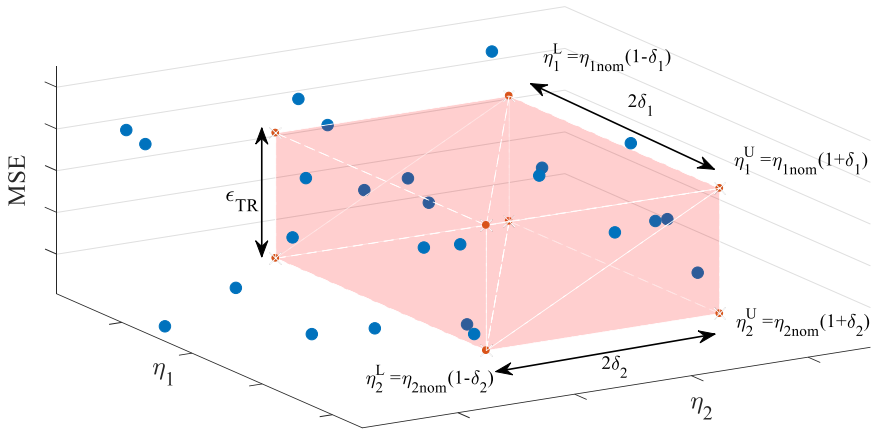

Figure 5-3: Schematic of the trust-region concept

The formulation of Problem (5-7) results in a sequential optimization strategy since the simulation of the actual nonlinear model is required for the evaluation of the MSEs. Thus, the DAE model (*F* in Problem (2-

1)) is solved in an inner loop using integration algorithms and the information is directed to the NLP solver as shown in Figure 5-4.

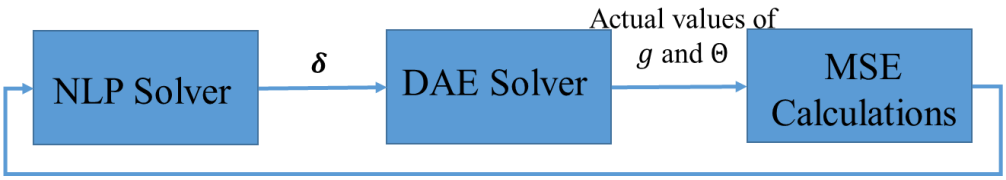

Figure 5-4: Sketch of sequential optimization

Although the implementation of the approach is relatively simple, it is prone to some deficiencies. First, only partial information from DAE is exchanged with the NLP; in particular, the DAE solver acts as a black-box for the optimization. This integration scheme might affect the pursuit of the optimal solution. Second, excessive iterations in the optimization approach might be required as the NLP attempts to find a descent direction which may result in high computational demands. Furthermore, the convergence is highly influenced by the length of the integration of the DAE solver, i.e. interval$(0, t_f]$. Above all, in the case of an unstable system that is highly sensitive to initial conditions, the sequential method might remain insufficient (Biegler, 2010). To circumvent these issues, an alternative approach is proposed next, which aims to search for the trust-region using an iterative method.

5.1.1 Stepwise search (alternative method for *Step 3*)

Here a systematic stepwise search method is introduced to identify the trusted region. The presented stepwise search method is an alternative in case the sequential formulation of trust-region shown in Problem (5-7) fails to converge or leads to unacceptable computational costs. The schematic of this algorithm is shown in Figure 5-5.

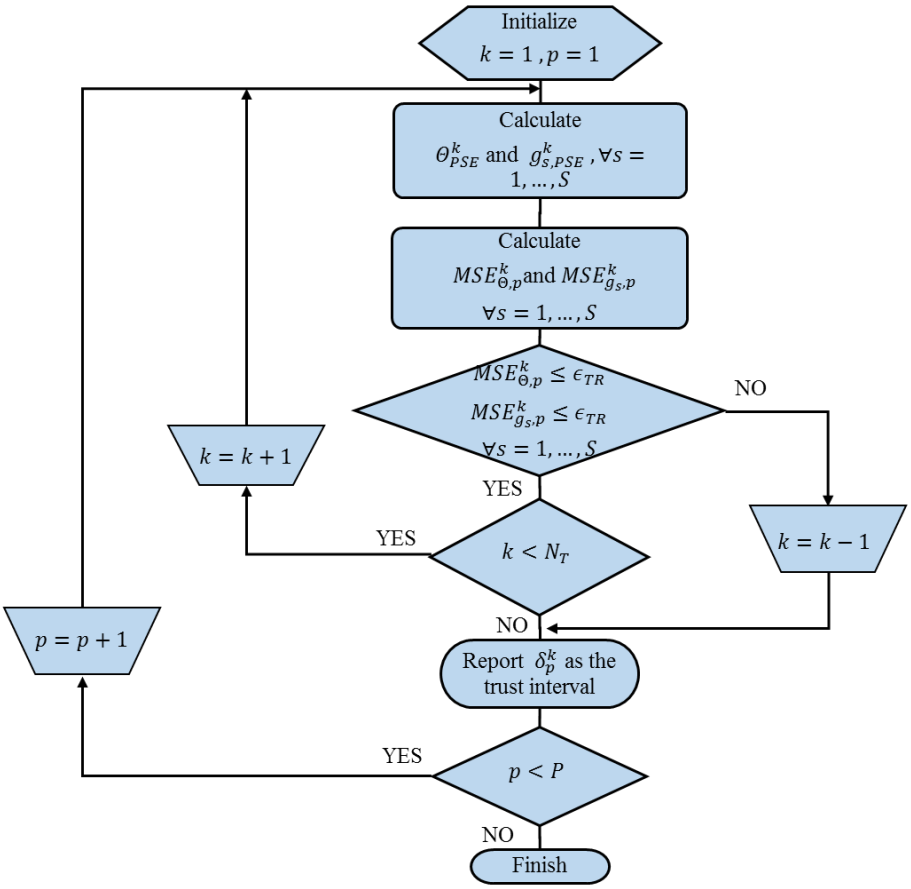

Figure 5-5: Schematic of the stepwise search for trust-region

This procedure of searching for the trusted region is as follows:

a) Specify a maximum number of steps (N_T) and a tolerance criterion to check for the validity of the PSE estimation of the cost function and constraints (ϵ_{TR}). Also, initialize an index (k), which keeps track of the increments in the search space, i.e. set $k = 1$. Start from the first decision variable, i.e. $p = 1$. The initial interval is defined according to the step size of the finite-difference ($\Delta\eta$) as follows:

$$\delta^k_p = \eta_{p_{nom}} \Delta\eta, \qquad k = 1, \qquad \forall p = 1, \dots P \tag{5-8}$$

b) The PSE sensitivities generated in *Step 2* of the general procedure shown in Equation (5-5) and (5-5) are used to estimate the cost function and constraint values at a new interval. The p^{th} decision

variable is changed while keeping the rest of the decision variables at their nominal value. The PSE at the corresponding interval is calculated as follows:

$$\Theta_{PSE}^{k}(\eta_{p_{nom}}+\delta_p^k)=\Theta(\eta_{p_{nom}})\big|_{t_{wc},\zeta_j}+\frac{\partial\Theta}{\partial\eta_p}\bigg|_{t_{wc},\zeta_j}(\delta_p^k)+\frac{1}{2}\frac{\partial^2\Theta}{\partial\eta_p^2}\bigg|_{t_{wc},\zeta_j}(\delta_p^k)^2+R_2(\delta_p^k) \tag{5-9}$$

$$g_{s,PSE}^{k}(\eta_{p_{nom}}+\delta_p^k)=g_s(\eta_{p_{nom}})\big|_{t_{wc},\zeta_j}+\frac{\partial g_s}{\partial\eta_p}\bigg|_{t_{wc},\zeta_j}(\delta_p^k)+\frac{1}{2}\frac{\partial^2 g_s}{\partial\eta_p^2}\bigg|_{t_{wc},\zeta_j}(\delta_p^k)^2+R_2(\delta_p^k) \tag{5-10}$$

c) MSE is used to measure the differences between the PSE estimation and the actual cost function and process constraints. The MSEs for the constraints and cost function at the k^{th} step of interval increase for the p^{th} decision variable are as follows:

$$MSE_{g_s,p}^{k}=\frac{1}{2}\Bigg\{\Big(g_s(\eta_{p_{nom}}+\delta_p^k)\big|_{t_{wc},\zeta_j}-g_{s,PSE}(\eta_{p_{nom}}+\delta_p^k)\big|_{t_{wc},\zeta_j}\Big)^2+\Big(g_s(\eta_{p_{nom}}-\delta_p^k)\big|_{t_{wc},\zeta_j}-g_{s,PSE}(\eta_{p_{nom}}-\delta_p^k)\big|_{t_{wc},\zeta_j}\Big)^2\Bigg\},\ \forall s=1,\dots,S \tag{5-11}$$

$$MSE_{\theta,p}^{k}=\frac{1}{2}\Bigg\{\Big(\Theta(\eta_{p_{nom}}+\delta_p^k)\big|_{t_{wc},\zeta_j}-\Theta_{PSE}(\eta_{p_{nom}}+\delta_p^k)\big|_{t_{wc},\zeta_j}\Big)^2+\Big(\Theta(\eta_{p_{nom}}-\delta_p^k)\big|_{t_{wc},\zeta_j}-\Theta_{PSE}(\eta_{p_{nom}}-\delta_p^k)\big|_{t_{wc},\zeta_j}\Big)^2\Bigg\} \tag{5-12}$$

where $MSE_{g,s}^{k}$ is the error in the s^{th} inequality constraints caused by the changes in p^{th} decision variable at k^{th} interval. Similarly, MSE_{Θ}^{k} is the error of the cost function due to the changes in p^{th} decision variable at k^{th} interval.

d) In principle, the interval is gradually increased and at each step of increase (k) it is determined whether the error is acceptable or not. If MSEs calculated in 5-11 and 5-12 fall beyond a user-defined threshold (ϵ_{TR}), then STOP, a trusted interval has been identified for the p^{th} decision variable (δ_p) at the previous increment $(k-1)$. Otherwise, while $k<N_T$ update $k=k+1$ and go back to *Step b*, i.e. increase the interval size and calculate the updated MSE. Note that k represents the index that keeps track of the number of times that the step is changing, i.e.

If $MSE_{g_s,p}^{k} \leq \epsilon_{TR}, \forall s = 1, \dots, S$ and $MSE_{\Theta}^{k} \leq \epsilon_{TR}$
Then
$\delta_p^{k+1} = \delta_p^k + \eta_{p_{nom}} \Delta\eta\,, \qquad \forall p = 1, \dots P$ (5-13)

Also, if the maximum allowable increase (N_T) is reached, then STOP, a trusted interval has been identified for the p^{th} decision variable (δ_p). The interval is calculated for decision variables one at a time. Once the interval is confirmed for p^{th} decision variables, update the decision variable ($p = p + 1$) and go back to *Step b*. Thus, the MSE at the new interval is calculated and tolerance criterion ϵ_{TR} is checked for the errors created by changing the decision variables. If the changes in a certain decision variable create larger deviations, the corresponding decision variable will remain constant and the sensitivity to other decision variables will be examined. The search continues until the maximum allowable deviations for all decision variables have been identified. The step size in the current work has a linear growth starting from the step size used to calculate numerical gradients, i.e. $\Delta\eta$. The step-growth can also be geometric if the system allows severe changes in the step size. The effect of the combination of changes in decision variables on the error-index is missing since the stepwise approach identifies the trust-region changing one decision variable at a time while keeping the rest of the decision variables at their nominal values.

Problem (5-7) simultaneously changes the decision variables and thus captures the effects of the changes of decision variables, i.e. trust-regions, on the error-index. However, the stepwise search (Section 5.1.1) independently identifies the effect of changes in every decision variable, i.e. the contribution of the trust-region of one decision variable to the error-index is measured while the rest of the variables are set to their nominal values. Ideally, the solution of Problem (5-7) is preferred; however, the optimization problem may become challenging for large-scale systems and also result in high computational costs as discussed above.

In summary, I define an individual interval for each decision variable, i.e. allowable search space for pth decision variable (δ_p). Identifying $\boldsymbol{\delta}$ is a considerable improvement to the previously introduced back-off methodology. The unique search space for each decision variable enables the algorithm to solve, at each

iteration step, PSE-based optimization problems that would approach the local optimal solution of the original problem in a systematic manner. Although identification of the trust-region requires higher CPU times, the algorithm performs efficiently in terms of the number of successive iterations required to converge, i.e. some decision variables are explored in a wider region compared to others thus allowing the algorithm to converge faster. Furthermore, the quality of the PSEs is preserved within a certain threshold during the execution of the algorithm.

Step 5 (Optimization of the PSE-based functions):

The PSE functions of the cost function and the constraints built-in *Step 3* are embedded within a PSE-based optimization problem defined as follows:

$$
\begin{aligned}
&\min_{\boldsymbol{\eta},\boldsymbol{\lambda},\boldsymbol{\mu}} \ \Theta_{PSE}(\boldsymbol{\eta})|_{t_{wc},\zeta_j} + \sum_{s}^{S} M_1\,\lambda_s + \sum_{q}^{Q} M_2\,\mu_q \\
&\text{Subject to:} \\
&\quad h_{PSE_q}(\boldsymbol{\eta}))\Big|_{t_{wc},\zeta_j} - \mu_q = 0\,, \forall q = 1,\dots,Q \\
&\quad g_{PSE_s}(\boldsymbol{\eta}))\Big|_{t_{wc},\zeta_j} - \lambda_s \le 0\,, \forall s = 1,\dots,S \\
&\quad \eta_{p_{nom}}\left(1-\delta_p\right) \le \eta_p \le \eta_{p_{nom}}\left(1+\delta_p\right)\,, \forall p = 1,\dots,P \\
&\quad \lambda_s \ge 0\,, \forall s = 1,\dots,S \\
&\quad \mu_q \ge 0\,, \forall q = 1,\dots,Q
\end{aligned}
\qquad (5\text{-}14)
$$

where the search space for the p^{th} decision variables is limited to δ_p identified from *Step 4*; λ_s and μ_q are optimization variables used to avoid infeasibility in the s^{th} and q^{th} constraint function ($g_{PSE\,s}$ and $h_{PSE\,q}$), respectively. The weights M_1 *and* M_2 are sufficiently large penalty terms used to drive the feasibility variables ($\boldsymbol{\lambda}, \boldsymbol{\mu}$) to zero and enable the specification of a dynamically feasible system that minimizes the cost function. The latter also referred to as the big-M method, is used here to ensure feasible solutions in Problem (5-14), particularly in the first iterations of the algorithm where the process constraints cannot accommodate dynamic feasibility with the limited search space region defined by $\boldsymbol{\delta}$. The selection of M_1 and M_2 heavily dictate the path to reach to the feasible region in the proposed back-off procedure. Therefore, the system might take different pathways to encounter the infeasibility in the constraint concerning the weights assigned to the infeasibility of the constraints and corresponding penalty terms. Although some

heuristics can be used to specify appropriate penalty terms, adopting the weights and penalty terms are user-defined and are mostly decided based on the nature of the process. Typically, assigning a penalty term which is at least two orders of magnitudes higher than the highest cost observed in the system provides acceptable results.

Step 6 (Convergence Criterion):

A floating average convergence technique, i.e. the difference in means, is considered here as a stopping criterion and is defined as follows:

$$Tol_{float}^{\Theta} = \left(\sum_{v=i-2N_c+1}^{i-N_c} \Theta_v - \sum_{r=i-N_c+1}^{i} \Theta_r\right) \Big/ \sum_{r=i-N_c+1}^{i} \Theta_r \tag{5-15}$$

where Θ_v and Θ_r represent the cost function values obtained from the solution of Problem (5-14) at the v^{th} and r^{th} iterations, respectively. If $\left|Tol_{float}^{\Theta}\right| \leq \epsilon$, then STOP, the method converged to an optimal solution. Otherwise, set $i = i + 1$, update the optimization variables ($\boldsymbol{\eta}_{nom}$) with the most recent solution obtained from Problem (5-14) and go back to *Step 3*. Alternatively, the algorithm is also terminated if the maximum number of iterations is reached, i.e. $i \geq N_{iter}$. A summary of the steps of the current trust-region method is available on Appendix A. Table 5-1 lists the tuning parameters required by the present method and their recommended values.

Table 5-1: Tuning parameters of the trust-region technique

Tuning parameter	Description	Recommended values
N_c	Convergence examination period, the higher the value the longer to check for convergence of the algorithm	10-30
N_{iter}	Maximum number of iterations allowed in the algorithm	≥300
ϵ	Termination tolerance for the algorithm	≤1x10^{-3}
ϵ_{TR}	Tolerance criteria for the validation of PSE expansions of cost and constraints	5-10%
$\boldsymbol{\delta}^U$	Maximum allowable trust-region in Problem (5-7)	$0.1\eta_{nom}$
PSE order	Order of the PSE expansion. Problem-specific and directly correlated to the nonlinearity of the problem under consideration- default value can be set to 2 and it will be updated if necessary	2-4
$\Delta\eta$	Step size considered to estimate the sensitivity of the cost function and process constraints with respect to the optimization variables	$0.01\eta_{nom}$-$0.02\eta_{nom}$
M_1, M_2	Penalty term that forces the system to move within the dynamic feasibility region	$10^3\Theta$-$10^5\ \Theta$

5.1.2 Optimality conditions

In this section, the equivalence of the simultaneous optimization of the design and control formulated as a dynamic optimization (i.e. Problem (2-1)) and the PSE-based optimization (Problem (5-14)) and its significance to the first-order optimality conditions in the proposed trust-region method is discussed. Typically, feasibility has a higher priority than optimality in the solution of optimization problems (Biegler, 2010). Accordingly, in the back-off formulation due to the existence of the penalty terms in the cost function (i.e. $\sum_s^S M_1\ \lambda_s$ and $\sum_q^Q M_2\ \mu_q$) and the higher weights assigned to the infeasibility (M_1, M_2), the PSE-based optimization prioritizes the search for a feasible direction by forcing the feasibility variables $(\boldsymbol{\lambda}, \boldsymbol{\mu})$ to zero. Once the feasibility is maintained, the optimization searches for a descent direction to reduce the objective function in such a way that it contains local optimality characteristics.

Let impose some restrictions on the formal integration of design and control problem introduced in Problem (2-1). The bounded optimization Problem (5-14) can be reformulated as follows:

$$\min_{\boldsymbol{\eta}} \Theta\,(\dot{\boldsymbol{x}}, \boldsymbol{x}, \boldsymbol{y}, \boldsymbol{\eta}, \boldsymbol{d}, \boldsymbol{\zeta}, t) \tag{5-16}$$

Subject to:

$$H: \begin{cases} F_{model}(\dot{\boldsymbol{x}}, \boldsymbol{x}, \boldsymbol{y}, \boldsymbol{\eta}, \boldsymbol{d}, \boldsymbol{\zeta}, t) = 0 \\ h_q(\dot{\boldsymbol{x}}, \boldsymbol{x}, \boldsymbol{y}, \boldsymbol{\eta}, \boldsymbol{d}, \boldsymbol{\zeta}, t) = 0\ , \forall q = 1, \dots Q \end{cases}$$

$$g_s(\dot{\boldsymbol{x}}, \boldsymbol{x}, \boldsymbol{y}, \boldsymbol{\eta}, \boldsymbol{d}, \boldsymbol{\zeta}, t) \leq 0 \,, \forall s = 1, \dots S$$
$$\eta_p^L < \eta_{p_{nom}}(1 - \delta_p) < \eta_p < \eta_{p_{nom}}(1 + \delta_p) < \eta_p^U \;\; , \forall p = 1, \dots N_{Dec}$$

where H is the combination of the dynamic model and the equality constraints since these are the constraints that must be persistently satisfied. In what it follows, it is assumed that the optimization problem has reached the region where there exists a feasible solution that can be achieved for the bounded decision variables, i.e. all feasibility variables ($\boldsymbol{\lambda}, \boldsymbol{\mu}$) have approached zero. Otherwise, the optimization might fail to identify a solution since the decision variables are bounded to a limited search space defined by $\boldsymbol{\delta}$. The boundaries imposed on the decision variables are the same obtained in *Step 4* using the trust-region interval (δ_p) for each p^{th} decision variable. If a local solution can be obtained from Problem (5-16), then the first-order Karush-Kuhn-Tucker (KKT) optimality conditions are as follows:

$$\nabla_\eta L(\boldsymbol{\eta}^*, \boldsymbol{u}^*, \boldsymbol{v}^*, \boldsymbol{u}_L^*, \boldsymbol{u}_U^*) = \nabla_{\boldsymbol{\eta}} \Theta + \nabla_{\boldsymbol{\eta}} g^T \boldsymbol{u}^* + \nabla_{\boldsymbol{\eta}} H^T \boldsymbol{v}^* - \boldsymbol{u}_L^* + \boldsymbol{u}_U^*$$

Feasibility: (5-17)

$$H(\dot{\boldsymbol{x}}, \boldsymbol{x}, \boldsymbol{y}, \boldsymbol{\eta}, \boldsymbol{d}, \boldsymbol{\zeta}, t) = 0 \,,$$
$$g_s(\dot{\boldsymbol{x}}, \boldsymbol{x}, \boldsymbol{y}, \boldsymbol{\eta}, \boldsymbol{d}, \boldsymbol{\zeta}, t) \leq 0 \,, \forall s = 1, \dots S$$

Complementarity:

$$g^T \boldsymbol{u}^* = 0 \,, \boldsymbol{u}^* \geq 0$$

where $\boldsymbol{u}^*$ and $\boldsymbol{v}^*$ are corresponding multipliers for the inequality and equality constraints, respectively whereas $\boldsymbol{u}_L^*$ and $\boldsymbol{u}_U^*$ are the corresponding bound multipliers for the decision variables.

On the other hand, PSEs are obtained under the assumption that the surrogate dynamic models are given by Equation (3-1) capture the characteristics of the actual constraints and cost function around a nominal point ($\boldsymbol{\eta}_{nom}$). Although the dynamic model does not appear in the PSE-based formulation, it is implicitly considered through the development and construction of the PSE functions. Thus, the dynamic model of the system is satisfied implicitly by the PSE-based optimization (Problem 5-14). Hence, the dynamic model associated with equality constraints (H_{PSE}) is considered as they both are intrinsically fulfilled in the development of the PSE functions. Based on the above, the KKT conditions for the PSE-based problem are as follows:

$$\nabla_{\boldsymbol{\eta}} L(\boldsymbol{\eta}^*, \boldsymbol{u}^*, \boldsymbol{v}^*, \boldsymbol{u}_L^*, \boldsymbol{u}_U^*) = \nabla_{\boldsymbol{\eta}} \Theta_{PSE} + \nabla_{\boldsymbol{\eta}} g_{PSE}^T \boldsymbol{u}^* + \nabla_{\boldsymbol{\eta}} h_{PSE}^T \boldsymbol{v}^* - \boldsymbol{u}_L^* + \boldsymbol{u}_U^*$$

Feasibility:

$$H_{PSE}(\boldsymbol{\eta}) = 0$$
$$g_{PSE_s}(\boldsymbol{\eta}) \leq 0 \,, \forall s = 1, \dots S \qquad (5\text{-}18)$$

Complementarity:

$$g^T \boldsymbol{u}^* = 0 \,, \boldsymbol{u}^* \geq 0$$

By comparing equations (5-17) and (5-18) it can be observed that both problems are equivalent in the neighborhood of the nominal condition if the numerical derivation of the PSE functions and actual functions are equivalent (Biegler et al., 1985). A sufficient condition is as follows:

$$\nabla_{\boldsymbol{\eta}} \Theta_{PSE} = \nabla_{\boldsymbol{\eta}} \Theta, \qquad \nabla_{\boldsymbol{\eta}} g = \nabla_{\boldsymbol{\eta}} g_{PSE}, \qquad \nabla_{\boldsymbol{\eta}} h = \nabla_{\eta} h_{PSE} \qquad (5\text{-}19)$$

As shown in *Step 3* and Equation (5-1) and (5-2), during the development of the PSE approximations we obtain the gradients of the cost function and constraints with respect to the decision variables, i.e. $\nabla \Theta(\boldsymbol{\eta})|_{t_{wc}, \zeta_j}$ and $\nabla g_s(\boldsymbol{\eta})|_{t_{wc}, \zeta_j}$. The only difference between the two formulations originates from the numerical error in the sensitivity calculations. Thus, it can be concluded that the PSE-based optimization in the present approach is equivalent to the bounded formal integration in the vicinity of the nominal condition. Therefore, an optimal solution to the bounded formal integration shown in Problem (5-16) can be translated into an optimal solution for PSE-based optimization in Problem (5-14). If the proposed algorithm converges, then the solution satisfies first-order KKT local optimality conditions and is equivalent to the solution obtained from a formal integration around that optimal point. In summary, the trust-region method guarantees convergence to a local optimum if at all iterations there is a local solution for the PSE-based optimization. At each iteration, the PSE-based optimization is required to converge to a local optimum solution; otherwise, the procedure may result in sub-optimal solutions due to a misleading search direction in the decision variables.

The proposed trust-region method still carries some limitations that can be further explored. For instance, structural (integer) decision variables involving changes in the design and/or control structure cannot be considered at this point and is a part of the future work considered in this research. The proposed approach can be extended to simultaneously design and control of batch processes. In batch processes, the dynamic behaviour of the system is closely tied with the design parameters and may extremely affect the performance of the process. Consequently, simultaneous design and control provides an attractive opportunity for further improvements in batch processes, in particular for biological systems. The biological systems are associated with multiple uncertain parameters and are typically designed as batch processes. Moreover, most of the biological processes consider manual or open-loop control strategies that require deliberate tuning considerations at the design stage. The current back-off approach is capable of performing integration design and control for batch processes with multiple uncertain parameters with open-loop or manual control strategies as long as the model of the system is available.

5.2 Illustrative case study: wastewater treatment plant

The wastewater treatment plant introduced in Chapter 3 was used as a case study to test the proposed trust-region framework. The process is designed to regulate the level of the substrate concentration (s_w) in the biodegradable waste stream. Table 5-2 provides the cost function and the process constraints that determine the feasible operating region for this process. The disturbance profile comprises step changes in the inlet flowrate (q_i) that happen at multiple time intervals (i.e. every 10 hours). The magnitudes of step changes are reported in Table 5-2. The computational experiments performed in this chapter were conducted using a computer running Microsoft Windows Server 2016 Standard. The computer was equipped with 96 GB RAM and 2 processors of Intel® Xeon® CPU E5-2620 v4 @ 2.10GHz.

Table 5-2: Model equations of the wastewater treatment plant

Description	Equations
Cost function: • CC_w : capital cost • OC_w : operating cost	$\Theta_W = \underbrace{0.16(3500\,V_r + 2300\,A_d)}_{CC_w} + \underbrace{870(f_k + q_p)}_{OC_w}$
Constraints:	
• Maximum allowable substrate concentration in the treated water that leaves the decanter	$s_w(t) \leq 100$
• Minimum and maximum allowed ratio between the purge to the recycle flowrates	$0.01 \leq \frac{q_p(t)}{q_2(t)} \leq 0.2$
• Allowed purge age in the decanter	$0.8 \leq \frac{V_r x_w(t) + A_d l r x_r(t)}{24\ q_p x_r(t)} \leq 15$
Optimization variables	$[A_d, V_r, s_{w_{sp}}, c_{w_{sp}}, K_{c1}, K_{c2}, \tau_{i1}, \tau_{i2}]$
Disturbance realizations (q_i)-step changes	{600, 630, 580,610,580}

5.2.1 Results

This case study is primarily used to test the capabilities of the trust-region method for a medium-scale application. The simultaneous design and control of this plant has been studied using three different approaches, formal integration approach (Problem (2-1)), basic back-off with a fixed search space (Chapter 3), and the trust-region algorithm proposed in the current chapter. Moreover, the trust-region is identified using two distinct methods, i.e. standard search for the validation region using the formulation presented in Problem (5-7), and an alternative stepwise iterative strategy proposed to identify the trusted interval, shown Section 5.1.1. The implementation of the formal integration of design and control optimization problem was performed in Pyomo (version 3.6) using a simultaneous discretization approach for dynamic optimization with and automatic discretization scheme (backward/collocation point). The tuning parameters and details regarding the basic back-off with a fixed search space have been reported in Chapter 3. For the trust-region method, the acceptable error range for the PSE validation (ϵ_{TR}) is set to 5%. The initial condition for all three methods is set to steady-state optimum under the assumption of no uncertainty and disturbances. Table 5-3 summarizes the results for the four different approaches considered for this case study.

Table 5-3: Summary of the results: formal integration, basic back off, and trust-region

	Formal integration	**Basic back-off (fixed search space)**	**Trust-region method**	**Trust-region method using the stepwise search**
Decision variables				
Area (m^2)	1,165.7	1,197.7	1,165.38	1,164.75
Volume (m^3)	1,437.7	1,421.7	1,438.4	1,438.9
$s_{w_{sp}}$	90	90.4	90	90
$c_{w_{sp}}$	0.06	0.06	0.06	0.06
K_{c1}	0.30	0.32	0.30	0.30
K_{c2}	0.11	0.31	0.69	0.83
Cost ($/a)	$4.965x10^8$	$5.013x10^8$	$5.003 x10^8$	$5.003x10^8$
Converged iteration	-	62	42	42
CPU (s)	14.15	20.13	1,226	167

As indicated in Table 5-3, all approaches converged to approximately similar results (i.e. less than 1% differences in cost function values and significant decision variables). The similarity in the outcomes obtained from these methods demonstrates the ability of the techniques to perform simultaneous design and control. The solutions obtained from the basic back-off and the trust-region are equal to the optimal solution of formal integration framework and the gradients of the first order KKT conditions are the same (not shown for brevity). The discrepancy in the gain of the second controller (K_{c2}) is because the optimization is not that sensitive to changes in this decision variable. As listed in Table 5-3, the formal integration technique requires relatively short CPU times and performs faster than other techniques; however, the application of formal integration is limited to relatively small or medium-scale problems. As the size and complexity of the process increase, e.g. by adding more uncertain scenarios combined with additional time-dependent disturbances, the implementation of formal integration (i.e. dynamic optimization) becomes challenging and computationally demanding. For the basic back-off, a constant search space (2% of the nominal value of the decision variables) was used that was specified offline. A fixed search space must be chosen in a way that provides validity of the PSE function for all decision variables during the entire back-off procedure; therefore, a conservative search space according to the smallest acceptable region was defined for this case study. On the other hand, the trust-region method is able to systematically choose different regions for decision variables at different stages of the integration procedure. Accordingly, the trust-region converged to the optimal solution after 42 iterations since the PSE-based optimization has more freedom to change the

decision variable's search space per iteration, whereas the basic back-off reaches to the same solution after 62 iterations. The proposed trust-region is capable of updating the order of PSE systematically based on a user-defined level of accuracy. Accordingly, the order of PSE may change at each iteration. For the current case study, second-order PSE remains sufficient for most of the iterations. Note that the CPU time for the trust-region is 2 orders of magnitude higher than the basic back-off. Since the current case study is a medium-scale problem, it is non-trivial to find a suitable search space for the basic back-off while the trust-region finds that value systematically at the expense of higher CPU times. As will be shown in the next section, the systematic identification of trusted interval is crucial for large-scale processes with highly nonlinear behaviour since the appropriate fixed search space is difficult to detect. Figure 5-6 shows a comparison between the two trust-region identification methods proposed in this study (see *Step 4* in Section 5.2). One method represents the solution of the problem (5-7) while the other is the stepwise method presented in Section 5.1.1. Both methods can capture the sensitivity of error-index (MSE) to the changes in the decision variables. Problem (5-7) is designed in a way that all decision variables are changing at the same time and the correlated impact on the error-index can be measured. On the other hand, the stepwise search (Section 5.1.1) independently identifies the effect of changes in every decision variable. The differences between the two approaches shown in Figure 5-6 stem from the correlation between the changes of decision variables. Solving Problem (5-7) in a sequential approach carries out the main portion of computations in the procedure and thus causes high CPU demands (see Table 5-3). The stepwise iterative search for the validation region with a lower CPU cost can replace the standard procedure of defining the region attained from Problem (5-7). Other than low CPU demands, the stepwise iterative approach is an attractive alternative for cases when the optimization in Problem (5-7) becomes challenging and computational taxing.

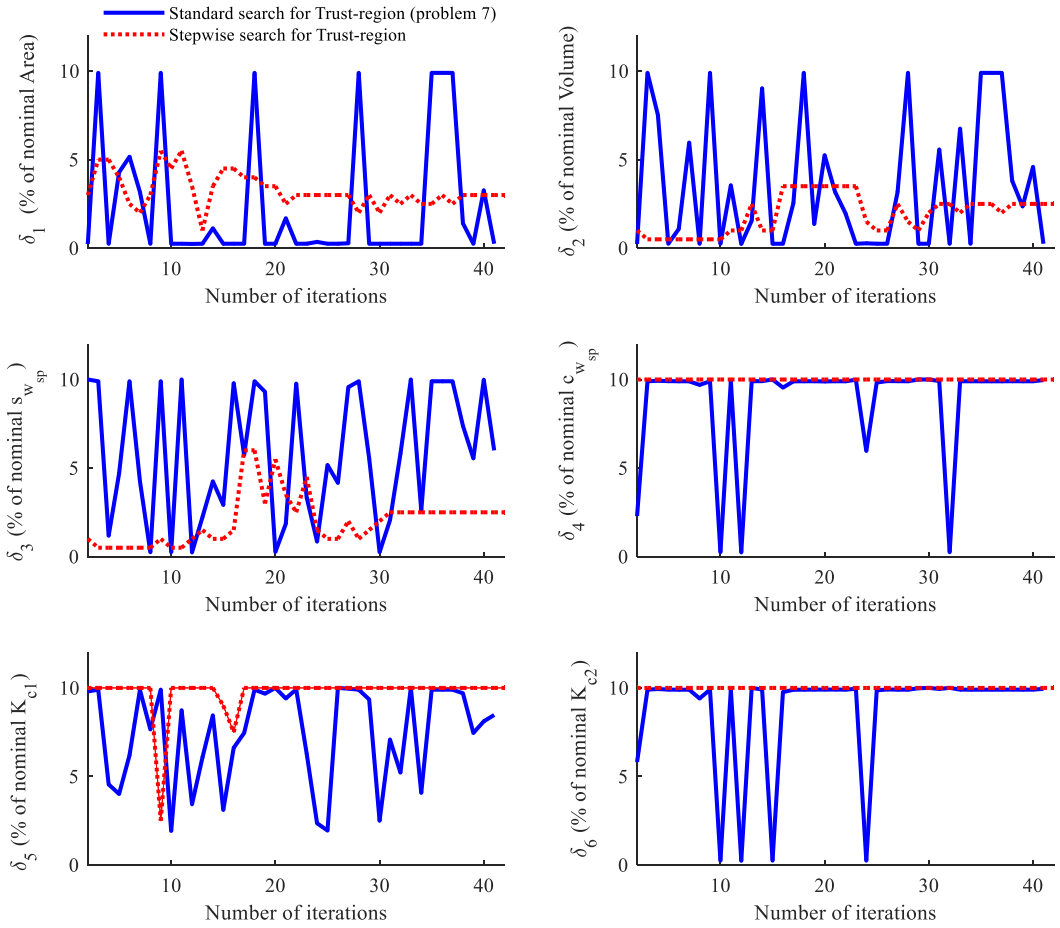

Figure 5-6: Comparison of the trust interval obtained from (Problem (5-7)) and alternative stepwise search

5.3 Large-scale case study: the Tennessee Eastman plant

In order to show the capabilities of the proposed trust-region method on a large-scale system, the method was used to perform integration of design and control of the Tennessee Eastman (TE) plant (Downs and Vogel, 1993). This process produces two main products (G and H) and a by-product (F) from four main reactants (A, C, D, and E) and an inert reactant (B). The process includes five major units: a two-phased exothermic reactor, the product condenser, a vapor-liquid separator, a recycle compressor, and a product stripper column. The mechanistic model of the process is not explicitly available, which restricts the application of model-based techniques for process optimization such as formal integration of design and

control. Instead, a Fortran code is available to simulate the plant under different operating scenarios. The TE plant is designed in a way that includes 12 manipulated variables, 41 output measurements, 19 composition measurements, and 20 potential disturbances. Multiple process goals and constraints including product composition, product rate, control scheme, and operating conditions have been defined for this plant (Downs and Vogel, 1993). Main goals are as follow, i.e.

- Product composition: process variability restrictions are applied on the product's stream, e.g. fluctuations exceeding 5% variations in the product stream are not desired in the process.
- Production rate: Six modes of operation have been defined for the TE plant according to the mix of products and the total mass flow of the production stream. The production rate must remain within a certain limit of the desired target product, e.g. 5% variations.
- Operation conditions: Those must remain within the equipment constraints including liquid levels, reactor pressure, and other safety constraints.
- Control goals: Minimum movements required for the valves and smooth disturbance rejection.

The control of the TE plant has been widely investigated (Larsson et al., 2001; Luyben, 1996; Lyman and Georgakis, 1995; McAvoy and Ye, 1994; Ricker, 1996; Sriniwas and Arkun, 1997). A previous study used process heuristics to develop a decentralized control configuration for this plant (Ricker, 1996). Figure 5-7 shows a schematic of the decentralized control strategy proposed in that study, which consists of 17 PI controllers spread throughout the plant. In the present study, the decentralized control configuration has been used; however, some of the optimal tuning parameters were obtained for the controllers in a simultaneous design and control framework. Downs and Vogel, (1993) identified multiple operating modes for the TE plant. For the purposed of current research, the 50/50-G/H operating mode is only considered.

The operating cost is defined according to the total operating cost at the base case specified by Downs and Vogel (1993). The capital cost function is adopted from the cost considered in a previous study (Ricardez-Sandoval et al., 2011). Therefore, the process units are considered as pressure vessels made of carbon steel with a length/diameter ratio of 4 and the bare module cost for each unit is calculated using diameter (D_{unit})

and maximum allowed working pressure (P_{unit}). Similarly, multiple process constraints according to the process goals and equipment safety are defined. Table 5-4 provides the objective and constraints of the process considered in this study.

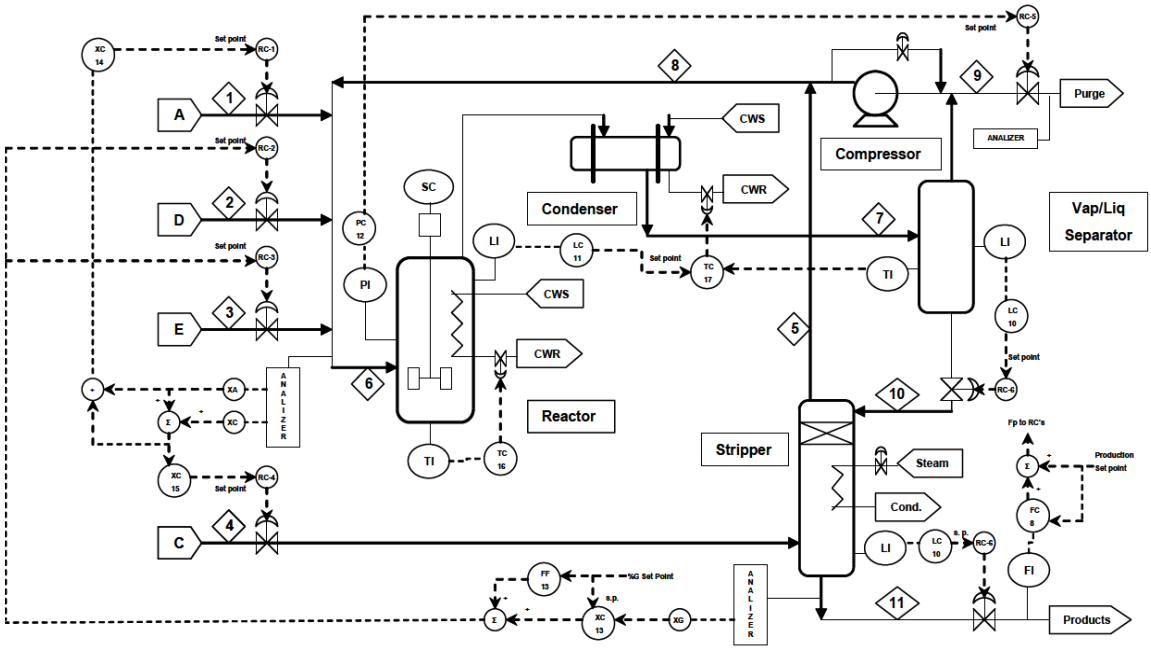

Figure 5-7: Schematic of the decentralized control strategy (Ricker, 1996)

Table 5-4: Key optimization characteristics of the TE process

Objectives:	
Capital cost ($/a) : $CC = r(5946D^{2.1}(19.82 - 12.55\ln \mathrm{P} + 2.36(\ln \mathrm{P})^2)360/315$	
Operating cost ($/hr) : $OP = (\text{purge \$})(\text{purge rate}) + (\text{product \$})(\text{product rate}) + (\text{compressor \$})(\text{compressor work}) + (\text{steam \$})(\text{steam rate})$	
Total cost ($/a) $= CC + (8760)O\mathrm{P}$	
Constraints:	
Variation in the product stream	±5% Variability in the product's G mol fraction
	±5% Variation in the product's stream flowrate
Safety	Reactor's Pressure ≤ 2895 kPa
	Reactor's Temperature ≤ 150 °C
	30 ≤ Reactor's Liquid level ≤ 100
Minimum target product (50/50-G/H)	Product's G mass flowrate ≥7038 kg/hr
	Product's H mass flowrate ≥7038 kg/hr

5.3.1 Scenario I: reactor only

The implementation of the formal integration on the TE process as a large-scale process with a black-box model is computationally challenging and overly demanding. Thus, the trust-region framework proposed in this work is a powerful candidate to simultaneously consider the design and control of a plant whose dynamic behaviour is only available through external sources, e.g. chemical engineering software such as Aspen dynamics or HYSYS. In this study, the Fortran code has been used to conduct the sensitivities computations of the process to the decision variables and construct the piecewise PSE functions.

In this section, the reactor section of the TE plant is only studied. Hence, design and control parameters of the reactor section are only considered as decision variables for this problem whereas the rest of the process variables and controller tuning parameters were set at their nominal values as specified by Ricker (1996, 1995). Accordingly, 13 decision variables for optimization are considered, i.e. reactor design capacity, operating conditions for the reactor unit and the controller tuning parameters of the surrounding control loops. Table 5-5 summarizes the optimization variables for the implementation of the trust-region on the TE plant. The dynamic model of the TE plant has been used that includes all process units. Changes in the

reactor may affect other sections of the plant and are defined as optimization variables in the present analysis. Although the rest of the sections of the plant were not explicitly considered in the present analysis, e.g. operation and design of the separator and stripper, their effects on the reactor performance are explicitly considered in the proposed trust-region approach through the use of the dynamic model for the complete TE plant. The objective of this problem is to define the design and control of the reactor section of this plant that minimizes the annualized capital and operating costs for this unit. Since the reactor section of this plant is studied, the reactor's capacity is a decision variable whereas the flash unit and the stripper column's bare module costs remained fixed to their constant values, i.e. 99.1 m^3 and 4.43 m^3.

Table 5-5: Decision variables for the reactor section

Decision variable (η)	
Design	Reactor's design capacity (m^3)
Adjustable set-points	Reactor's pressure set-point (kPa) Reactor's liquid level set-point (%) Reactor's temperature set-point (°C) Production set-point (m^3/hr);
PI tuning parameters	Kc, τ_I : Purge valve (stream 9) Kc, τ_I : Reactor liquid level (loop17) Kc, τ_I : Reactor pressure (loop5) Kc, τ_I : Reactor temperature

Multiple disturbances affecting the reactor unit introduced by Downs and Vogel (1993) are considered for the present scenario. Table 5-6 shows the step changes in 5 different disturbances along with the corresponding magnitudes of the changes with respect to their nominal value. These disturbances are time-dependent and occur at different intervals throughout the process. The combination of the disturbances creates highly challenging scenarios for the dynamic operation of the reactor unit (Ricker, 1996).

Table 5-6: Disturbances in the TE

	Type	Nominal	Magnitudes	Description
idv(1)	step	95%	4	A/C feed ratio, B composition constant (stream 4)
idv(2)	step	0.5 mol%	1	B composition, A/C ratio constant (stream 4)
idv(3)	step	45°C	2	D feed temperature (stream 2)
idv(4)	step	35°C	2	Reactor cooling water inlet temperature
idv(6)	step	396.1 kmol/hr	2	A feed loss (stream 1)

In the current case study, the stepwise search for the trusted interval has been employed since the implementation of standard search using a sequential optimization approach (Problem (5-7)) was computationally taxing. The tuning parameters of the trust-region method used for the TE plant have been summarized in Table (5-7).

Table 5-7: Tuning parameters of the trust-region method used for the TE plant

Tuning parameter	Description	Recommended values
N_c	Convergence examination period	10
N_{iter}	Maximum number of iterations	500
ϵ	Termination tolerance for the algorithm	$1x10^{-2}$
ϵ_{TR}	Tolerance criteria for the validation of PSEs	10%
$\Delta\eta$	Finite-difference step size	$0.0051\boldsymbol{\eta}_{nom}$
M_1, M_2	Infeasibility penalty terms	$10^5\boldsymbol{\Theta}$

Although the optimal steady-state operation of the TE problem has been considered before, those studies were conducted for specific design factors and focused on the optimal operation at steady-state (Bahakim et al., 2014; Ricker, 1995). The optimal steady-state operating mode (50/50) and current reactor capacity (McAvoy and Ye, 1994) reported in the literature is used as the initial point to implement the trust-region framework (see Table 5-8).

As shown in Figure 5-8, the trust-region introduces a more economically attractive design compared to the base case design currently considered for the reactor unit. As indicated in the figure, a 36% positive back-off is obtained from the base case design and control configuration. The solution from the trust-region framework is the closest feasible solution to the initial base case while the cost is improved and dynamic feasibility is maintained in the presence of the disturbances considered for this study. As discussed in Section 5.1.2, the feasible and near-optimal solution offered by the trust-region has the potential to be a

locally optimal point for this process. Figure 5-9 shows how the system satisfies the process constraints and maintains feasibility by forcing feasibility variables ($\boldsymbol{\lambda}$) to zero. Once the feasibility variables $\boldsymbol{\lambda}$ for all constraints are approaching zero, the dynamic feasibility of the system has been satisfied for the worst-case variability in the TE reactor's operation due to the disturbances considered in the analysis. Some of the constraints remained active at the beginning of the algorithm and thus the proposed method gradually forced the feasibility variables ($\boldsymbol{\lambda}$) and penalty function towards zero to retain dynamic feasibility.

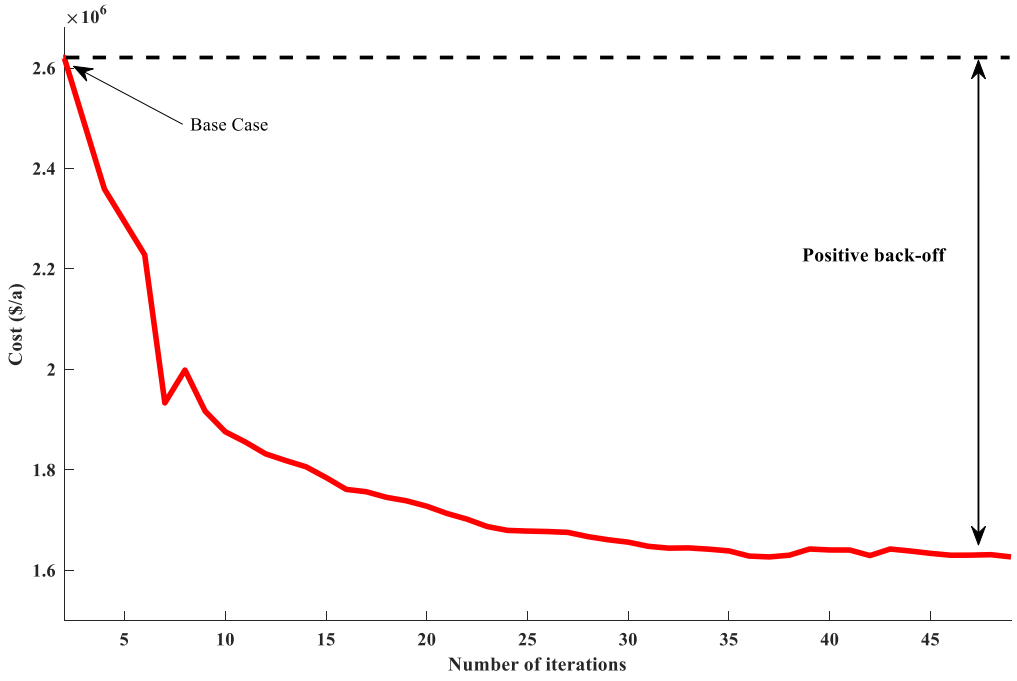

Figure 5-8: Cost function of TE using the trust-region method

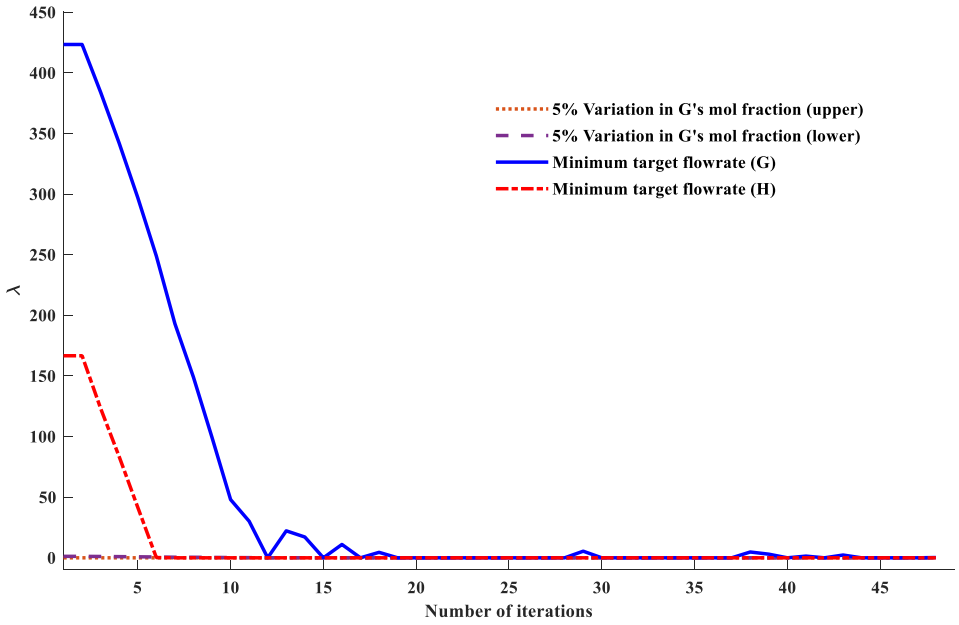

Figure 5-9: The behaviour of feasibility variables (λ) for the rust-region algorithm

The solution obtained from the trust-region is summarized for all the decision variables along with their initial value (base case) in Table 5-8. As discussed above, the trust-region successfully moved the process variables and resulted in a lower annualized cost compared to the base case while maintaining dynamic feasibility under process constraints. As indicated in Table 5-8, increasing the capacity of the reactor allows the system to operate at higher pressure; hence, the set-point was set to 2,894 kPa while it was 2,800 kPa at the base case. The maximization of reactor pressure is in favor of the process economics (Ricker, 1995). The trust-region method suggests a higher-pressure set-point close to the upper bound while avoiding a shut-down. To avoid poor controllability issues at high pressures, the method requires a larger reactor that makes control of the process smoother.

Table 5-8: TE decision variables along with their base case values

Decision variables	Base case (initial condition)	Trust-region method
Reactor's design capacity (m^3)	36.8	45.3
Reactor's pressure set-point (kPa)	2,800	2,894
Reactor's liquid level set-point (%)	65	55.5
Reactor's temperature set-point (°C)	122.9	124.6
Production set-point (m^3/hr)	22.9	23.8
Kc, purge valve (loop5)	0.010	0.034
τ_I ,purge valve (loop5)	$1x10^{-3}$	$5.71x10^{-4}$
Kc, reactor liquid level (loop11)	0.8	0.81
τ_I , reactor liquid level (loop11)	60	60
Kc, reactor pressure (loop12)	$-1x10^{-4}$	$-7.2x10^{-4}$
τ_I , reactor pressure (loop12)	20	16.93
Kc, reactor temperature (loop16)	-8	-1.2
τ_I , reactor temperature (loop16)	7.5	3.8
Converged iteration	NA	52
Total cost ($/a)	$2.55x10^6$	$1.63x10^6$

To compare the advances of the proposed trust-region framework with the original back-off technique, the basic back-off method (Chapter 3) with a fixed search space on the reactor section of the TE plant was implemented. Although a conservative search space was used, i.e. $\delta_p = 1\%$ of all the nominal decision variables, the methodology was not able to converge to a solution even after 500 iterations. The basic back-off with a fixed search space method drives decision variables to different outcomes, which indicates that the PSE representation of the system may not be accurate around some of the nominal operating conditions explored by the fixed search space region. The cost function values obtained from these methods are compared in Figure 5-10. As shown in this figure, using a fixed search space causes a negative total cost at some iterations, e.g. 200- 207-232, which indicates that PSE-based optimization converged to an infeasible point due to misrepresentation of the actual model at those iterations. As mentioned before, failure of the system to identify local optimum at every iteration deteriorates the identification of a local optimum at the convergence of the procedure; thus, an optimal local solution cannot be guaranteed.

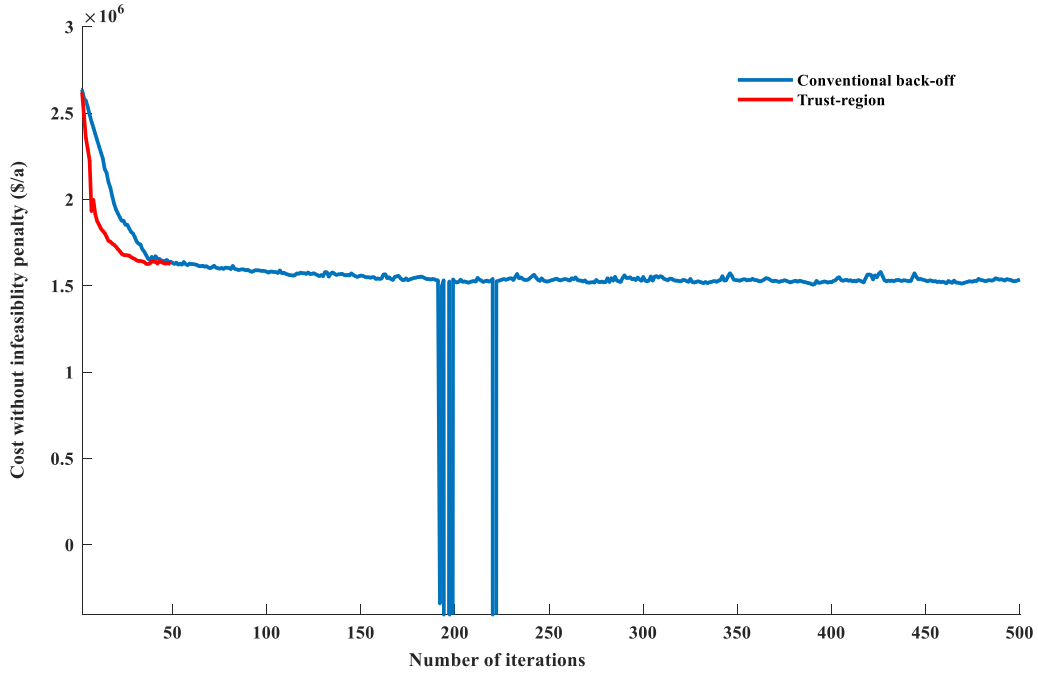

Figure 5-10: Cost function of basic back-off with fixed search space and trust-region algorithm

Figure 5-11 shows the performance of the feasibility variables ($\boldsymbol{\lambda}$) for the basic back-off approach with a fixed search space. Although the cost of the basic back-off shows a converging behaviour, the procedure cannot maintain dynamic feasibility in the system; hence, process constraints are not satisfied, as shown in Figure 5-11.

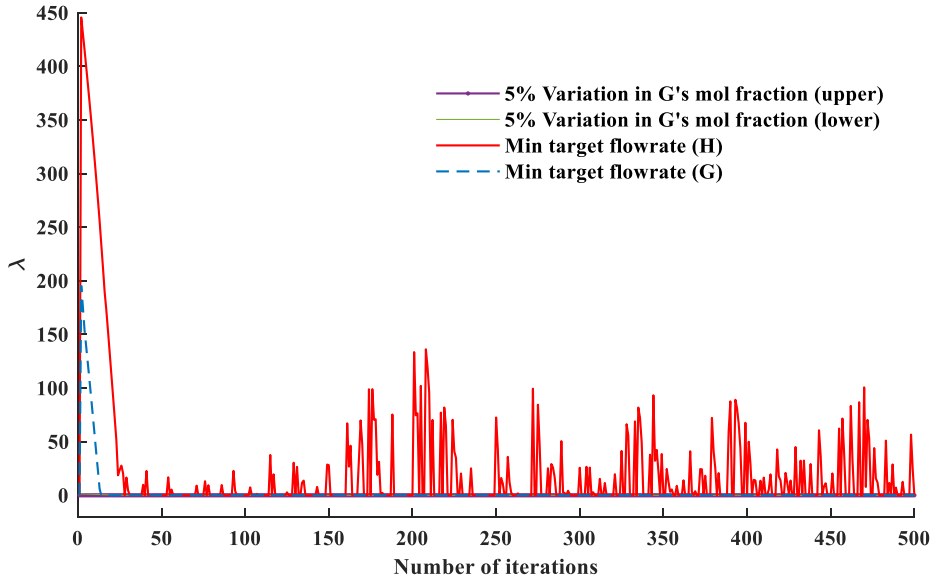

Figure 5-11: The behaviour of feasibility variables ($\boldsymbol{\lambda}$) for the basic back-off approach with a fixed search space.

Figure 5-12 shows the search space for the key decision variables of the TE while using the trust-region algorithm. As indicated above, the method maintains the validity of the PSE in the entire trust-region technique by choosing different trust intervals for decision variables and the size of the search space changes as the iterations proceed. At some iterations, changes in one decision variable are restricted to small variations while the other decision variables can be explored in a wider range. Hence, the trust-region for some variables is smaller compared to the others and this can change as the algorithm proceeds. This result shows that specifying the search space is non-trivial and requires a sophisticated method to select suitable search space regions for each decision variable on which the PSE functions remain valid.

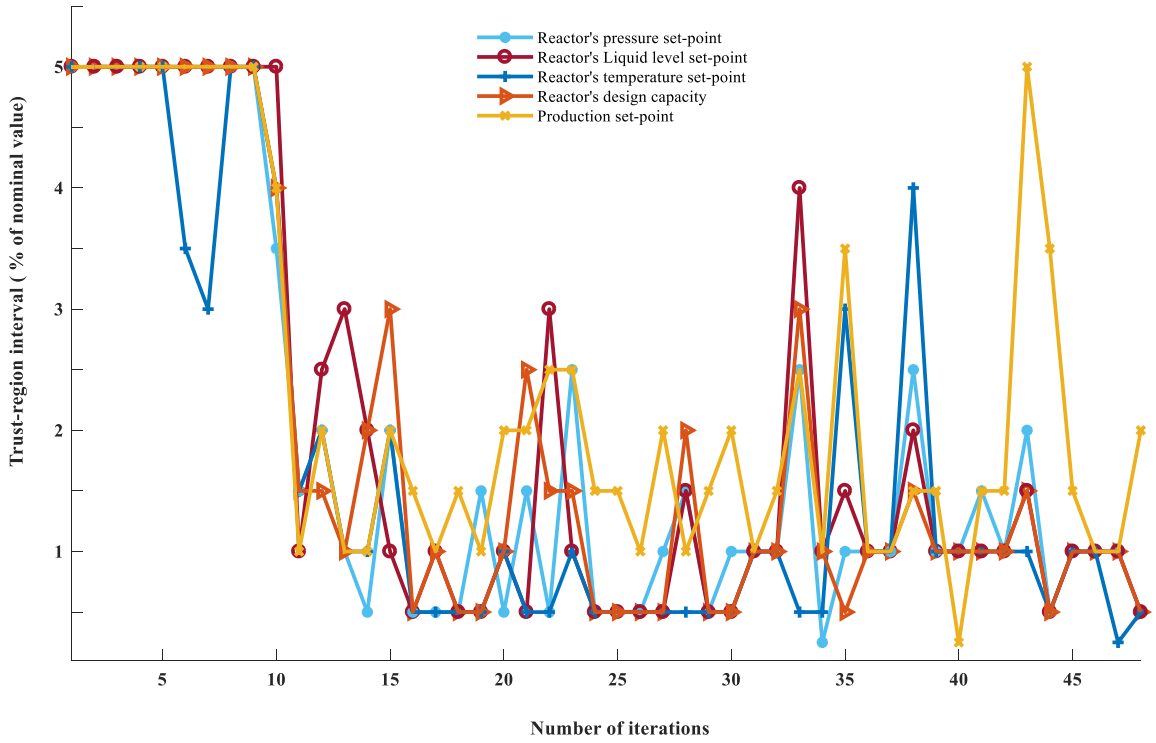

Figure 5-12: Search space for individual decision variables

The high CPU cost (approximately 38.2 hours) is the price needed to ensure the quality of PSE function at each nominal condition and thus convergence of the trust-region method. Although the implementation of the trust-region algorithm requires higher computational costs, the method guarantees that an optimal local solution could be identified. As discussed in Section 5.2, for the wastewater treatment plant, the satisfactory search space can be obtained from offline sensitivity analysis and implementation of the trust-region method remains insignificant. However, in the case of the large-scale industrial processes such as the TE plant, the back-off with the fixed search space failed to converge to a dynamically feasible and near-optimal solution. Moreover, the formal integration of design and control cannot be performed because a process model for this plant is not explicitly available. The latter highlights the benefits of using the presented trust-region framework for large-scale applications.

5.3.2 Scenario II: comparison with previous studies

The integration of design and control of the TE plant has been previously studied under different scenarios (Ricardez-Sandoval, 2008; Ricardez-Sandoval et al., 2011, 2010). In the current section, the results obtained from the proposed trust-region method have been compared to those from the literature. Ricardez-Sandoval (2008) used random variations in the A, B and C feed composition in stream 4 (see Figure 5-7). The disturbance specification is shown in Table 5-9. Despite the small changes in the disturbance, it has a significant effect on product's flowrate. Also, this disturbance has been reported as one of the most challenging disturbances to handle for the TE process (Ricker, 1996).

Table 5-9: Disturbance specifications

Component	Nominal value	Lower Bound	Upper bound
A	0.485	0.475	0.495
B	0.005	0.002	0.008
C	0.510	0.480	0.540

Ricardez-Sandoval (2008) employed a robust modeling approach based on structured singular value (SSV) analysis for simultaneous design and control. Accordingly, the author estimated the critical time-dependent profile in the disturbance that generates the maximum variability in the process outputs. The SSV-based method results in conservative designs that remained feasible for the calculated critical disturbance profile, which generates the highest variability in the process constraints and cost function (Ricardez-Sandoval, 2008; Ricardez-Sandoval et al., 2011). On the other hand, the proposed trust-region method results in robust designs since the surrogate models are developed around the worst-case variability in the constraints and cost function. However, in the current trust-region method the critical disturbance profile is defined *a priori* and remains unchanged during the calculations. That is, the critical disturbance is not estimated at each step of the iterations as it is performed in Ricardez-Sandoval (2008). To make a fair comparison, a similar disturbance profile to the critical time-dependent profile found at the optimal solution by Ricardez-Sandoval (2008) for the TE plant is considered in this work. Hence, a disturbance profile involving a series of steps, with magnitudes in the step changes and average frequency similar to those specified by Ricardez-Sandoval (2008), has been generated for the present scenario. The resulting disturbance profile in the feed

composition (stream 4) is used to implement the proposed trust-region method for simultaneous design and control of the TE plant. The cost, process design and adjustable set-points for the reactor section obtained from the trust-region method and SSV-based approach are reported in Table 5-10. Note that both approaches converge to design and control schemes that remained dynamically feasible under the disturbances in stream 4 (see Table 5-9). In the SSV-based approach, a variability cost was considered in the analysis to explicitly account for the largest (worst-case) variability in products G and H. The process variability of product G and H is defined as the deviation of the product's mass flowrate with respect to their corresponding nominal value at steady-state (Ricardez-Sandoval, 2008). The present trust-region approach handles the maximum process variability in a different way. The PSEs are developed for the maximum deviation in the cost function of the process, including the cost due to the variability of product G and H. Thus, the variability of the cost function is taken to account. Note that the worst-case is defined for a disturbance that remained fixed in the calculations as opposed to is estimated from a robust analysis in the SSV-based approach. As shown in Table 5-10, the current trust-region method specified a design and control scheme that is 27% less expensive than that obtained from the SSV-based approach. The variability cost considered in the SSV-based method commits to 36% of the total cost, which aims to maintain the dynamic behaviour of the system around the nominal condition, whereas the capital cost has the lowest contribution to the total cost (5%). Consequently, in order to compensate for the variability cost and decrease the deviation in products' flowrate, the SSV-based approach specifies a larger reactor capacity, which is approximately 2 times the capacity obtained from the trust-region. On the other hand, the capital cost contributes to a greater portion of the total cost in the trust-region method, thus, the approach does not result in large reactor capacities. The solution of simultaneous design and control obtained in the trust-region can maintain feasibility under the specified disturbances with a smaller reactor capacity and at a higher pressure set-point. Nevertheless, there is no guarantee that the system remains feasible if the disturbance profile changes for the obtained solution.

Table 5-10: Comparison of results between SSV-based and trust-region method

	SSV-based approach (Ricardez-Sandoval, 2008)	**Trust-region method**
Reactor's design capacity (m^3)	84.19	39.84
Reactor's pressure set-point (kPa)	2,600	2,847.3
Reactor's liquid level set-point (%)	63.20	59.60
Reactor's temperature set-point (°C)	117.0	123.4
Production set-point (m^3/hr)	23.11	23.2
CPU time	~100 hr	~30 hr
Total cost ($/a)	$1.681x10^6$	$1.230x10^6$

5.3.3 Scenario III: complete TE plant

Simultaneous design and control of the reactor section using the proposed trust-region has been addressed in the earlier sections. In those analyses, only design and control factors of the reactor are considered. Note that for analysis of the reactor section the design and control tuning parameters of the other units remained constant at their base case values. Although the effects of other units on the overall process performance are captured through the use of the dynamic model for the complete TE plant, their design and control parameters are not considered as optimization variables. Changes in the parameters of other units of the process, e.g. separator and stripper, may affect the process performance and economics. Thus, in this section, the optimal design and control of the three major units of the TE process are simultaneously considered.

Table 5-4 provides the cost and constraints of the TE process. Equivalent objective and constraint functions are used for the reactor section and complete model. Table 5-11 present the set of optimization variables include 46 decision variables that are basically for all main units of the process.

Table 5-11: Decision variables for the complete model

Decision variable (η)	
Design	Reactor capacity (m^3) Flash separator (m^3) Stripper column (m^3)
Adjustable set-points	Reactor pressure set-point (kPa) Reactor liquid level set-point (%) Reactor temperature set-point (°C) Production set-point (m^3/hr) Separator liquid level set-point (%) Stripper liquid level set-point (%) y_A set-point (%) y_{AC} set-point (%) Mol % G set-point
PI controller tuning parameters	Kc, τ_I : Reactor liquid level (loop17) Kc, τ_I : Reactor pressure (loop5) Kc, τ_I : A feed rate (stream1) Kc, τ_I : D feed rate (stream 2) Kc, τ_I : E feed rate (stream 3) Kc, τ_I : C feed rate (stream 4) Kc, τ_I : Purge rate (stream 9) Kc, τ_I : Separator liquid flow (stream 10) Kc, τ_I : Stripper liquid flow (stream 11) Kc, τ_I : Production rate Kc, τ_I : Stripper liquid level (loop7) Kc, τ_I : Separator liquid level (loop6) Kc, τ_I : Mol % G in stream 11 Kc, τ_I : Ration in loop 1 (y_A) Kc, τ_I : Ration in loop 4 (y_{AC}) Kc, τ_I : Reactor coolant valve Kc, τ_I : Separator coolant valve

The same disturbance configuration used in scenario I (see Section 5.3.1) shown in Table 5-6 has been used for the integrated design and control of the complete TE plant. Table 5-12 shows the results of the implemented trust-region for the complete TE plant. These results are compared to those obtained for the reactor section only (Section 5.3.1). As shown in the table, the integrated design and control of the complete TE plant results in 11% lower costs compared to the reactor section analysis. The complete TE problem has more freedom in terms of additional decision variables that can be adjusted to reduce the cost. The contribution of those decision variables to the economics and dynamic performance of the process has been captured and thus the proposed plant design is able to reduce the cost and maintain dynamic feasibility. The integration of design and control of the entire TE plant suggests different values for the parameters which were set to their base case values in the reactor analysis section. Considering additional decision variables

improves the economics of the plant; on the downside, the size of the problem and thus the computational cost increases as shown in Table 5-12. The capital cost takes up to 10% of the overall cost of the process; while 90% of the total cost is due to the operating costs. Reasonably, the trust-region approach decreases the overall cost by choosing larger capacities for the reactor, stripper, and separator (see Table 5-12). Consequently, the operational costs decrease and the system can operate at closer conditions to the specified margins, e.g. the system operates at a higher pressure adjacent to the upper limit.

Table 5-12: Results of complete model

Decision variables	**Complete TE plant**	
Design		
Reactor (m^3)	45.30	
Flash separator (m^3)	117.12	
Stripper column (m^3)	5.66	
Adjustable set-points		
Reactor's pressure set-point (kPa)	2,893	
Reactor's liquid level set-point (%)	54.60	
Reactor's temperature set-point (°C)	123.3	
Production set-point (m^3/hr)	23.49	
Separator's liquid level set-point (%)	56.96	(50 at Base case)
Stripper's liquid level set-point (%)	50.55	(50 at Base case)
y_A set-point (%)	34.79	(32.2 at Base case)
y_{AC} set-point (%)	19.05	(18 at Base case)
Mol % G set-point	54.5	(55.83 at Base case)
CPU time (hr)	~110	
Total cost ($/a)	1.45×10^6	
Converged iteration	62	

Figure 5-13 shows the convergence of both reactor and complete TE plant (reactor, separator, and stripper). The complete TE plant requires additional iterations in the trust-region procedure to satisfy the convergence criterion when compared to Scenario I; however, it results in a larger amount of back-off, i.e. lower cost compared to the initial base case value and therefore more economic benefits. Figure 5-13 clearly shows the trade-offs between computational costs and additional economic savings, i.e. while Scenario I (reactor only) required approximately one-third of CPU time of the present scenario (complete TE plant), it identified an optimal design and control solution that is 11% more economical than that obtained by Scenario I. This result illustrates the benefits of considering the optimal design and control of a large-scale plant and also is indicative of the corresponding CPU costs that will be incurred when attempting to solve such a problem.

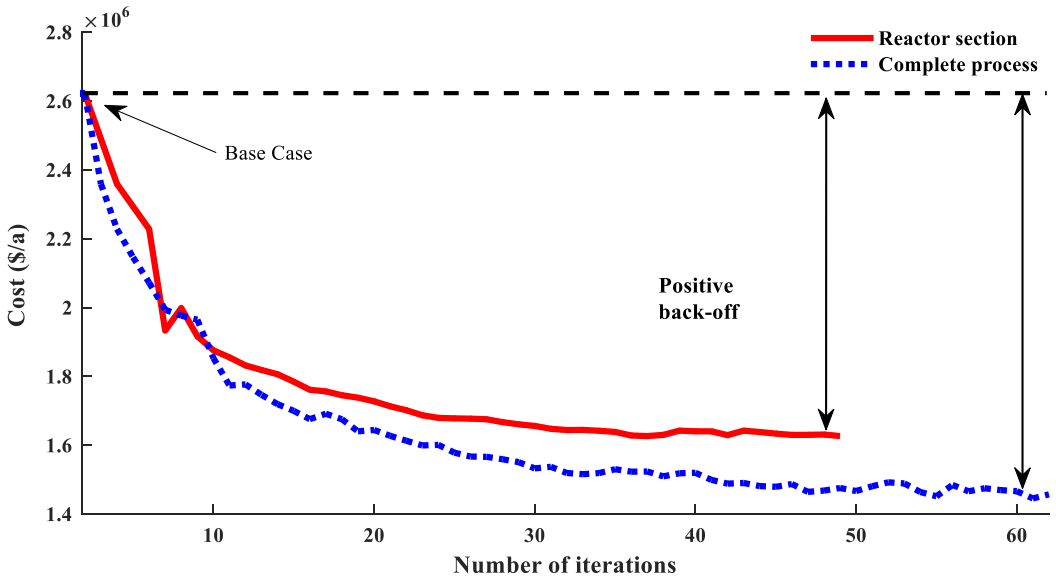

Figure 5-13: Cost function of complete TE and reactor section using the trust-region method

Figure 5-14 shows the performance of some of the nonzero feasibility variables (λ) for the trust-region approach. As illustrated in the figure, the feasibility in the process is maintained since the trust-region method forces all the feasibility variables to zero at the convergence.

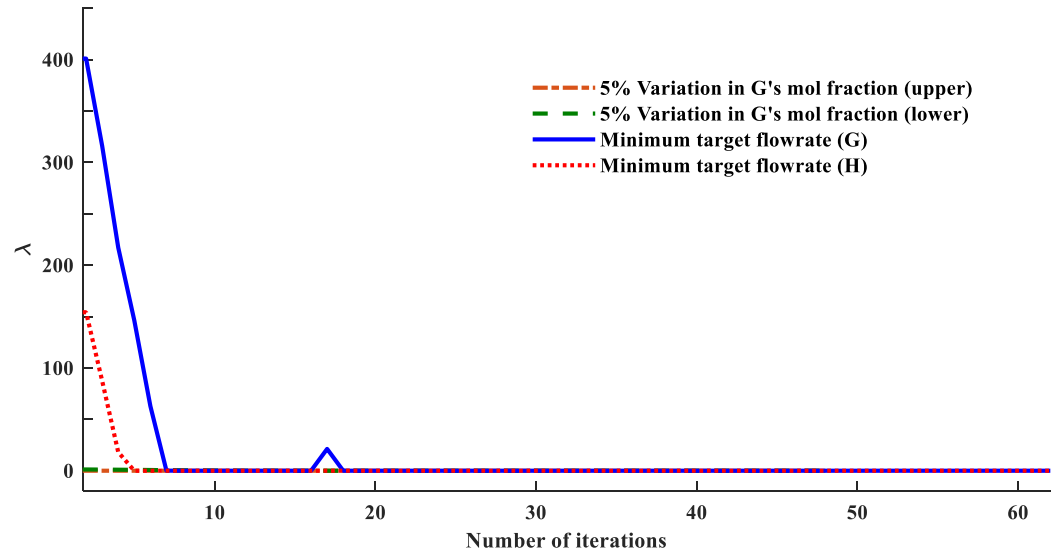

Figure 5-14: The behaviour of feasibility variables for the complete TE plant

As discussed in Section 5.1, the current trust-region method is capable of updating the order of PSE with respect to the region that is being explored at each iteration step. At certain nominal conditions, if the system has a highly nonlinear behaviour or the identified trust-regions too small the procedure adopts to increase the order of the PSE to improve the accuracy of the approximation. Figure 5-15 shows the order of the PSE that was employed among the iteration of the trust-region approach. As expected, at the early iterations, the low order of PSE shows satisfactory performance. Due to the changes in optimization variables, the system might show highly nonlinear behaviour at some iterations and thus higher-order PSEs may be required.

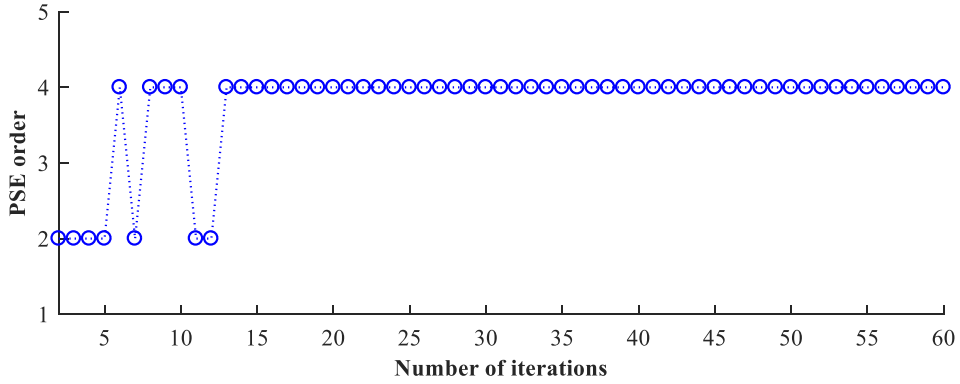

Figure 5-15: PSE order during the trust-region procedure

The search spaces obtained for individual decision variables of the three main units of the process, i.e. reactor, stripper, and separator, are shown in Figure 5-16. As indicated in the figure, the trust-region method maintains the validity of the PSE functions by choosing different trust intervals for decision variables at each iteration of the trust-region procedure. At some iterations, changes in one decision variable are restricted to a small search space while other decision variables can be explored in a wider range. In general, if large changes in one decision variable deteriorate the error-index, i.e. accuracy of the PSE, the procedure chooses to limit the allowable search space. Although small trusted intervals for specific decision variables may delay convergence, the accuracy of the PSE function due to the changes in the decision variables is ensured through the user-defined tolerance (see *Step 4* in Section 5.1).

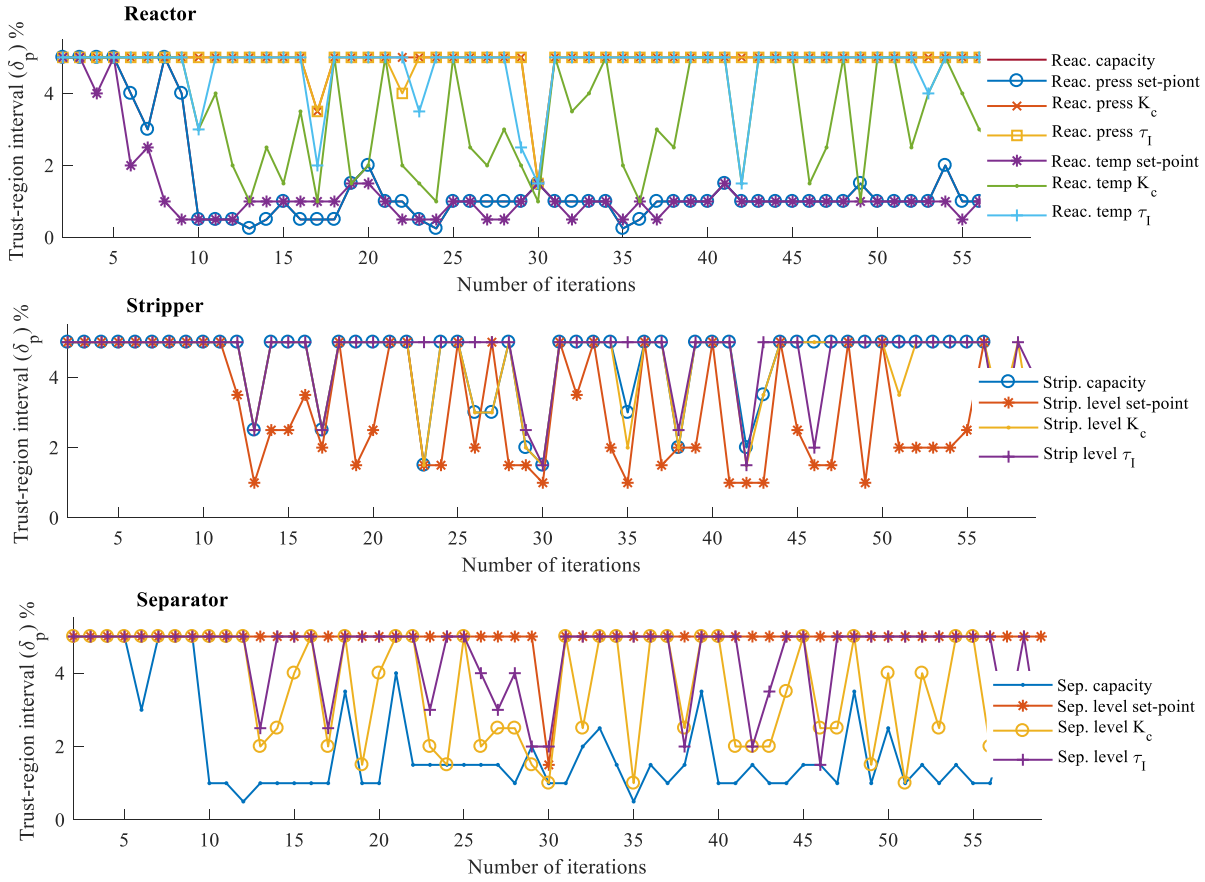

Figure 5-16: Trust-region intervals for individual decision variables

To validate the design, the solution obtained from the trust-region method was tested using the disturbance specified for the process (Table 5-6). Figure 5-17 illustrates the variation in the product stream qualifications, i.e. G mol% and flowrate in stream 11, which must remain under 5% (see Table 5-4). As indicated, stream 11 (i.e. product stream) remains within their corresponding limits in the presence of the disturbance.

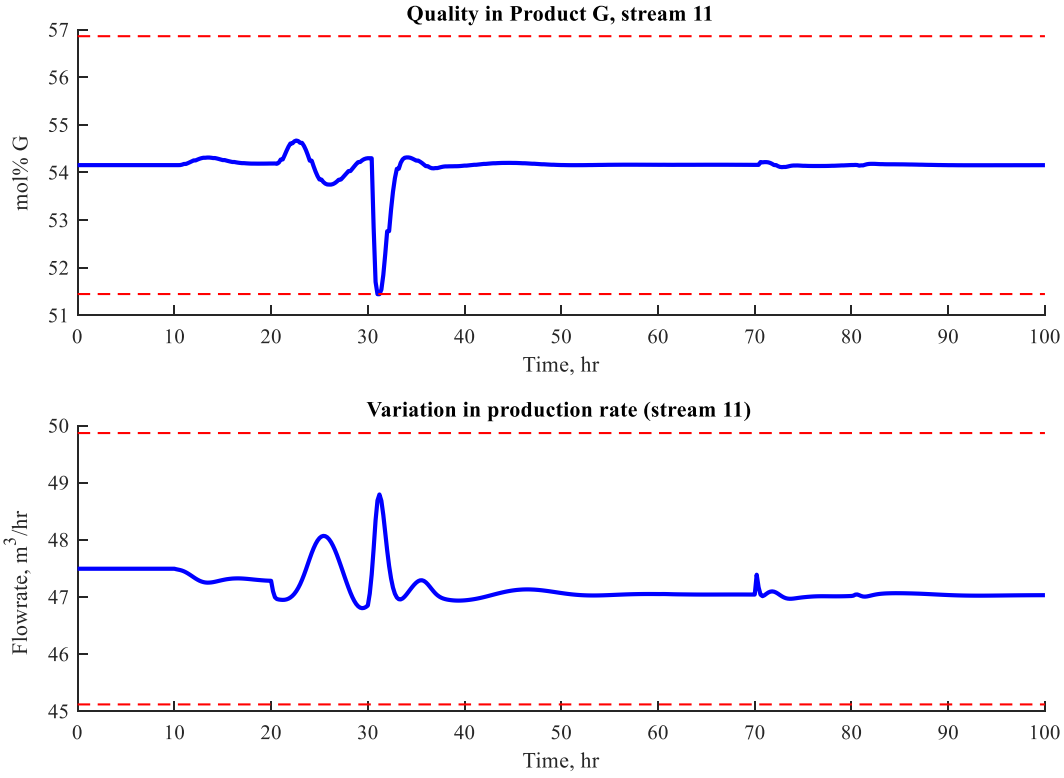

Figure 5-17: Variation in the product stream (stream 11)

The dynamic operation of the reactor is illustrated in Figure 5-18. As shown in the figure, all three operating conditions, i.e. reactors' pressure, temperature, and liquid level, remain feasible during the process time under specified disturbances. Accordingly, the system can operate at a higher pressure without any violations to its safety margin for the specified disturbance profile. Figure 5-19 shows the product variability in terms of variability of flowrate of product G and H. For the 50/50 operating mode, both G and H product flowrates must be greater than (7,038 kg/hr). Accordingly, the design obtained by the present method maintains the minimum target product for 50/50-G/H operating mode. For the solution obtained from the proposed trust-region method the minimum target value is active at some conditions but it does not present any constraint violation.

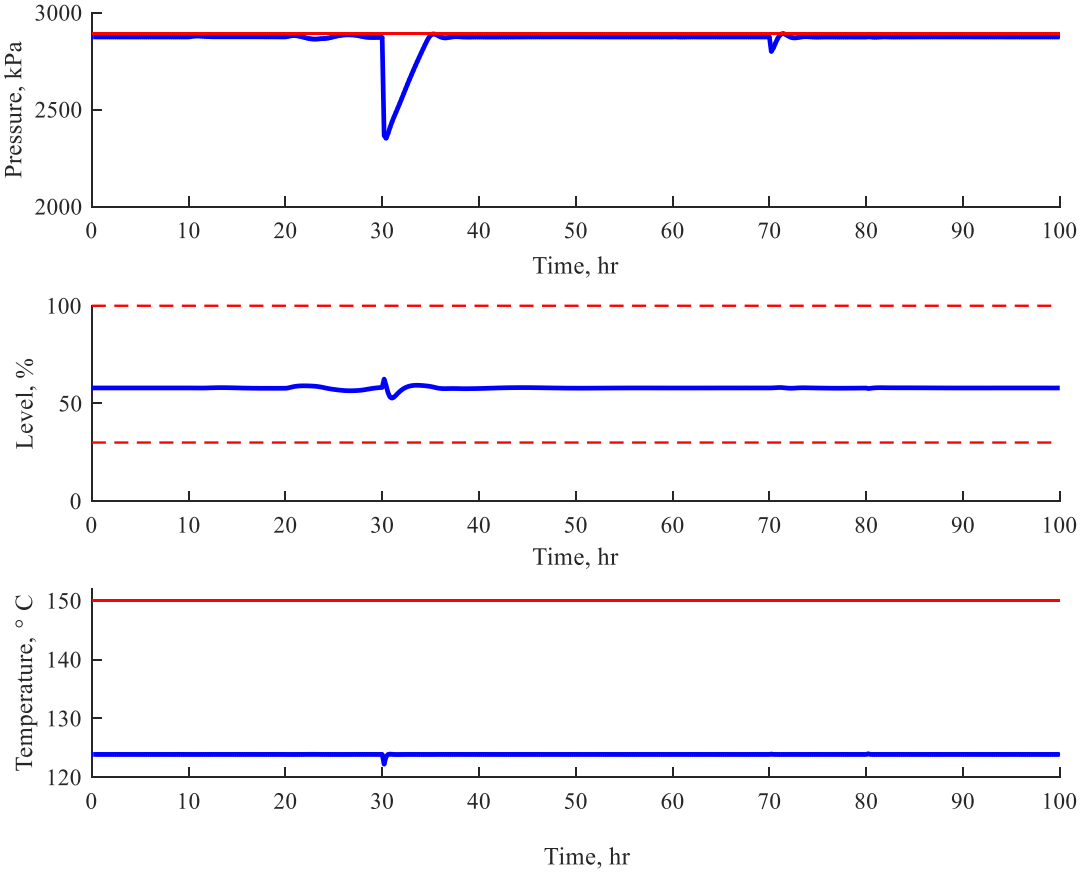

Figure 5-18: Reactor operating constraints

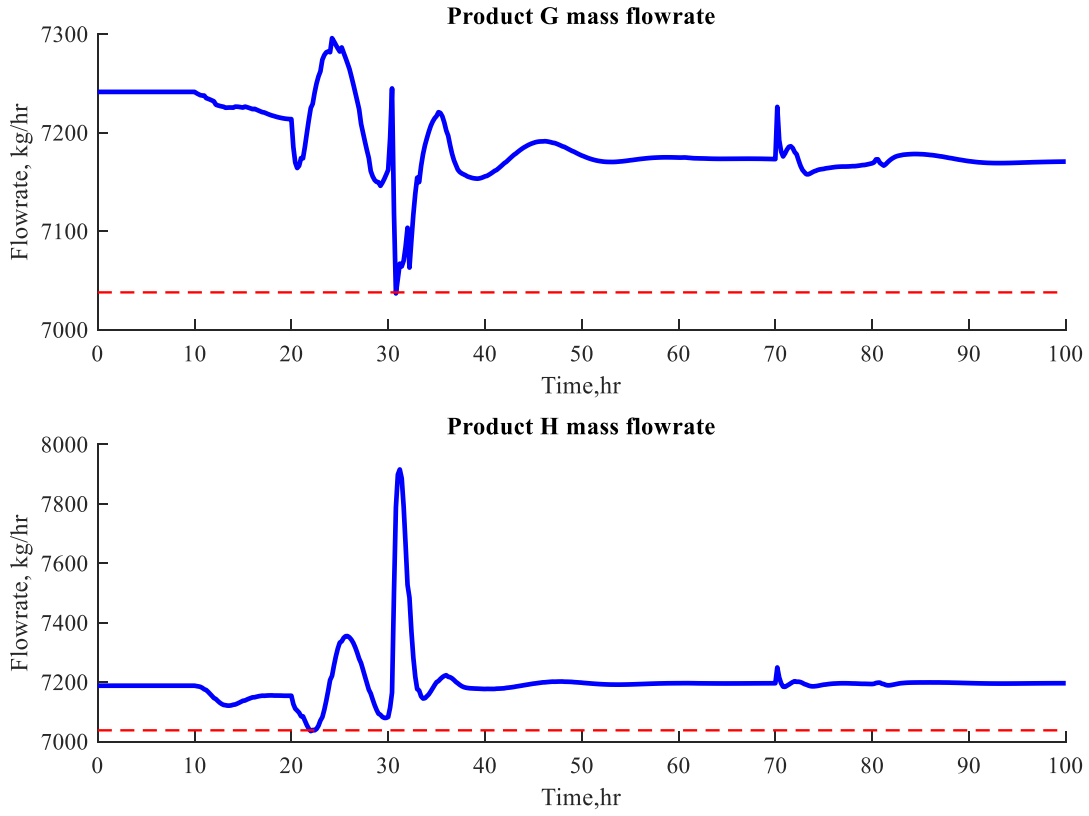

Figure 5-19: Minimum target product for (50/50-G/H)

In summary, this chapter presented the trust-region approach which is an extension of the basic back-off approach. The proposed trust-region method can be applied for simultaneous design and control of large-scale systems. The approach is designed in a way that systematically selects the size of the trusted interval region in which the error between the actual function and its PSE remains in a certain tolerance. The procedure is capable of updating the order of PSE regarding the area that is being explored or the desired accuracy of the PSE approximations. The quality of the solution obtained from the current region was also studied. If the proposed algorithm converges, then the solution satisfies first-order KKT local optimality conditions and is equivalent to the solution obtained from a formal integration problem around that optimal point. The methodology was implemented on a wastewater treatment plant and the TE process. The results indicate that the proposed methodology leads to more economically attractive and reliable designs while maintaining the dynamic operability of the system in the presence of multiple disturbances. The trust-region

method with adaptive search space shows a significant accomplishment in simultaneous design and control of the large-scale process while the basic back-off approach that uses a constant search space may fail to converge.

6 Emerging trends

Today's dynamic business market nature requires fast adaptation in the production process. To remain competitive, industries need to modify their production strategies and adjust to the rapidly evolving market demands as quickly as possible and in a safe and environmentally-friendly manner. Decision layers of process strategies, i.e. strategic/logistics, tactical, and operational, happen at different time and length scales. Traditionally, the settlements for each layer are acquired independently or inadequately combined with the adjacent layer. Central to the entire discipline of the integrated approach is maintaining an efficient flow of information between the multiple aspects of the process. The emerging trends in the field mainly include expanding the decision-making strategies to consider multiple layers of the process from different perspectives.

This chapter presents ideas to support the development of new and more efficient opportunities for an integrated framework. My central goal is to highlight open problems and future research perspectives. Then, incentives directed towards the evolution of an integrated approach are identified. Future directions are suggested as the possible pathways the industry and academy might take to achieve the ideal framework of integrating all the decision levels, considering the complexities, obligations, and dimensions of a real-world enterprise. Promising strategies that are often implemented individually and that can expand the operating window of an integrated approach are outlined here. The discussions presented in this chapter have published in (Rafiei and Ricardez-Sandoval, 2020a).

Emerging trends in the field are identified in 5 different categories which are discussed next.

6.1 Design, control, scheduling, and planning

The need for simultaneous design and control has already been established and widely discussed in the literature. Design parameters can dominate the dynamic behaviour of the system; hence, they have a pivotal role in reducing the complexity to operate and control the process at their desired targets. Illustrative

examples can be found in (Luyben, 2004). In the industrial processes, however, various time scales with the corresponding decision layers are often established that would also be affected by process design decisions. These layers often involve planning (long-term decisions, months to years), scheduling (short-term decisions, days to months) and process control (operational, seconds to minutes) decisions. This intensified consideration should include design, planning, scheduling and control of the process as depicted in Figure 6-1.

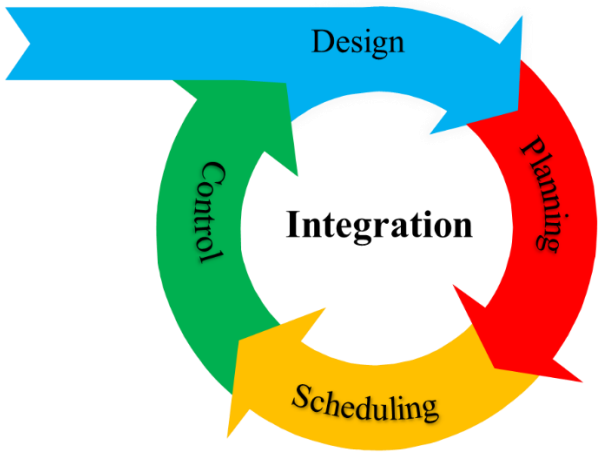

Figure 6-1: Integration of design, control, scheduling and planning

To date, the research of the integrated framework has been mostly focused on the integration of design and control (Ricardez-Sandoval et al., 2009a; Vega et al., 2014a; Yuan et al., 2012), integration of control and scheduling (Baldea and Harjunkoski, 2014; Chu and You, 2015; Dias and Ierapetritou, 2016; Engell and Harjunkoski, 2012; Flores-Tlacuahuac and Grossmann, 2011; Harjunkoski et al., 2009; Valdez-Navarro and Ricardez-Sandoval, 2019a), integration of planning and scheduling (Maravelias and Sung, 2009), and integration of control, scheduling and planning (Chu and You, 2015). Simultaneous integration of all four aspects (i.e. planning, scheduling, control, and design) has yet to be attempted. Shobrys and White (2002) reported the major benefits for the integration of planning, scheduling, and control. They also discussed the barriers that need to be overcome to achieve a technically feasible integration. Grossmann (2005, 2012) reviewed the scope and application of mathematical programming techniques to Enterprise-wide Optimization (EWO) problems where planning, scheduling, real-time optimization, and control are

included. Economic MPC (EMPC) has emerged as an attractive alternative to account for the process economic at the control stage. The key goal is to replace the standard tracking objective function with an objective function that captures the economics of the process in the transient domain (Ellis et al., 2014; Müller et al., 2014; Rashid et al., 2016). Correspondingly, for most of the scheduling and planning problems, the design is assumed to remain fixed. However, there has been evidence of a correlation between design and process scheduling. There are few studies that have recently investigated the simultaneous consideration of design, control, and scheduling (Koller et al., 2018; Koller and Ricardez-Sandoval, 2017; Patil et al., 2015; Pistikopoulos et al., 2015; Pistikopoulos and Diangelakis, 2016). Logically, in any aspect that the control performance of the system is a subject of interest, the design of the system should be taken into consideration to yield a stable, feasible and flexible control scheme. The integration of each of the components of the process advances the resilience and operability of the process along with the performance of the process. Furthermore, considering all aspects of the process appears to positively shift the short-term and long-term profits of the entire system. The ever-increasing interest in optimal and efficient operations would thus motivate process industrial practitioners to implement intensified considerations at the early stages of the design. Considering the design features together with decisions made at the different layers of control, scheduling and planning offers more room for improvement of the sustainability of the entire process by directly affecting the control and indirectly affecting scheduling and planning. A comprehensive study using simple to medium-size case studies could assess the benefits and limitations emerging from the simultaneous consideration of the multiple aspects and/or levels of the process.

The chemical supply chain is a sequence of processes and activities from production to distribution that includes the transformation of raw material to desired products. The chemical supply chain components have different time scales. Naturally, judgments at each layer are made by different decision-makers with diverse expertise, i.e. management experts at headquarters and process engineers at plant operation. Those experts have internal or local objectives that are often different from others and that can even contradict the objectives considered on other layers. As a result, the decision at each layer can be transferred as hard

(aggressive) constraints to the other layers in a sequential approach. The outputs of a block set decision rules for the following block, which would aim to meet their own targets in an optimal fashion and satisfy imposed decision rules. Thus, the internal decisions and actions at each layer are vague to the other layers, which may contradict the actions in the other layers. This inconsistency itself adds another source of uncertainty to the system which is not favorable. Additionally, all individual layers have their own uncertainties coming from different sources. In a sequential or disintegrated approach, uncertainties might be ignored at some levels since they have no effect on the outcome of the current level. In contrast, the ignored uncertainty generates severe deviations in a subsequent layer in which the origin of disruptions does not exist. Likewise, uncertainties might overlap in different layers and if considered separately, it will be a source of a higher redundant conservative policy. Consistent information flow between these layers is possible using an integrated approach which is the key component to align the short-term milestones with the long-term decisions. Moreover, resolutions at each layer can be carried out to the other layers not only as boundaries but also as objectives and operational constraints.

On the basis of the aforementioned definition of planning and scheduling, the integration of design, control, scheduling, and planning suggests modifications that are not beyond the battery limits of a plant. Thus, the decisions are internal and require adaptation to external situations such as feed quality variations, availability of the utilities, and distribution. For example, price fluctuations and distribution to retailers are handled as external uncertainties that can affect the plant; however, the reverse does not apply. Recently, the topic of multi-enterprise instead of single enterprise has gained interest (Sahay and Ierapetritou, 2016). The approach illustrates some of the external unknown factors and decreases the magnitude of unpredictable factors. Therefore, the systems instead of operating with those external variables as complete unknown dynamics can somehow manipulate those externally imposed variations. The role of a single plant as an item from a larger collection of systems can be considered in a chemical supply chain framework. The chemical supply chain offers large saving opportunities for companies at the expense of solving larger

(intensive) optimization formulations. An interconnected approach is key to define aligned activities for several portions of the process.

6.2 Supply chain optimization

The decision layers with highly diverse time scales are interconnected though they are typically treated independently. Integration of the multiple aspects increases the profitability of the process in terms of shortening product manufacturing, improving product quality, widening the process capabilities, etc. Grossmann and Westerberg (2000) stated that: "*Process Systems Engineering is concerned with the improvement of decision making processes for the creation and operation of the chemical supply chain. It deals with the discovery, design, manufacture, and distribution of chemical products in the context of many conflicting goals."* According to the updated definition of process system engineering (PSE), the key goals of the discipline can be broadened from process unit operation to the chemical supply chain. The chemical supply chain starts at small scales categorized as molecules, molecular clusters, and small particles or entities for single and multi-phase systems. The design and analysis of process units as a part of the flowsheet are referred to as intermediate scales. The collection of suppliers, warehouses and distribution centers defines a commercial enterprise at the macroscale level.

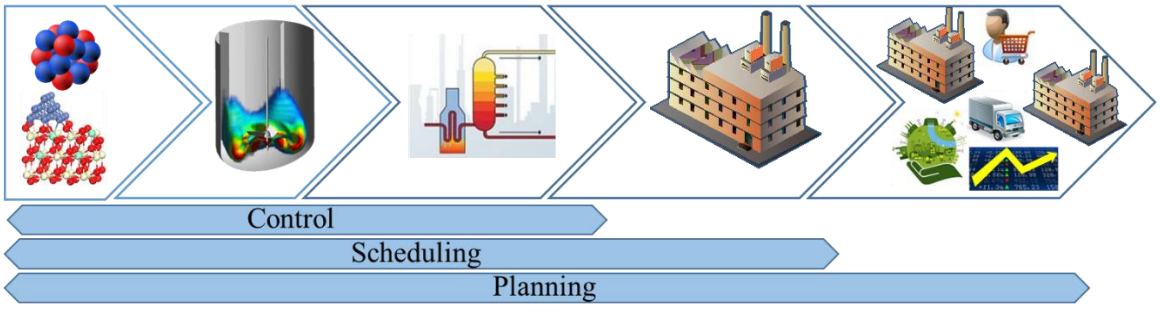

Figure 6-2: Chemical supply chain

Multiple blocks of a chemical supply chain are shown in Figure 6-2. Each of these blocks is different in time-, length-scales, and objectives to fulfill. However, the ultimate goal of all the blocks is to achieve a level of profitability and sustainability that is acceptable for the company. Through the chemical supply

chain, fundamental scientific discoveries at the molecular or microscopic level (i.e. discovery and design of new molecular structures) are highly interconnected with the logistics for manufacturing and production planning (i.e. supply chain planning and scheduling) (Grossmann, 2004). Each of these levels is briefly discussed next.

Microscopic level: a systematic procedure for setting up, solving and analyzing Computer-aided Molecular Design (CAMD) problems has been proposed (Harper et al., 1999; Harper and Gani, 2000). Gani (2004) described product design based on the needs and desires that can form the fundamental of the first node in the chemical supply chain. The author discussed the challenges and opportunities of a systematic CAMD to identify/ design new products and processing routes. The concept of CAMD has been implemented in computer-aided software-tool for sustainable process synthesis-intensification of a bio-diesel system (Tula et al., 2017). Economic and environmental sustainability targets are also considered for a systematic optimal product−process design by (Cignitti et al., 2018). The second node of the supply chain is defined based on the fluid-flow phenomena based on the conservation laws. For example, computational fluid dynamics (CFD) enables the quantifications of the fluid-flow and multi-phase characteristics of the system (see Section 5.3).

Intermediate level: decisions of design characteristics (e.g. capacity), the control of a single unit, and the intensified flowsheet design and control take place at this level. Demand forecasts are depicted to the supply chain network as the external conditions over a short- to medium- time horizon (Schulz et al., 2005; Shah, 2005). Scheduling and planning are strategic decisions made at this level. A detailed discussion of the key modeling approaches that can address the practical integration of medium-term production planning and short-term scheduling problems are provided elsewhere (Maravelias and Sung, 2009).

Macroscopic level: forecasting ultimate goals of the process including but not limited to future market demands, production capacity, raw material availability, production targets and other logistic decisions take place at this level. Furthermore, the connection of the enterprise with other supply chain contributors is considered at this stage, which may lead to a multi-enterprise network.

Supply chain optimization is emerging as a modern research direction that involves manufacturers, suppliers, retailers, and distributors at the enterprise level. In addition, the current manufacturing environment for the modern process industry moves companies toward collaborative strategies in which multiple enterprises instead of acting independently are tied together and serve as a large incorporated complex to the global market. In the multi-enterprise network, additional factors of collaboration and competition inevitable increases the problem's complexity. However, collaborative approaches carry higher constructive potentials and convenient outcomes for involved partners. The studies presented thus far in the literature have made use of simplified models and provided some insights allowing a narrow understanding of some particular scenarios. The issues of a multi-enterprise supply chain and an overview of integrated decision-making have been discussed by (Dias and Ierapetritou, 2017). These advances facilitate the reduction of the gap between the current state of the manufacturing industry and an enterprise-wide optimum condition for operational management.

One example involving the supply chain is in the food sector. Food processing units such as thermal and non-thermal processing are classic unit operations that can be designed and controlled using available simultaneous design and control strategies. Food processes are subject to large deviations in raw materials. The availability of raw material is mostly seasonal and directly related to the availability of agricultural products. The efficient production of a company in food manufacturing is also tied to multiple contributors including raw material suppliers (agriculture), distributors, retailers, and customers. Thus, integration of design and control seems to be limited to tackle the large variations and external decisions for these systems. Strategic planning and scheduling decisions also need to be considered in the decision-making process to meet market demands. There is a great potential of increasing the flexibility and the optimality of the companies by including strategic planning and scheduling aspects. In order to meet the market demand in an optimal and sustainable manner, the organizations should act as a cooperative organization (supply chain management). This outlook is possible while the whole process is addressed in an integrated framework.

In summary, a natural progression in the field of integrated process design is expanding the integration framework to include the supply chain optimization and maintaining a transparent link between key aspects of the process. This is a bigger picture compared to the scheduling and planning which expands the vision of the process design farther and provides broad enhancement possibilities. Supply chain management is a large-scale multi-period optimization problem that will grow exponentially if it is combined with design and control decisions. A legitimate connection between contributors to the supply chain improves the sustainability of the process as well as profitability for a longer time scale. Consideration of process design aspects at larger time scales requires the development of efficient multi-scale modeling and optimization techniques. Fortunately, computers are rapidly evolving and becoming more powerful, which would enable us to formulate and attempt to solve large-scale integrated problems. The current potentials in computing technology support (until some extend) the solution of complex problems originated from the combination of supply chain optimization with design and control decisions.

6.2.1 Multi-scale optimization

Modern technologies aim at particular materials with specific qualifications, e.g. synthesis of nanomaterials with a certain particle size distribution. To capture key atomistic processes, specific molecular modeling tools such as kinetic Monte Carlo and/or molecular dynamics can be implemented. Macroscopic conditions such as temperature have the potential to shape the morphology and structure of fine-scale (molecular) materials. Thus, control of the events at the macroscale level affects the properties at the molecular scale. In materials science, simultaneous design and control of the micro/nanoscales and macroscales aims to target specific properties more efficiently by designing a material at the molecular scale with ad hoc characteristics. the combination of these two scales forms a basic multi-scale system. In order to maintain the connection between the molecular and macroscopic scale, an intermediate tool is needed for the multi-scale scheme. Therefore, model behaviour at the molecular level is linked to the macroscopic behaviour by means of reduced-order (surrogate) models. Biegler et al. (2014) considered a heterogeneous collection of device scale and process scale models; those authors captured the multi-scale, multi-fidelity model

behaviour by means of distributed and lumped parameter models of varying complexity. Simultaneous optimization of design and control can be implemented to optimally determine the macroscopic conditions in which the molecular dynamics will satisfy the objectives of the process. More broadly, supply chain contains a wide range of time and spatial scales from the molecular to the macroscale levels that necessitate the existence of multi-scale modeling and optimization methods. Efficient and accurate model reduction strategies are applied to integrate the multiple scales of the problem within the optimization framework. The critical challenge in that approach is the handling of uncertainty and disturbances along with the disparity of time scales in the optimization framework. Uncertainty can be quite diverse in nature and also scale-dependent, e.g. uncertainty in the process model parameters and product demands may occur at different time scales. Moreover, the level of detail and the magnitude of the uncertainty and variables are different at each layer. As a result, multi-scale modeling and optimization require the consideration of meticulously balanced links between the different time and spatial scales. These links are representative of model behaviour of a level into another level. Typically, reduced-order models (RMs) are employed as agents that maintain the link between the current level and the previous one. Figure 6-3 shows a schematic of the multi-scale optimization of chemical supply chain linked through RMs. The significant parameters in an RM can be identified using standard systems identification techniques. RMs have been developed to transfer the behaviour of the corresponding level to the other level. Those RMs should be constructed according to the significant properties that will be optimized. Selecting the significant parameters at each level raises another challenge that might require intense identification steps and hence increase the computational burden.

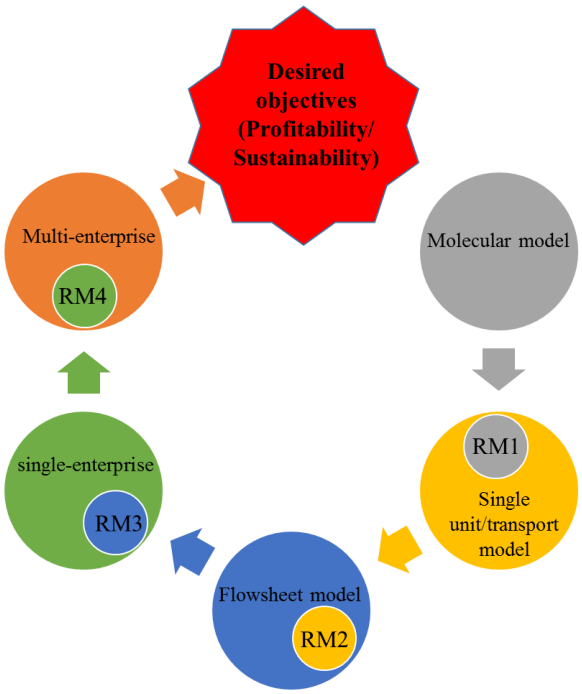

Figure 6-3: Multi-scale optimization of chemical supply chain linked through RMs

In summary, efficient techniques are required to recognize the key parameters and reduce the full model to a significant and descriptive set of parameters. Also, it is critical for maintaining a well-adjusted link between stages that carries the necessary information to achieve an optimal process design that considers the multiple scales of the process. The multi-scale subject is an emerging area that can be further explored in the future. For instance, the design of the system at the molecular level using Kinetic Monte Carlo simulations can be related to the controllability and other design and operational management factors at larger scales.

6.3 Computational fluid dynamics (CFD)

Typically, process simulation models are built on the basis of a number of ideal assumptions with lumped parameter descriptions. Likewise, surrogate models are widely used to handle large-scale and complex models. Generally, those models are incapable of distinguishing the interactions between material design, complex fluid behaviour and transport effects (Biegler et al., 2014). Failure in capturing the equitable

behaviour of the system might eventually drive the model-based optimization to sub-optimal or even unrealistic solutions. Computational Fluid Dynamics (CFD) has been developed as a standard numerical tool to capture the interaction between the process components, such as flow, heat and mass transfer, phase change and mechanical movements. CFD is a sophisticated modeling approach that tends to provides detailed knowledge, e.g. spatial information on flow patterns, turbulence conditions, mixing behaviour. The information could be highly precise and effective in forecasting the performance of the system that cannot be described using conventional (low-order) models. For instance, CFD modeling has found its place in the modeling of bioreactors and fermentation processes (Farzan and Ierapetritou, 2017; Singh and Hutmacher, 2009; Tajsoleiman et al., 2019) while other modeling techniques fail to accurately model them. Up to now, far too little attention has been paid to integration approaches using CFD. The main challenge faced during the integration of multiple aspects of the process using CFD technique is the high computational burden. Nowadays, it is still challenging to solve integration of design and control problems involving CFD applications; however, advances in computing science appear to be promising for such pathways in the future. On the one hand, the inclusion of CFD will deteriorate the performance of the current integration approaches by increasing the computational demands; on the other hand, CFD model can provide additional insights regarding the behaviour of the process that the conventional modeling techniques might fail to capture. Accordingly, hybrid models are potential remedies to avoid the high computational times needed for solving complex problems resulting from the application of integrated approaches. The key idea in these models is to combine mechanistic knowledge-based models with data-driven approaches to capture convoluted process relationships (Venkatasubramanian, 2009). For example, a low computational cost hybrid multi-scale thin film deposition model that couples artificial neural networks (ANNs) with a mechanistic (first-principles) multi-scale model was constructed by Chaffart and Ricardez-Sandoval (2018). They combined continuum differential equations, which describe the transport of the precursor gas phase, with a stochastic partial differential equation (SPDE) that predicts the evolution of the thin film surface in a multi-scale framework. In a similar way, CFD modeling can be used to model the second node (from left to right) of the chemical supply chain shown in Figure 6-2 using a multi-scale or hybrid technique;

thus, the behaviour of small-scale components in the supply chain can be related to the other layers using standard multi-scale modeling techniques. Furthermore, CFD is capable of modeling irregular geometries in the form of a mesh. The application of CFD simulation software is widespread and is becoming a standard tool in the chemical industry. For further work, CFD techniques could be integrated into the design and control framework as a modeling tool to consider the geometry of the process. In the meantime, integrated approaches are based on the assumption of a fixed (known) geometry of the process, e.g. a reactor with unknown capacity but with a fixed shape. Changes in the geometry will affect the process model extensively; conversely, CFD models are developed based on the fundamental physics that makes them independent of the geometry. This ability of CFD can provide an additional degree of freedom which turns geometry into a decision (optimization) variable and therefore offers the potential to identify novel and optimal process designs. Defining physical boundaries in the numerical simulations, i.e. meshing, impose limitations on the application of CFD in the design process; however, recent advances in this field aim to embed the physical boundaries into the CFD problem using methods such as the fictitious domain, immersed boundary, and diffuse domain/interface methods (Aland et al., 2010; Patankar et al., 2000; Sotiropoulos and Yang, 2014). Using such methods, the simulation of moving boundaries without the need for manipulation of the underlying mesh/grid becomes possible. Hence, the geometry of the domain of interest (i.e. process equipment) can be easily modified if the design of the process is involved in the optimization procedure (Treeratanaphitak, 2018). This dominant feature is of great interest for a wide range of fields including nanotechnology, materials' design and reaction engineering. Moreover, CFD models are scale independent and remain valid for a wide range in the design parameters. The validity of the model enables the optimization to pursue the optimum condition in a broad variety of choices. To authors' knowledge, integration of CFD models while performing simultaneous design and control has not been explored in the literature; hence, the motivation to advance the field in this front and provide new insight into optimal process design.

6.4 Expert decisions

Other areas that are critical to advance this field are integration of expert decisions into the process design. Expert decisions still play a crucial role at almost all levels of decision layers in the industries. Artificial intelligence (AI) techniques can be used to obtain systematic coordination between data and act as a decision-supporting tool. Usually, a massive amount of data is available that might be obtained from the historical data of similar processes; however, often these data are ignored particularly when the enterprises exclude systematic strategic decisions. Additionally, the integration of multiple aspects of the chemical supply chain consists of an enormous set of uncertainties that differ extremely in nature, i.e. sources, quantities, patterns. AI techniques can then be used to capture complex patterns and handle a large set of data with the aim to specify low-order though highly predictive surrogate (ANN) models. Figure 6-4 shows a schematic application of AI in the integrated algorithms. Recent advances in machine learning and big data analysis for decision-making provide additional support to capture useful uncertainty information and handle large data that lights up further improvements in this field (Ning and You, 2018). Additionally, AI enables the system to insert some sort of tactical planning decisions such as suggesting the course of action for the decision-making process. This is expected to be a fruitful research area in the near future.

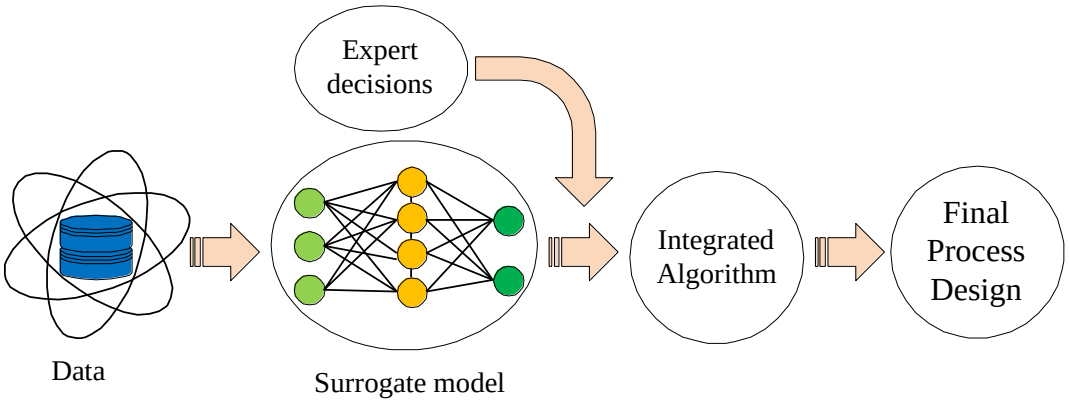

Figure 6-4: Schematic of AI application in the integrated algorithms

Having discussed the emerging trends, integration of such aspects and expanding the simultaneous design and control may open new research avenues to companies and improve their position in terms of being agile

and responsive to the dynamic and rapidly evolving global market. Clearly, new frontiers are not limited to the emerging trends discussed in this paper. Further advances in all individual sub-problems involving process integration as well as efficient optimization techniques, sophisticated data analysis procedures, and high-performance computing environments would also become a major breakthrough in the future. All these improvements support the attachment of the components of a multi-enterprise system shown in Figure 6-2 and practically implement the all-inclusive integrated problem. Implementation of an inclusive integrated scheme requires a platform that enables the connection and information flow between different factors.

6.5 Potential applications

The simultaneous design and control concepts have the potential to be broadened to fields beyond the chemical engineering discipline. Specific applications in other research fields can also be considered, e.g. nanotechnology (catalyst materials design), biotechnology (biological and biomedical systems), health (drug delivery), food engineering (thermal/non-thermal processing), agriculture (eco-friendly pesticides and fertilizers), business (investment decisions), advanced manufacturing (production of thin films), etc. To the best knowledge of the authors, no one has attempted to implement the integrated approach in such fields. Figure 6-5 shows a schematic of the currently explored and potential future applications of integrated approaches. Systematic integrated decision-making strategies, i.e. integration of design and control as the initial step, offer considerable benefits for the modern industries. Undoubtedly, such integrated attitudes are extremely appealing for companies which are seeking automation and building systematically links between the multiple aspects of this problem. A potential new application where integration of design and control has not been considered yet is presented next.

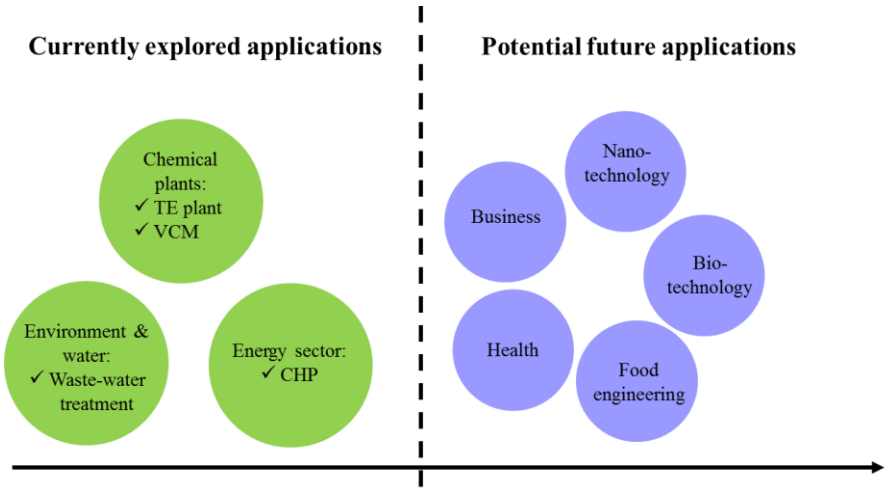

Figure 6-5: Schematic for the current and potential applications of integrated approaches

One of the applications of the integrated approach and systematic decision-making could be in the area of healthcare. In modern healthcare, technology combined with medical expertise can be used to improve patient care. Data based and systematic decision-making supports the treatment procedure and increases the effectiveness of the treatment. The quality of treatment can potentially increase by effectively providing the correct medication to the patient and at optimal success rate while maintaining close surveillance and monitoring of the patient's health and improvement. Health information incorporates information technologies and handles a large set of data coming from the patients' medical records, clinical documentation, and related research. Primarily, AI techniques can be implemented to classify and narrow down the possible diagnoses according to the symptoms to aid the assessment procedure commonly referred to as computer-aided diagnosis. For instance, AI technology can be used to identify the correct treatment for a patient or to specify the uncertainty description for key events that may affect the patient during the treatment. Biomedical modeling techniques can then be employed to obtain a model that can describe the patient's response to various treatments, the uncertainties surrounding the treatment and the disease, and external events that can affect the patient's treatment. Surrogate models could be developed to model these characteristics and assess the patient's performance in response to specific treatments under the effect of uncertain or unexpected events. Data collected from the research and medical records can be used to

validate those models. Moreover, it is possible to personalize and validate the obtained model for a specific patient using personal medical records. This problem can be formulated as a simultaneous design, control, and scheduling problem. The specification of the treatment method, which could be considered as the design variables, size and frequency of a dose of a medicine or drug, and the optimal treatment intervals can all be considered as decision variables of the integrated problem. The schematic of the integration of design and control concept for the healthcare problem is shown in Figure 6-6. The conceptual problem has the potential to add more factors and combine technology with medical expertise.

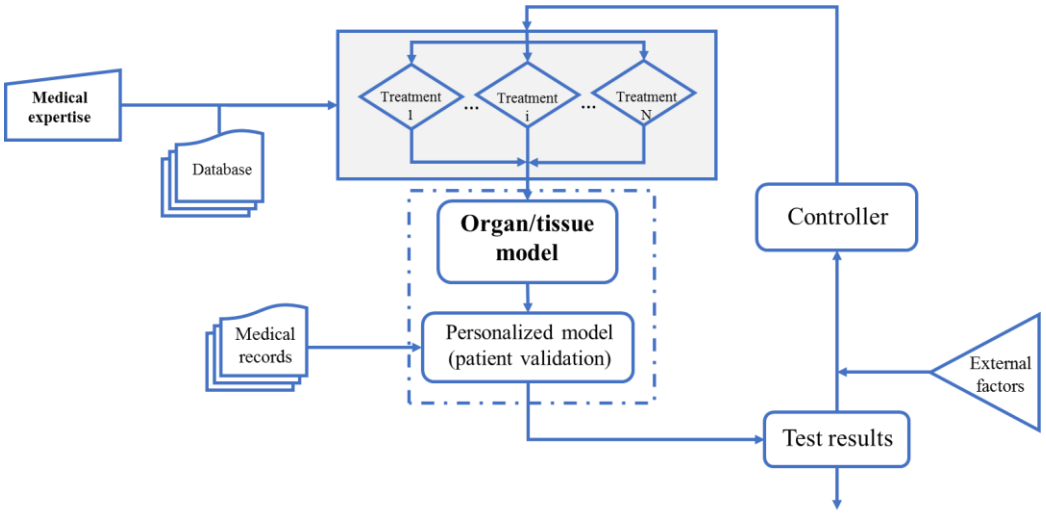

Figure 6-6: Conceptual integration of design and control for a healthcare system

This technology enables the implementation of a specific control strategy (either in closed-loop or open-loop) to decide the dosage and the treatment frequency, systematically. For instance, an MPC controller scheme can be used to provide optimal control actions in the system. Therefore, feedback from the patients is inserted into the curing process. Optimization can alternatively specify optimal open-loop control actions instead of feedback control actions for the problem. In addition to the patients' model, external factors can be added to the integrated framework which affects the curing process, e.g. reducing the average patient's waiting time, preparing and analyzing the test results in-between treatments. All these considerations in the treatment process can eventually increase the success rate of the treatment procedure and improve the patient's health. To the authors' knowledge, case studies addressing integration of design and operations

management in this critical area are not available; hence the need to develop such benchmark studies to evaluate the benefits and limitations of existing approaches to advance this field.

6.6 Outlook

Sustainable enterprises aim to protect nature and human and ecological health without sacrificing economic efficiency, innovations and business improvements. Within the framework of trade globalization and the dynamic market, quick adaptation is an essential policy that companies should pursue to remain as leaders in their sectors and enhance profits and sustainability. Every process incorporates a diverse set of conflicting objectives that need to be considered to achieve a sustainable and near-optimal operation. Inclusive awareness of the several features of the process, i.e. sustainability, can be obtained in an integrated approach. The integration of multiple aspects of the process aims for the consideration of the correlation between different layers of the process that results in flexible designs that can handle unpredictable disruptions efficiently. The integrated approaches have been mainly explored in terms of the integration of design and control; control and scheduling; scheduling and planning; and recently design, control, and scheduling. In general, the inherent interconnection between process design and control decisions with the upper manufacturing layers motivates the need to pursue the development of efficient techniques that can take those aspects into account and enable a formal process integration.

There are still a few open questions and challenges in the field that require further investigation, which can be summarized as follows:

- Sustainability can be improved by employing an integrated approach that leads to an overall environmentally-friendly, safe, profitable and energy-efficient process. Instead of addressing each aspect (or a combination of those) independent of other aspects, the inherent interconnection between these aspects, combined with the specification of suitable sustainability metrics, would enhance process sustainability. Thus, taking several aspects of the process into account would

streamline the decision-making procedure since it would enable the simultaneous selection of multiple decision variables affecting the operability, lifetime and economics of the process.

- Future directions tend to include wider decision layers in a bigger picture ranging from microscopic to macroscopic time and length scales. The provision of the chemical supply chain into the process design will enhance the profit of commercial enterprises. The collaborative strategies of an incorporated complex of multiple enterprises carry higher promises in the success of sustainable processes.
- A successfully integrated methodology requires recognition of dominant factors in multiple layers referred to as the multi-scale modeling techniques. Maintaining a good qualitative and quantitative information flow between the stages of the process is key to efficiently optimize multi-scale systems. Moreover, new computational tools enabling the optimization of key linking variables between the different scales are needed to allow the integration of systems at multiple time and spatial scales.
- More research is needed to assess the addition of advanced control strategies in an integrated framework and investigate the benefits and limitations of sophisticated control schemes such as NMPC and eventually EMPC. Issues such as closed-loop stability, state estimation and fast convergence of the control algorithms are still open challenges that may also impact process integration. In addition, global optimization approaches are subject to certain limitations; particularly for large-scale and highly constrained (non-convex) case studies under uncertainty. Thus, further algorithmic research and solver software developments are required to bring the promise of efficient global optimization closer to reality.
- Future work needs to be conducted to establish the incorporation of CFD into the integrated approach as a modeling tool that can capture the interaction between the different process components and therefore accomplish a highly detailed process integration for CFD systems.

Chemical reactor engineering, in particular, heterogeneous catalytic processes, are expected to greatly benefit from future developments in this area.

- In the modern world, the development of methods that can handle massive data for systematic decision-making is extremely desired. Additionally, AI enables the system to insert expert opinions into systematic decision-making. Applications of AI technology, in particular, machine learning techniques such as artificial neural networks, can become a breakthrough in this area to attempt the optimal integration of industrial-scale applications.
- The application of an integrated approach is not limited to the PSE discipline and development of applications in other fields such as healthcare, systems biology and agriculture are needed to gain insight into the existing integrated technologies.

Furthermore, there is still a large gap between the academia and industry to place the suggested methods into practice for real-life applications. The gap stems from the complex nature of the problem; nevertheless, the current advances in computer science signals confidence in converting integrated (complex) problems into achievable (solvable) goals in the future. Greater efforts are needed to include efficient uncertainty quantification techniques as well as the addition of sophisticated modeling techniques into the formulations. In brief, the integrated approach has a bright and promising future, though many challenges have yet to be overcome before a standard industrial-oriented framework can be devised.

7 Conclusions and future work

Moving towards optimal and sustainable operations has become a key concern for most of the industries to remain competitive in the current dynamic global market. The optimal operation of a process is highly tied with the design aspects of the process as they are inherently co-dependent. Integration of design and control aims to improve the efficiency of a plant during operation. The simultaneous consideration of design and control mostly results in the specification of complex and computationally demanding problems, particularly for industrial-scale applications.

In the current research, a new back-off approach for the integration of design and control of chemical processes has been presented using PSE functions. The key idea is to back-off from the optimal steady-state design to identify a new dynamically feasible operating condition at low computational costs. The work focuses on calculating various optimal design and control parameters by solving a set of optimization problems in an iterative fashion using PSE expressions. The PSE functions represent the actual process constraints and the cost function, which are explicitly defined in terms of the optimization variables expanded around the worst-case scenario. Computation of the PSE sensitivity terms using an analytical and a numerical approach was compared. The results show that both methods are equally efficient to calculate the PSE sensitivity terms; however, proper tuning of the finite-difference calculation is required offline. Higher computational costs were observed from the analytical calculation when compared with the numerical technique as more ODE's have to be solved in the first. Most of the CPU time required by the present approach is spent on the computation of the PSE sensitivity terms; thus, the total CPU time is expected to increase as more complex and highly nonlinear systems are considered.

The trust-region method is an extension of the basic back-off approach to address large-scale industrial systems. The key idea in this work is the development of the PSE function of the cost function and constraints while the validity of those expansions is certified in a trusted interval. The basic back-off approach remains insufficient for highly nonlinear and large-scale processes since the identification of a

trust-region around a nominal value that remains valid for the entire back-off procedure is a challenging task and might become intractable. Alternatively, the trust-region approach uses an adaptive search strategy to identify the validity region for each decision variable systematically. The trust-region is identified for every decision variable at each iteration. Accordingly, the adaptive approach may impose some restrictive boundaries on some decision variables regarding the effect of the decision variables in the deviation of the PSE function from the actual nonlinear process behaviour. Particularly for highly nonlinear systems, while the procedure chooses to retain those decision variables at their nominal values on some iterations, the rest of the decision variables may be allowed to be explored in a wider region. The system successively seeks for local optimality under disturbances. The convergence to a local optimum is assured since the representation of the approximate functions is maintained. The convergence of the approach to a locally optimal solution extremely depends on the qualifications of the PSE approximations during the entire sequence of the procedure. The system moves towards a descent direction and the convergence can satisfy the first-order KKT conditions. Furthermore, the approach can systematically update the order of PSE based on a user-defined level of accuracy. Black-box models can also be addressed using the proposed trust-region technique. The results indicate that the proposed methodology leads to more economically attractive and reliable designs while maintaining the dynamic operability of the system in the presence of multiple disturbances. Also, the application of the method on a large-scale system has been compared to the method previously reported in the literature for the TE plant.

A stochastic back-off methodology that addresses simultaneous design and control using stochastic uncertainty descriptions was also developed in this research. The key idea is to describe the confidence interval of process constraints at user-defined coverage probabilities using PSE-based functions. The method provides an additional degree of freedom since it can allocate different levels of confidence for the process constraints using coverage probability of confidence intervals. The results indicate that the proposed stochastic back-off approach leads to more economically attractive designs when compared to the

worst-case and variance-based approaches. The high computational demand is the main barrier for the implementation of the stochastic back-off on large-scale processes such as the TE plant.

7.1 Future work

The findings of this study have a number of important implications for future practice and can potentially be extended in different ways as explained below.

- Process synthesis and control structure selection have not been addressed in the current research. That is, continuous decision variables are considered for the integration of design and control concept. Integer variables associated with the topology of the process and the control scheme, e.g. control structure selection, are assumed to be known *a priori*. Evidently, considering integer decision variables along with the continuous variables provide much greater flexibility for improving the economics and performance of a large variety of problems. However, discontinuity of the derivatives due to the presence of integer variables extends the formulations to MINLP thereby increasing the problem's complexity. For future research directions, the addition of integer decision variables is highly recommended.
- One key future objective in this research is to achieve an optimal process design within an acceptable computational cost, in particular for large-scale systems. The foremost barrier to the implementation of the stochastic-based methodology is computational costs. The main burden of the proposed stochastic-based technique is the need for numerous simulations of the closed-loop system in order to obtain satisfactory accuracy of the PSE functions. For that reason, the next step in this research is to reduce the number of required samples in the analysis to achieve a certain level of accuracy in the calculations. Propagation of the uncertainties using MC sampling can be relatively straightforward to perform. Depending on the application, however, using other uncertainty propagation techniques such as Multilevel Monte Carlo (MLMC) may strongly reduce the computational demands (Kimaev and Ricardez-Sandoval, 2018). MLMC is considered as an

alternative which takes advantage of a geometric sequence of time steps that reduces the required numbers of samples using a range of different levels of discretization. The application of MLMC technique may result in attractive computational times compared to the standard MC sampling method. Once the computational burden of the stochastic back-off is relieved the probabilistic-based realization of uncertainty and disturbances for large-scale applications can be considered.

- In this research, PSE functions have been used as the modeling tool to propose a new methodology for the optimal design and control of dynamic systems under uncertainty. PSE functions represent the analytical expressions of the cost and constraints in the optimization problem. Simulation results are used to approximate the sensitivities of the PSE functions by means of finite-difference technique. Accordingly, the need to have access to the explicit closed-loop process model equations in the PSE approach is not required. That is, the present approach only requires access to the process outputs due to changes in the inputs. Following this reasoning, the automated communication between different programming languages such as MATLAB where the proposed back-off methodology can be implemented, and common process simulators available in the market is possible. Particularly, process simulators such as ASPEN and HYSYS are powerful tools used to develop comprehensive dynamic plant models. A communication link between a process simulator and a programming language, e.g. HYSYS and MATLAB, can be developed to implement the proposed back-off methodology for large-scale applications. The main challenge would be the difficulty of the convergence of the system in the dynamic mode. This difficulty might be due to the changes in the design parameters that affect the convergence of the dynamic mode. Indeed, dynamic simulation requires a good sense of appreciation of margins of design parameters and all related issues, e.g. complexity of obtaining physical property data at each nominal condition. Restrictions of the design variables, i.e. upper/lower bounds on decision variables, should be specified cautiously to avoid potential numerical instabilities while performing the simultaneous design and control using the proposed back-off methodology.

- The incorporation of advanced control strategies is expected to improve the performance of the designed system. The integration of a sophisticated control scheme such as model predictive control (MPC) into the design process results in significant advantages in process economics and performance. MPC is an advanced method of process control algorithm that has been in use in chemical process industries for decades. The ability of the MPC to handle the interactions and process constraints among the process variables may result in better optimal process designs than those obtained from decentralized control strategies. Enhanced control performance of the system improves the process economics and leads to short-term and long-term profits of the entire system.
- The straightforward implementation of the proposed technique allows further incorporation of the other aspects such as planning and scheduling into the integration framework. Accordingly, the procedure can be potentially extended to include transitions in the operating modes of the process. For example, the optimal transition between several modes of operation can also be addressed using decision variables that can take different values at different time intervals.
- The proposed methodology can be extended for simultaneous design and control of applications beyond the chemical engineering discipline such as nanotechnology (catalyst materials design), biotechnology (biological and biomedical systems), food engineering (thermal/non-thermal processing), agriculture (eco-friendly pesticides and fertilizers), and advanced manufacturing (production of thin films).
- Mathematical treatment that provides convergence guarantee along with theorems and proofs of the optimality of the final design is part of the future work. Similar concepts taken for the convergence of the derivative free optimization can be used to initiate the mathematical proof. Although the proposed methodology shares the common features of conventional trust-region methods that examine the validity of the approximation, it differs from those methods as the surrogate models at each iteration may be different. In the proposed trust-region method, surrogate models, i.e. PSEs, are developed for different nominal conditions of the process at each iteration.

Accordingly, the behavior of the actual nonlinear models should be studied at certain conditions to reinforce consistency between the iterations; for example, PSEs should be developed at a certain time at all iterations instead of the worst-case scenario.

Bibliography

Abd Hamid, M.K., Sin, G., Gani, R., 2010. Integration of process design and controller design for chemical processes using model-based methodology. Comput. Chem. Eng. 34, 683–699. doi:10.1016/j.compchemeng.2010.01.016

Aland, S., Lowengrub, J., Voigt, A., 2010. Two-phase flow in complex geometries: A diffuse domain approach. C. - Comput. Model. Eng. Sci. 57, 77–106.

Alhammadi, H.Y., Romagnoli, J.A., 2004. Process design and operation incorporating environmental, profitability, heat integration and controllability considerations, in: Seferlis, P., Georgiadis, M.C. (Eds.), The Integration of Process Design and Control. ELSEVIER, Amsterdam, pp. 264–305.

Alves, M.J., Clímaco, J., 2007. A review of interactive methods for multiobjective integer and mixed-integer programming. Eur. J. Oper. Res. 180, 99–115. doi:10.1016/j.ejor.2006.02.033

Andersen, B.B., Nielsen, R.F., Udugama, I.A., Papadakis, E., Gernaey, K. V., Huusom, J.K., Mansouri, S.S., Abildskov, J., 2018. Integrated Process Design and Control of Cyclic Distillation Columns. IFAC-PapersOnLine 51, 542–547. doi:10.1016/j.ifacol.2018.09.368

Asteasuain, M., Bandoni, A., Sarmoria, C., Brandolin, A., 2006. Simultaneous process and control system design for grade transition in styrene polymerization. Chem. Eng. Sci. 61, 3362–3378. doi:10.1016/j.ces.2005.12.012

Babi, D.K., Lutze, P., Woodley, J.M., Gani, R., 2014. A process synthesis-intensification framework for the development of sustainable membrane-based operations, in: Chemical Engineering and Processing: Process Intensification. Elsevier B.V., pp. 173–195. doi:10.1016/j.cep.2014.07.001

Bahakim, S.S., Rasoulian, S., Ricardez-Sandoval, L.A., 2014. Optimal Design of Large-Scale Chemical Processes Under Uncertainty: A Ranking-Based Approach. AIChE J. 60, 405–410.

Bahakim, S.S., Ricardez-Sandoval, L.A., 2015. Optimal design of a postcombustion CO2capture pilot-scale plant under process uncertainty: A ranking-based approach. Ind. Eng. Chem. Res. 54, 3879–3892.

Bahakim, S.S., Ricardez-Sandoval, L.A., 2014. Simultaneous design and MPC-based control for dynamic systems under uncertainty: A stochastic approach. Comput. Chem. Eng. 63, 66–81. doi:10.1016/j.compchemeng.2014.01.002

Bahri, P.A., Bandoni, J.A., Barton, G.W., Romagnoli, J.A., 1995. Back-off calculations in optimising control: A dynamic approach. Comput. Chem. Eng. 19, 699–708.

Bahri, P.A., Bandoni, J.A., Romagnoli, J.A., 1996. Effect of Disturbances in Optimizing Control : Steady-State Open-Loop Backoff Problem. AIChE J. 42, 983–994.

Bajaj, I., Iyer, S.S., Faruque Hasan, M.M., 2018. A trust region-based two phase algorithm for constrained black-box and grey-box optimization with infeasible initial point. Comput. Chem. Eng. 116, 306–321. doi:10.1016/j.compchemeng.2017.12.011

Baldea, M., 2015. From process integration to process intensification. Comput. Chem. Eng. 81, 104–114. doi:10.1016/j.compchemeng.2015.03.011

Baldea, M., Harjunkoski, I., 2014. Integrated production scheduling and process control: A systematic review. Comput. Chem. Eng. 71, 377–390. doi:10.1016/j.compchemeng.2014.09.002

Bansal, V., Sakizlis, V., Ross, R., Perkins, J.D., Pistikopoulos, E.N., 2003. New algorithms for mixed-integer dynamic optimization. Comput. Chem. Eng. 27, 647–668. doi:10.1016/S0098-1354(02)00261-2

Bernal, D.E., Carrillo-Diaz, C., Gomez, J.M., Ricardez-Sandoval, L.A., 2018. Simultaneous Design and Control of Catalytic Distillation Columns Using Comprehensive Rigorous Dynamic Models. Ind. Eng. Chem. Res. 57, 2587–2608. doi:10.1021/acs.iecr.7b04205

Bettebghor, D., Bartoli, N., Grihon, S., Morlier, J., Samuelides, M., 2011. Surrogate modeling approximation using a mixture of experts based on em joint estimation. Struct. Multidiscip. Optim. 43, 243–259. doi:10.1007/s00158-010-0554-2

Bhosekar, A., Ierapetritou, M., 2018. Advances in surrogate based modeling, feasibility analysis, and optimization: A review. Comput. Chem. Eng. 108, 250–267. doi:10.1016/j.compchemeng.2017.09.017

Biegler, L.T., 2010. Nonlinear Programming: Concepts, Algorithms, and Applications to Chemical Processes, 1st ed. SIAM, Philadelphia, PA, USA.

Biegler, L.T., Grossmann, I.E., 2004. Retrospective on optimization. Comput. Chem. Eng. 28, 1169–1192. doi:10.1016/j.compchemeng.2003.11.003

Biegler, L.T., Grossmann, I.E., Westerberg, A.W., 1985. A Note on Approximation Techniques Used for process Optimization. Comput. Chem. Eng. 9, 201–206.

Biegler, L.T., Lang, Y. dong, Lin, W., 2014. Multi-scale optimization for process systems engineering. Comput. Chem. Eng. 60, 17–30. doi:10.1016/j.compchemeng.2013.07.009

Blanco, A.M., Bandoni, J.A., 2003. Interaction between process design and process operability of chemical processes: An eigenvalue optimization approach. Comput. Chem. Eng. 27, 1291–1301. doi:10.1016/S0098-1354(03)00053-X

Brengel, D., Seider, W., 1992. Coordinated design and control optimization of nonlinear Process. Comput. Chem. Eng. 16, 861–886.

Burnak, B., Diangelakis, N.A., Katz, J., Pistikopoulos, E.N., 2019a. Integrated process design, scheduling, and control using multiparametric programming. Comput. Chem. Eng. 125, 164–184. doi:10.1016/j.compchemeng.2019.03.004

Burnak, B., Diangelakis, N.A., Pistikopoulos, E.N., 2019b. Towards the Grand Unification of Process Design, Scheduling, and Control—Utopia or Reality? Processes 7, 461. doi:10.3390/pr7070461

Chaffart, D., Ricardez-Sandoval, L.A., 2018. Optimization and control of a thin film growth process: A hybrid first principles/artificial neural network based multiscale modelling approach. Comput. Chem. Eng. 119, 465–479. doi:10.1016/j.compchemeng.2018.08.029

Chan, L.L.T., Chen, J., 2017. Probabilistic Uncertainty Based Simultaneous Process Design and Control with Iterative Expected Improvement Model. Comput. Chem. Eng. 106, 609–620. doi:10.1016/j.compchemeng.2017.07.011

Chawankul, N., Budman, H., Douglas, P.L., 2005. The integration of design and control: IMC control and robustness. Comput. Chem. Eng. 29, 261–271. doi:10.1016/j.compchemeng.2004.08.034

Chawankul, N., Ricardez-Sandoval, L.A., Budman, H.M., Douglas, P.L., 2007. Integration of Design and Control : A Robust Control Approach Using MPC. Can. J. Chem. Eng. 85, 433–446. doi:10.1002/cjce.5450850406

Chu, Y., You, F., 2015. Model-based integration of control and operations: Overview, challenges, advances, and opportunities. Comput. Chem. Eng. 83, 2–20. doi:10.1016/j.compchemeng.2015.04.011

Chu, Y., You, F., 2013. Integrated scheduling and dynamic optimization of complex batch processes with general network structure using a generalized benders decomposition approach. Ind. Eng. Chem. Res. 52, 7867–7885. doi:10.1021/ie400475s

Chu, Y., You, F., 2012. Integration of scheduling and control with online closed-loop implementation: Fast computational strategy and large-scale global optimization algorithm. Comput. Chem. Eng. 47, 248–268. doi:10.1016/j.compchemeng.2012.06.035

Cignitti, S., Mansouri, S.S., Woodley, J.M., Abildskov, J., 2018. Systematic Optimization-Based Integrated Chemical Product-Process Design Framework. Ind. Eng. Chem. Res. 57, 677–688. doi:10.1021/acs.iecr.7b04216

Dakin, R.J., 1965. A tree-search algorithm for mixed integer programming problems. Comput. J. 8, 250–255.

Davison, A.C., Hinkley, D. V., 1997. Bootstrap Methods and their Application.

Demirel, S.E., Li, J., Hasan, M.M.F., 2017. Systematic process intensification using building blocks. Comput. Chem. Eng. 105, 2–38. doi:10.1016/j.compchemeng.2017.01.044

Diangelakis, N.A., Avraamidou, S., Pistikopoulos, E.N., 2016. Decentralized Multiparametric Model Predictive Control for Domestic Combined Heat and Power Systems. Ind. Eng. Chem. Res. 55, 3313–3326. doi:10.1021/acs.iecr.5b03335

Diangelakis, N.A., Burnak, B., Katz, J., Pistikopoulos, E.N., 2017. Process design and control optimization: A simultaneous approach by multi-parametric programming. AIChE J. 63, 4827–4846. doi:10.1002/aic.15825

Diangelakis, N.A., Pistikopoulos, E.N., 2017. A multi-scale energy systems engineering approach to residential combined heat and power systems. Comput. Chem. Eng. 102, 128–138. doi:10.1016/j.compchemeng.2016.10.015

Dias, L.S., Ierapetritou, M.G., 2019. Optimal operation and control of intensified processes — challenges and opportunities. Curr. Opin. Chem. Eng. 8–12. doi:10.1016/j.coche.2018.12.008

Dias, L.S., Ierapetritou, M.G., 2017. From process control to supply chain management: An overview of integrated decision making strategies. Comput. Chem. Eng. 106, 826–835. doi:10.1016/j.compchemeng.2017.02.006

Dias, L.S., Ierapetritou, M.G., 2016. Integration of scheduling and control under uncertainties: Review and challenges. Chem. Eng. Res. Des. 116, 98–113. doi:10.1016/j.cherd.2016.10.047

Diehl, M., Bock, H.G., Kostina, E., 2006. An approximation technique for robust nonlinear optimization. Math. Program. 107, 213–230. doi:10.1007/s10107-005-0685-1

Dimitriadis, V.D., Pistikopoulos, E.N., 1995. Flexibility Analysis of Dynamic Systems. Ind. Eng. Chem. Res. 34, 4451–4462.

Downs, J.J., Vogel, E.F., 1993. A Plant-wide Industrial Problem Process. Comput. Chem. Eng. 17, 245–255. doi:10.1016/0098-1354(93)80018-I

Duran, M.A., Grossmann, I.E., 1986. An outer-approximation algorithm for a class of mixed-integer nonlinear programs. Math. Program. 36, 307–339. doi:10.1007/BF02592064

Ellis, M., Durand, H., Christofides, P.D., 2014. A tutorial review of economic model predictive control methods. J. Process Control 24, 1156–1178. doi:10.1016/j.jprocont.2014.03.010

Engell, S., Harjunkoski, I., 2012. Optimal operation: Scheduling, advanced control and their integration. Comput. Chem. Eng. 47, 121–133. doi:10.1016/j.compchemeng.2012.06.039

Exler, O., Antelo, L.T., Egea, J.A., Alonso, A.A., Banga, J.R., 2008. A Tabu search-based algorithm for mixed-integer nonlinear problems and its application to integrated process and control system design. Comput. Chem. Eng. 32, 1877–1891. doi:10.1016/j.compchemeng.2007.10.008

Farzan, P., Ierapetritou, M.G., 2017. Integrated modeling to capture the interaction of physiology and fluid dynamics in biopharmaceutical bioreactors. Comput. Chem. Eng. 97, 271–282. doi:10.1016/j.compchemeng.2016.11.037

Figueroa, J.L., Bahri, P.A., Bandoni, J.A., Romagnoli, J.A., 1996. Economic impact of disturbances and uncertain parameters in chemical processes - A dynamic back-off analysis. Comput. Chem. Eng. 20, 453–461.

Flores-Tlacuahuac, A., Biegler, L.T., 2007. Simultaneous mixed-integer dynamic optimization for integrated design and control. Comput. Chem. Eng. 31, 588–600. doi:10.1016/j.compchemeng.2006.08.010

Flores-Tlacuahuac, A., Grossmann, I.E., 2011. Simultaneous cyclic scheduling and control of tubular reactors: Parallel production lines. Ind. Eng. Chem. Res. 50, 8086–8096. doi:10.1021/ie101677e

Forrester, A.I.J., Keane, A.J., 2009. Recent advances in surrogate-based optimization. Prog. Aerosp. Sci. 45, 50–79. doi:10.1016/j.paerosci.2008.11.001

Francisco, M., Vega, P., Álvarez, H., 2011. Robust Integrated Design of processes with terminal penalty model predictive controllers. Chem. Eng. Res. Des. 89, 1011–1024. doi:10.1016/j.cherd.2010.11.023

Gani, R., 2004. Chemical product design: Challenges and opportunities. Comput. Chem. Eng. 28, 2441–2457. doi:10.1016/j.compchemeng.2004.08.010

Gebreslassie, B.H., Yao, Y., You, F., 2012. Design Under Uncertainty of Hydrocarbon Biorefinery Supply Chains: Multiobjective Stochastic Programming Models, Decomposition Algorithm, and a Comparison Between CVaR and and Downside Risk. AIChE J. 58, 2155–2179. doi:10.1002/aic.13844

Gentle, J.E., Härdle, W.K., Mori, Y. (Eds.), 2012. Handbook of Computational Statistics, 2nd ed, Handbook of Computational Statistics. Springer-Verlag. doi:10.1007/978-3-642-21551-3

Geoffrion, A.M., 1972. Generalized Benders Decomposition. J. Optim. Theory Appl. 10, 237–260. doi:10.1097/ACI.0000000000000254

Gerhard, J., Marquardt, W., Mönnigmann, M., 2008. Normal Vectors on Critical Manifolds for Robust Design of Transient Processes in the Presence of Fast Disturbances. SIAM J. Appl. Dyn. Syst. 7, 461–490. doi:10.1137/070698981

Gerhard, J., Mönnigmann, M., Marquardt, W., 2005. Constructive nonlinear dynamics - foundations and application to robust nonlinear control, in: Control and Observer Design for Nonlinear Finite and Infinite Dimensional Systems. Springer-Verlag, pp. 165–182.

Grossmann, I., 2005. Enterprise-wide optimization: A new frontier in process systems engineering. AIChE J. 51, 1846–1857. doi:10.1002/aic.10617

Grossmann, I.E., 2012. Advances in mathematical programming models for enterprise-wide optimization. Comput. Chem. Eng. 47, 2–18. doi:10.1016/j.compchemeng.2012.06.038

Grossmann, I.E., 2004. Challenges in the new millennium: Product discovery and design, enterprise and supply chain optimization, global life cycle assessment. Comput. Chem. Eng. 29, 29–39. doi:10.1016/j.compchemeng.2004.07.016

Grossmann, I.E., Westerberg, A.W., 2000. Research Challenges in Process Systems Engineering. AIChE J. 46, 1700–1703.

Gupta, O.K., Ravindran, A., 1985. Branch and bound experiments in convex nonlinear integer programming. Manage. Sci. 31, 1533–1546.

Gutierrez, G., Ricardez-Sandoval, L.A., Budman, H., Prada, C., 2014. An MPC-based control structure

selection approach for simultaneous process and control design. Comput. Chem. Eng. 70, 11–21. doi:10.1016/j.compchemeng.2013.08.014

Harjunkoski, I., Nyström, R., Horch, A., 2009. Integration of scheduling and control-Theory or practice? Comput. Chem. Eng. 33, 1909–1918. doi:10.1016/j.compchemeng.2009.06.016

Harper, P.M., Gani, R., 2000. A multi-step and multi-level approach for computer aided molecular design. Comput. Chem. Eng. 24, 677–683. doi:10.1016/S0098-1354(00)00410-5

Harper, P.M., Gani, R., Kolar, P., Ishikawa, T., 1999. Computer-aided molecular design with combined molecular modeling and group contribution. Fluid Phase Equilib. 158–160, 337–347. doi:10.1016/s0378-3812(99)00089-8

Jones, D.R., 2001. A Taxonomy of Global Optimization Methods Based on Response Surfaces. J. Glob. Optim. 21, 345–383. doi:10.1023/A:1012771025575

Kalakul, S., Malakul, P., Siemanond, K., Gani, R., 2014. Integration of life cycle assessment software with tools for economic and sustainability analyses and process simulation for sustainable process design. J. Clean. Prod. 71, 98–109. doi:10.1016/j.jclepro.2014.01.022

Kimaev, G., Ricardez-Sandoval, L.A., 2018. Multilevel Monte Carlo for noise estimation in stochastic multiscale systems. Chem. Eng. Res. Des. 140, 33–43. doi:10.1016/j.cherd.2018.10.006

Koller, R.W., Ricardez-Sandoval, L.A., 2017. A dynamic optimization framework for integration of design, control and scheduling of multi-product chemical processes under disturbance and uncertainty. Comput. Chem. Eng. 106, 147–159. doi:10.1016/j.compchemeng.2017.05.007

Koller, R.W., Ricardez-Sandoval, L.A., Biegler, L.T., 2018. Stochastic back-off algorithm for simultaneous design, control, and scheduling of multiproduct systems under uncertainty. AIChE J. doi:10.1002/aic.16092

Kookos, I.K., Perkins, J.D., 2016. Control Structure Selection Based on Economics: Generalization of the Back-Off Methodology. AIChE J. 62, 3056–3064. doi:10.1002/aic.15284

Kookos, I.K., Perkins, J.D., 2004. The back-off to simultaneous design and control, in: Seferlis, P., Georgiadis, M.C. (Eds.), The Integration of Process Design and Control. ELSEVIER, Amsterdam, pp. 216–234.

Kookos, I.K., Perkins, J.D., 2001. An Algorithm for Simultaneous Process Design and Control. Ind. Eng. Chem. Res. 40, 4079–4088. doi:10.1021/ie000622t

Kronqvist, J., Bernal, D.E., Lundell, A., Grossmann, I.E., 2019. A review and comparison of solvers for convex MINLP, Optimization and Engineering. Springer US. doi:10.1007/s11081-018-9411-8

Kuhlman, T., Farrington, J., 2010. What is sustainability? Sustainability 2, 3436–3448. doi:10.3390/su2113436

Laird, C.D., Biegler, L.T., 2006. Large-Scale Nonlinear Programming for Multi-scenario Optimization, in: Bock, H.G., Kostina, E., Phu, H.X., Rannacher, R. (Eds.), Modeling , Simulation of Complex Processes. Springer-Verlag, Hanoi, Vietnam, pp. 324–336.

Larsson, T., Hestetun, K., Hovland, E., Skogestad, S., 2001. Self-optimizing control of a large-scale plant: The Tennessee Eastman process. Ind. Eng. Chem. Res. 40, 4889–4901. doi:10.1021/ie000586y

Lenhoff, A.M., Morari, M., 1982. Design of resilient processing plants-I Process design under consideration of dynamic aspects. Chem. Eng. Sci. 37, 245–258. doi:10.1016/0009-2509(82)80159-0

Li, C., Zhang, X., Zhang, S., Suzuki, K., 2009. Environmentally conscious design of chemical processes and products: Multi-optimization method. Chem. Eng. Res. Des. 87, 233–243. doi:10.1016/j.cherd.2008.07.017

Li, S., Mirlekar, G., Ruiz-Mercado, G.J., Lima, F. V., 2016. Development of chemical process design and control for sustainability. Processes 4, 1–21. doi:10.3390/pr4030023

Li, X., Armagan, E., Tomasgard, A., Bart, 2011a. Stochastic Pooling Problem for Natural Gas Production Network Design and Operation Under Uncertainty. AIChE J. 57, 2120–2135. doi:10.1002/aic

Li, X., Chen, Y., Barton, P.I., 2012. Nonconvex generalized benders decomposition with piecewise convex relaxations for global optimization of integrated process design and operation problems. Ind. Eng. Chem. Res. 51, 7287–7299. doi:10.1021/ie201262f

Li, X., Tomasgard, A., Barton, P.I., 2011b. Nonconvex Generalized Benders Decomposition for Stochastic Separable Mixed-Integer Nonlinear Programs. J. Optim. Theory Appl. 151, 425–454. doi:10.1007/s10957-011-9888-1

Lu, X.J., Li, H.X., Yuan, X., 2010. PSO-based intelligent integration of design and control for one kind of curing process. J. Process Control 20, 1116–1125. doi:10.1016/j.jprocont.2010.06.019

Lutze, P., Babi, D.K., Woodley, J.M., Gani, R., 2013. Phenomena based methodology for process synthesis incorporating process intensification. Ind. Eng. Chem. Res. 52, 7127–7144. doi:10.1021/ie302513y

Lutze, P., Gani, R., Woodley, J.M., 2010. Process intensification: A perspective on process synthesis. Chem. Eng. Process. Process Intensif. 49, 547–558. doi:10.1016/j.cep.2010.05.002

Luyben, M.L., Floudas, C.A., 1994a. Analyzing the interaction of design and control-1. A multiobjective framework and application to binary distillation synthesis. Comput. Chem. Eng. 18, 933–969.

Luyben, M.L., Floudas, C.A., 1994b. Analyzing the interaction of design and control-2. reactor-separator-recycle system, in: Computers and Chemical Engineering. pp. 971–993. doi:10.1016/0098-1354(94)85006-2

Luyben, M.L., Floudas, C.A., 1992. A Multiobjective Optimization Approach for Analyzing the Interaction of Design and Control, in: IFAC Proceedings Volumes. Elsevier, pp. 101–106. doi:10.1016/s1474-6670(17)54017-3

Luyben, W.L., 2004. The need for simultaneous design education, in: Seferlis, P., Georgiadis, M.C. (Eds.), The Integration of Process Design and Control. Elsevier B.V., Amsterdam, pp. 10–41.

Luyben, W.L., 1996. Simple regulatory control of the Eastman process. Ind. Eng. Chem. Res. 35, 3280–3289. doi:10.1021/ie960162x

Luyben, W.L., 1992. Design and Control of Recycle Processes in Ternary Systems with Consecutive Reactions. IFAC Proc. Vol. 25, 65–74. doi:10.1016/s1474-6670(17)54013-6

Lyman, P.R., Georgakis, C., 1995. Plant-wide control of the Tennessee Eastman problem. Comput. Chem. Eng. 19, 321–331. doi:10.1016/0098-1354(94)00057-U

Malcolm, A., Polan, J., Zhang, L., Ogunnaike, B.A., Linninger, A.A., 2007. Integrating Systems Design and Control using Dynamic Flexibility Analysis. AIChE J. 53, 2048–2061. doi:10.1002/aic.11218

Maly, T., Petzold, L.R., 1996. Numerical methods and software for sensitivity analysis of differential-algebraic systems. Appl. Numer. Math. 20, 57–59. doi:10.1016/0168-9274(95)00117-4

Mansouri, S.S., Huusom, J.K., Gani, R., Sales-Cruz, M., 2016a. Systematic Integrated Process Design and Control of Binary Element Reactive Distillation Processes. AIChE J. 62, 3137–3154. doi:10.1002/aic.15322

Mansouri, S.S., Sales-Cruz, M., Huusom, J.K., Gani, R., 2016b. Systematic integrated process design and control of reactive distillation processes involving multi-elements. Chem. Eng. Res. Des. 115, 348–364. doi:10.1016/j.cherd.2016.07.010

Maravelias, C.T., Sung, C., 2009. Integration of production planning and scheduling: Overview, challenges and opportunities. Comput. Chem. Eng. 33, 1919–1930. doi:10.1016/j.compchemeng.2009.06.007

Marler, R.T., Arora, J.S., 2004. Survey of multi-objective optimization methods for engineering. Struct. Multidiscip. Optim. 26, 369–395. doi:10.1007/s00158-003-0368-6

Matallana, L.G., Blanco, A.M., Bandoni, J.A., 2011. Nonlinear dynamic systems design based on the optimization of the domain of attraction. Math. Comput. Model. 53, 731–745. doi:10.1016/j.mcm.2010.10.011

McAvoy, T.J., Ye, N., 1994. Base control for the Tennessee Eastman problem. Comput. Chem. Eng. 18, 383–413. doi:10.1016/0098-1354(94)88019-0

Meeuse, F.M., Tousain, R.L., 2002. Closed-loop controllability analysis of process designs: Application to distillation column design. Comput. Chem. Eng. 26, 641–647. doi:10.1016/S0098-1354(01)00791-8

Mehta, S., Ricardez-Sandoval, L.A., 2016. Integration of Design and Control of Dynamic Systems under Uncertainty: A New Back-Off Approach. Ind. Eng. Chem. Res. 55, 485–498. doi:10.1021/acs.iecr.5b03522

Meidanshahi, V., Adams, T.A., 2016. Integrated design and control of semicontinuous distillation systems utilizing mixed integer dynamic optimization. Comput. Chem. Eng. 89, 172–183. doi:10.1016/j.compchemeng.2016.03.022

Mohideen, M.J., Perkins, J.D., Pistikopoulos, E.N., 1997. Robust stability considerations in optimal design of dynamic systems under uncertainty. J. Process Control 7, 371–385. doi:10.1016/S0959-1524(97)00014-0

Mohideen, M.J., Perkins, J.D., Pistikopoulos, E.N., 1996a. Optimal design of dynamic systems under uncertainty. AIChE J. 42, 2251–2272. doi:10.1002/aic.690420814

Mohideen, M.J., Perkins, J.D., Pistikopoulos, E.N., 1996b. Optimal synthesis and design of dynamic systems under uncertainty. Science (80-.). 20, 895–900.

Moon, J., Kim, S., Linninger, A.A., 2011. Integrated design and control under uncertainty: Embedded control optimization for plantwide processes. Comput. Chem. Eng. 35, 1718–1724. doi:10.1016/j.compchemeng.2011.02.016

Müller, M.A., Angeli, D., Allgöwer, F., Amrit, R., Rawlings, J.B., 2014. Convergence in economic model predictive control with average constraints. Automatica 50, 3100–3111. doi:10.1016/j.automatica.2014.10.059

Narraway, L., Perkins, J.D., 1994. Selection of process control structure based on economics. Comput. Chem. Eng. 18, S511–S515. doi:10.1016/0098-1354(94)80083-9

Narraway, L.T., Perkins, J.D., 1993. Selection of process control structure based on linear dynamic economics. Ind. Eng. Chem. Res. 32, 2681–2692.

Narraway, L.T., Perkins, J.D., Barton, G.W., 1991. Interaction between process design and process control: economic analysis of process dynamics. J. Proc. Cont. 1, 243–250. doi:10.1016/0959-1524(91)85015-B

Nguyen, T.C., Barton, G.W., Perkins, J.D., Johnston, R.D., 1988. A condition number scaling policy for stability robustness analysis. AIChE J. 34, 1200–1206. doi:10.1002/aic.690340716

Nie, Y., Biegler, L.T., Villa, C.M., Wassick, J.M., 2015. Discrete Time Formulation for the Integration of Scheduling and Dynamic Optimization. Ind. Eng. Chem. Res. 54, 4303–4315. doi:10.1021/ie502960p

Ning, C., You, F., 2018. Data-driven decision making under uncertainty integrating robust optimization with principal component analysis and kernel smoothing methods. Comput. Chem. Eng. 112, 190–

210. doi:10.1016/j.compchemeng.2018.02.007

Palazoglu, A., Arkun, Y., 1986. A multiobjective approach to design chemical plants with robust dynamic operability characteristics. Comput. Chem. Eng. 10, 567–575.

Papalexandri, K.P., Pistikopoulos, E.N., 1996. Generalized modular representation framework for process synthesis. AIChE J. 42, 1010–1032. doi:10.1002/aic.690420413

Papalexandri, K.P., Pistikopoulos, E.N., 1994a. Synthesis and Retrofit Design of Operable Heat Exchanger Networks. 2. Dynamics and Control Structure Considerations. Ind. Eng. Chem. Res. 33, 1738–1755. doi:10.1021/ie00031a013

Papalexandri, K.P., Pistikopoulos, E.N., 1994b. Synthesis and Retrofit Design of Operable Heat Exchanger Networks. 1. Flexibility and Structural Controllability Aspects. Ind. Eng. Chem. Res. 33, 1718–1737. doi:10.1021/ie00031a012

Patankar, N.A., Singh, P., Joseph, D.D., Glwinski, R., Pan, T.-W., 2000. A new formulation of the distributed Lagrange multiplier/fictitious domain method for particulate flows. Int. J. Multiph. Flow 26, 1509–1524. doi:10.1016/s0301-9322(99)00100-7

Patil, B.P., Maia, E., Ricardez-sandoval, L.A., 2015. Integration of Scheduling, Design, and Control of Multiproduct Chemical Processes Under Uncertainty. AIChE J. 61, 2456–2470. doi:10.1002/aic

Perkins, J.D., 1989. Interactions Between Process Design and Process Control, in: IFAC Symposium on Dynamics and Control of Chemical Reactors and Columns. Pergamon Press, Maastricht, The Netherlands, pp. 195–203.

Perkins, J.D., Gannavarapu, C., Barton, G.W., 1989. Choosing Control Structures Based on Economics., in: Control for Profit. Newcastle, pp. 3/1-3/3.

Pistikopoulos, E.N., 1995. Uncertainty in Process Design and Operations. Comput. Chem. Eng. 19, S553–S563.

Pistikopoulos, E.N., Diangelakis, N.A., 2016. Towards the integration of process design, control and scheduling: Are we getting closer? Comput. Chem. Eng. 91, 85–92. doi:10.1016/j.compchemeng.2015.11.002 0098-1354/©

Pistikopoulos, E.N., Diangelakis, N.A., Oberdieck, R., Papathanasiou, M.M., Nascu, I., Sun, M., 2015. PAROC — An integrated framework and software platform for the optimisation and advanced model-based control of process systems. Chem. Eng. Sci. 136, 115–138. doi:10.1016/j.ces.2015.02.030

Rafiei-Shishavan, M., Mehta, S., Ricardez-Sandoval, L.A., 2017. Simultaneous design and control under uncertainty: A back-off approach using power series expansions. Comput. Chem. Eng. 99, 66–81. doi:10.1016/j.compchemeng.2016.12.015

Rafiei-Shishavan, M., Ricardez-Sandoval, L.A., 2017. A Stochastic Approach for Integration of Design and Control under Uncertainty: A Back-off Approach Using Power Series Expansions, in: Espuña, A., Graells, M., Puigjaner, L. (Eds.), 27th European Symposium on Computer Aided Process Engineering. Barcelona, Spain, pp. 1861–1866. doi:10.1016/B978-0-444-63965-3.50312-3

Rafiei, M., Ricardez-Sandoval, L.A., 2020a. New frontiers, challenges, and opportunities in integration of design and control for enterprise-wide sustainability. Comput. Chem. Eng. 132. doi:10.1016/j.compchemeng.2019.106610

Rafiei, M., Ricardez-Sandoval, L.A., 2020b. A Trust-Region Framework for Integration of Design and Control. AIChE J. doi:10.1002/aic.16922

Rafiei, M., Ricardez-Sandoval, L.A., 2018. Stochastic Back-Off Approach for Integration of Design and Control Under Uncertainty. Ind. Eng. Chem. Res. 57, 4351–4365. doi:10.1021/acs.iecr.7b03935

Rashid, M.M., Mhaskar, P., Swartz, C.L.E., 2016. Multi-rate modeling and economic model predictive control of the electric arc furnace. J. Process Control j 40, 50–61. doi:10.1007/978-3-030-04140-3_10

Rasoulian, S., Ricardez-Sandoval, L.A., 2016. Stochastic nonlinear model predictive control applied to a thin film deposition process under uncertainty. Chem. Eng. Sci. 140, 90–103.

Rasoulian, S., Ricardez-Sandoval, L.A., 2015. Robust multivariable estimation and control in an epitaxial thin film growth process under uncertainty. J. Process Control 34, 70–81.

Rasoulian, S., Ricardez-Sandoval, L.A., 2014. Uncertainty analysis and robust optimization of multiscale process systems with application to epitaxial thin film growth. Chem. Eng. Sci. 116, 590–600. doi:10.1016/j.ces.2014.05.027

Revollar, S., Francisco, M., Vega, P., Lamanna, R., 2010. Stochastic optimization for the simultaneous synthesis and control system design of an activated sludge process. Lat. Am. Appl. Res. 40, 137–146.

Ricardez-Sandoval, L.A., 2012. Optimal design and control of dynamic systems under uncertainty: A probabilistic approach. Comput. Chem. Eng. 43, 91–107.

Ricardez-Sandoval, L.A., 2008. Simultaneous design and control of chemical plants: A robust modelling approach.

Ricardez-Sandoval, L.A., Budman, H.M., Douglas, P.L., 2010. Simultaneous design and control: A new approach and comparisons with existing methodologies. Ind. Eng. Chem. Res. 49, 2822–2833. doi:10.1021/ie9010707

Ricardez-Sandoval, L.A., Budman, H.M., Douglas, P.L., 2009a. Integration of design and control for chemical processes: A review of the literature and some recent results. Annu. Rev. Control 33, 158–171. doi:10.1016/j.arcontrol.2009.06.001

Ricardez-Sandoval, L.A., Budman, H.M., Douglas, P.L., 2009b. Application of robust control tools to the simultaneous design and control of dynamic systems. Ind. Eng. Chem. Res. 48, 801–813. doi:10.1021/ie800378y

Ricardez-Sandoval, L.A., Budman, H.M., Douglas, P.L., 2009c. Simultaneous design and control of chemical processes with application to the Tennessee Eastman process. J. Process Control 19, 1377–1391.

Ricardez-Sandoval, L.A., Budman, H.M., Douglas, P.L., 2008. Simultaneous design and control of processes under uncertainty: A robust modelling approach. J. Process Control 18, 735–752. doi:10.1016/j.jprocont.2007.11.006

Ricardez-Sandoval, L.A., Douglas, P.L., Budman, H.M., 2011. A methodology for the simultaneous design and control of large-scale systems under process parameter uncertainty. Comput. Chem. Eng. 35, 307–318. doi:10.1016/j.compchemeng.2010.05.010

Ricker, N.L., 1996. Decentralized control of the Tennessee Eastman Challenge Process. J. Process Control 6, 205–221. doi:10.1016/0959-1524(96)00031-5

Ricker, N.L., 1995. Optimal steady-state operation of the Tennessee Eastman challenge process. Comput. Chem. Eng. 19, 949–959. doi:10.1016/0098-1354(94)00043-N

Ruiz, J.P., Grossmann, I.E., 2017. Global optimization of non-convex generalized disjunctive programs: a review on reformulations and relaxation techniques. J. Glob. Optim. 67, 43–58. doi:10.1007/s10898-016-0401-0

Sahay, N., Ierapetritou, M., 2016. Multienterprise Supply Chain: Simulation and Optimization. AIChE J. 62, 3392–3403. doi:10.1002/aic

Sakizlis, V., Perkins, J.D., Pistikopoulos, E.N., 2004. Recent advances in optimization-based simultaneous

process and control design. Comput. Chem. Eng. 28, 2069–2086.

Sakizlis, V., Perkins, J.D., Pistikopoulos, E.N., 2003. Parametric controllers in simultaneous process and control design optimization. Ind. Eng. Chem. Res. 42, 4545–4563.

Sanchez-Sanchez, K.B., Ricardez-Sandoval, L.A., 2013a. Simultaneous Design and Control under Uncertainty Using Model Predictive Control. Ind. Eng. Chem. Res. 52, 4815–4833.

Sanchez-Sanchez, K.B., Ricardez-Sandoval, L.A., 2013b. Simultaneous Process Synthesis and Control Design under Uncertainty: A Worst-Case Performance Approach. AIChE J. 59, 2497–2413. doi:10.1002/aic

Schluter, M., Egea, J.A., Antelo, L.T., Alonso, A.A., Banga, J.R., 2009. An Extended Ant Colony Optimization Algorithm for Integrated Process and Control System Design. Ind. Eng. Chem. Res. 48, 6723–6738. doi:10.1021/ie8016785

Schulz, E.P., Diaz, M.S., Bandoni, J.A., 2005. Supply chain optimization of large-scale continuous processes. Comput. Chem. Eng. 29, 1305–1316. doi:10.1016/j.compchemeng.2005.02.025

Shah, N., 2005. Process industry supply chains: Advances and challenges. Comput. Chem. Eng. 29, 1225–1235. doi:10.1016/j.compchemeng.2005.02.023

Sharifzadeh, M., 2013. Chemical Engineering Research and Design Integration of process design and control : A review, Chemical Engineering Research and Design. Institution of Chemical Engineers. doi:10.1016/j.cherd.2013.05.007

Sharifzadeh, M., Thornhill, N.F., 2013. Integrated design and control using a dynamic inversely controlled process model. Comput. Chem. Eng. 48, 121–134. doi:10.1016/j.compchemeng.2012.08.009

Sharifzadeh, M., Thornhill, N.F., 2012. Optimal selection of control structure using a steady-state inversely controlled process model. Comput. Chem. Eng. 38, 126–138. doi:10.1016/j.compchemeng.2011.12.007

Shi, J., Biegler, L.T., Hamdan, I., 2016. Optimization of grade transitions in polyethylene solution polymerization processes. AIChE J. 62, 1126–1142. doi:10.1002/aic.15113

Shobrys, D.E., White, D.C., 2002. Planning, scheduling and control systems: Why cannot they work together. Comput. Chem. Eng. 26, 149–160. doi:10.1016/S0098-1354(01)00737-2

Singh, H., Hutmacher, D.W., 2009. Bioreactor Studies and Computational Fluid Dynamics, in: Kasper, C., Griensven, M. van, Portner, R. (Eds.), Advances in Biomedical Engineering/Biotechnology. Springer, pp. 231–251. doi:10.4271/780316

Sotiropoulos, F., Yang, X., 2014. Immersed boundary methods for simulating fluid-structure interaction. Prog. Aerosp. Sci. 65, 1–21. doi:10.1016/j.paerosci.2013.09.003

Srinivasan, B., Bonvin, D., Visser, E., Palanki, S., 2003. Dynamic optimization of batch processes. Comput. Chem. Eng. 27, 27–44.

Sriniwas, G.R., Arkun, Y., 1997. Control of the Tennessee eastman process using input-output models. J. Process Control 7, 387–400. doi:10.1016/s0959-1524(97)00015-2

Swartz, C.L.E., Kawajiri, Y., 2019. Design for dynamic operation – A review and new perspectives for an increasingly dynamic plant operating environment Christopher. Comput. Chem. Eng. doi:https://doi.org/1https://doi.org/10.1016/j.compchemeng.2019.06.0020.1016/j.compchemeng.2019.06.002

Tajsoleiman, T., Spann, R., Bach, C., Gernaey, K. V., Huusom, J.K., Krühne, U., 2019. A CFD based automatic method for compartment model development. Comput. Chem. Eng. 123, 236–245. doi:10.1016/j.compchemeng.2018.12.015

Tawarmalani, M., Sahinidis, N. V, 2004. Global optimization of mixed-integer nonlinear programs: A theoretical and computational study. Math. Program. 591, 563–591.

Tian, Y., Demirel, S.E., Hasan, M.M.F., Pistikopoulos, E.N., 2018. An overview of process systems engineering approaches for process intensification: State of the art. Chem. Eng. Process. - Process Intensif. 133, 160–210. doi:10.1016/j.cep.2018.07.014

Tian, Y., Pistikopoulos, E.N., 2019. Synthesis of operable process intensification systems: advances and challenges. Curr. Opin. Chem. Eng. 1–7. doi:10.1016/j.coche.2018.12.003

Trainor, M., Giannakeas, V., Kiss, C., Ricardez-Sandoval, L.A., 2013. Optimal process and control design under uncertainty: A methodology with robust feasibility and stability analyses. Chem. Eng. Sci. 104, 1065–1080. doi:10.1016/j.ces.2013.10.017

Treeratanaphitak, T., 2018. Diffuse Solid-Fluid Interface Method for Dispersed Multiphase Flows. University of Waterloo.

Tsay, C., Pattison, R.C., Baldea, M., 2017. A Dynamic Optimization Approach to Probabilistic Process Design under Uncertainty. Ind. Eng. Chem. Res. 56, 8606–8621. doi:10.1021/acs.iecr.7b00375

Tula, A.K., Babi, D.K., Bottlaender, J., Eden, M.R., Gani, R., 2017. A computer-aided software-tool for sustainable process synthesis-intensification. Comput. Chem. Eng. 105, 74–95. doi:10.1016/j.compchemeng.2017.01.001

Valdez-Navarro, Y.I., Ricardez-Sandoval, L.A., 2019a. Integration between Dynamic Optimization and Scheduling of Batch Processes under Uncertainty : A Back-off Approach, in: 12th IFAC Symposium on Dynamics and Control of Process Systems, Including Biosystems. Elsevier B.V., Florianópolis - SC, Brazil, pp. 655–660. doi:10.1016/j.ifacol.2019.06.137

Valdez-Navarro, Y.I., Ricardez-Sandoval, L.A., 2019b. A Novel Back-off Algorithm for Integration of Scheduling and Control of Batch Processes under Uncertainty. Ind. Eng. Chem. Res. 58, acs.iecr.9b04963. doi:10.1021/acs.iecr.9b04963

Vega, P., Lamanna de Rocco, R., Revollar, S., Francisco, M., 2014a. Integrated design and control of chemical processes – Part I: Revision and classification. Comput. Chem. Eng. 71, 602–617. doi:10.1016/j.compchemeng.2014.05.010

Vega, P., Lamanna, R., Revollar, S., Francisco, M., 2014b. Integrated design and control of chemical processes – Part II: An illustrative example. Comput. Chem. Eng. 71, 618–635. doi:10.1016/j.compchemeng.2014.09.019

Venkatasubramanian, V., 2009. DROWNING IN DATA: Informatics and Modeling Challenges in a Data-Rich Networked World. AIChE J. 55, 1–8. doi:10.1002/aic

Viana, F.A.C., Haftka, R.T., Watson, L.T., 2013. Efficient global optimization algorithm assisted by multiple surrogate techniques. J. Glob. Optim. 56, 669–689. doi:10.1007/s10898-012-9892-5

Visser, E., Srinivasan, B., Palanki, S., Bonvin, D., 2000. A feedback-based implementation scheme for batch process optimization. J. Process Control 10, 399–410. doi:10.1016/S0959-1524(00)00015-9

Viswanathan, J., Grossmann, I.E., 1990. A combined penalty function and outer-approximation method for MINLP optimization. Comput. Chem. Eng. 14, 769–782. doi:10.1016/0098-1354(90)87085-4

Wang, B., Gebreslassie, B.H., You, F., 2013. Sustainable design and synthesis of hydrocarbon biorefinery via gasification pathway: Integrated life cycle assessment and technoeconomic analysis with multiobjective superstructure optimization. Comput. Chem. Eng. 52, 55–76. doi:10.1016/j.compchemeng.2012.12.008

Wang, S., Baldea, M., 2014a. Identification-based optimization of dynamical systems under uncertainty.

Comput. Chem. Eng. 64, 138–152. doi:10.1016/j.compchemeng.2014.02.001

Wang, S., Baldea, M., 2014b. Conservativeness and Stability Properties in the Optimal Design of Dynamical Systems Under Uncertainty, in: American Control Conference (ACC). Portland, OR, pp. 3524–3529.

Washington, I.D., Swartz, C.L.E., 2014. Design Under Uncertainty Using Parallel Multiperiod Dynamic Optimization. AIChE J. 60, 3151–3168. doi:10.1002/aic

Yuan, Z., Chen, B., Sin, G., Gani, R., 2012. State-of-the-Art and Progress in the Optimization-based Simultaneous Design and Control for Chemical Processes. AIChE J. 58, 1640–1659. doi:10.1002/aic.13786

Appendix A

The summary of the proposed trust-region algorithm introduced in chapter 5 is presented here.

Step 1: Define upper ($\boldsymbol{\eta}^U$) and lower bounds ($\boldsymbol{\eta}^L$) for optimization variables ($\boldsymbol{\eta}$), the maximum number of iterations (N_{iter}); PSE validation tolerance (ϵ_{TR}), convergence tolerance (ϵ), convergence examination period (N_c); step size for the finite difference calculations, which will be used as the smallest acceptable trust-region. Set the iteration index to $i = 1$.

Step 2: Set the uncertain parameters and disturbances to their nominal values and solve the steady-state optimization problem. Alternatively, one could use an educated initial guess in case the optimal steady-state solution is not available, e.g. process designs based on heuristics. Set the solution ($\boldsymbol{\eta_0}$) as the nominal optimization variables for the first iteration ($\boldsymbol{\eta}_{i=1} = \boldsymbol{\eta_0}$).

Step 3: Using $\boldsymbol{\eta_i}$ simulate the process under uncertainty and disturbances, identify the worst-case scenario (highest variability) for each constraint, i.e. the uncertain parameter (ζ_j) and the time that largest variability in each constraint occurs (t_{wc}). Simulate the model for $\boldsymbol{\eta}^+$and $\boldsymbol{\eta}^-$using ζ_j and record the cost and constraint values at t_{wc}. Use the collected data to calculate the sensitivity of the cost and constraints and thus PSE expansions of cost and constraint functions.

Step 4: Build the MSE for the cost and constraint functions according to equations (5-3 and 5-4) using the sensitivities calculated in *Step 3*.

Solve the trust-region optimization (problem (5-7)) and identify the search interval for each decision variable (you may use the stepwise search method described in section 5.1.1 as an alternative approach to estimate the search space interval for each decision variable). If the identified trust-region is too small, go back to *Step* 3 and increase the order of PSE function. If increased PSE order does not significantly improve the accuracy in the estimations, proceed with the small search space region.

Step 5: Construct and solve the PSE based optimization problem (problem (5-14)) using the PSE expansions built in *Step* 3 and the search space (trust-region) for each decision variable identified in *Step* 4.

Step 6: Check for convergence (equation (5-15)). If $\left|Tol_{float}^{o}\right| \leq \epsilon$, then STOP, the method converged to an potential optimal (local) solution. Otherwise, set $i = i + 1$, update the optimization variables ($\boldsymbol{\eta}_{nom}$) with the most recent solution obtained from *Step 5* and go back to *Step 3*.